NUREG/CR-2331
BNL-NUREG-51454
VOL. 4, NO. 2

SAFETY RESEARCH PROGRAMS SPONSORED BY OFFICE OF NUCLEAR REGULATORY RESEARCH

QUARTERLY PROGRESS REPORT
APRIL 1 — JUNE 30, 1984

Date Published — November 1984

DEPARTMENT OF NUCLEAR ENERGY, BROOKHAVEN NATIONAL LABORATORY
UPTON, NEW YORK 11973

Prepared for the U.S. Nuclear Regulatory Commission
Office of Nuclear Regulatory Research
Contract No. DE-AC02-76CH00016

NUREG/CR-2331
BNL-NUREG-51454
VOL. 4, NO. 2
AN, R-1,4,5,7,8, RD

SAFETY RESEARCH PROGRAMS SPONSORED BY OFFICE OF NUCLEAR REGULATORY RESEARCH

QUARTERLY PROGRESS REPORT
APRIL 1 — JUNE 30, 1984

Herbert J.C. Kouts, Department Chairman
Walter Y. Kato, Deputy Chairman

Principal Investigators:

R.A. Bari
R.J. Cerbone
C.J. Czajkowski
T. Ginsberg
G.A. Greene
J.G. Guppy
R.E. Hall
W.J. Luckas, Jr.
J.N. O'Brien
W.T. Pratt
M. Reich
P. Saha
C. Sastre
J.H. Taylor
J.R. Weeks
W. Wulff
D. van Rooyen

Compiled by: Allen J. Weiss
Manuscript Completed September 1984

DEPARTMENT OF NUCLEAR ENERGY
BROOKHAVEN NATIONAL LABORATORY, ASSOCIATED UNIVERSITIES, INC.
UPTON, NEW YORK 11973

Prepared for the
OFFICE OF NUCLEAR REGULATORY RESEARCH
U.S. NUCLEAR REGULATORY COMMISSION
CONTRACT NO. DE-AC02-76CH00016
FIN NOS. A-3014,-3015,-3016,-3024,-3041,-3208,-3215,-3219,-3225,
-3226,-3227,-3257,-3261,-3266,-3268,-3270,-3271,-3275

Available from
GPO Sales Program
Division of Technical Information and Document Control
U.S. Nuclear Regulatory Commission
Washington, D.C. 20555
and
National Technical Information Service
Springfield, Virginia 22161

FOREWORD

The Advanced and Water Reactor Safety Research Programs Quarterly Progress Reports have been combined and are included in this report entitled, "Safety Research Programs Sponsored by the Office of Nuclear Regulatory Research - Quarterly Progress Report." This progress report will describe current activities and techncial progress in the programs at Brookhaven National Laboratory sponsored by the Division of Accident Evaluation, Division of Engineering Technology, and Division of Risk Analysis and Operations of the U. S. Nuclear Regulatory Commission, Office of Nuclear Regulatory Research.

The projects reported are the following: High Temperature Reactor Research, SSC Development, Validation and Application, CRBR Balance of Plant Modeling, Thermal-Hydraulic Reactor Safety Experiments, Development of Plant Analyzer, Code Assessment and Application (Transient and LOCA Analyses), Thermal Reactor Code Development (RAMONA-3B), Calculational Quality Assurance in Support of PTS; Stress Corrosion Cracking of PWR Steam Generator Tubing, Probability Based Load Combinations for Design of Category I Structures, Mechanical Piping Benchmark Problems, Identification of Age Related Failure Modes; Analysis of Human Error Data for Nuclear Power Plant Safety Related Events, Human Factors Aspects of Safety/Safeguards Interactions, Emergency Action Levels, and Protective Action Decisionmaking. The previous reports have covered the period October 1, 1976 through March 30, 1984.

TABLE OF CONTENTS

TABLE OF CONTENTS (Cont'd.)

TABLE OF CONTENTS (Cont'd.)

FIGURES

FIGURES (Cont'd.)

FIGURES (Cont'd.)

TABLES

I. DIVISION OF ACCIDENT EVALUATION

SUMMARY

High Temperature Reactor Research

Three of the four oxidized medium sized Stackpole 2020 samples were taken to the Oak Ridge National Laboratory for nondestructive measurements. Eddy current responses were measured at different positions of the samples to see the density changes on the surface. Elastic moduli were estimated through ultrasonic wave velocity measurements, and x-ray radiographs were also made on the samples.

The results showed that there exists a large oxidation gradient on the surface of each sample. These results will be compared with those from the destructive measurements that are planned to be done in the near future.

The oxidation rate runs for Stackpole 2020 and PGX have been continuing in the helium impurity loop (HIL No. 1). Most of the planned experimental runs are completed. The results will be utilized to set the experimental conditions for the next PGX oxidation (1 year) experiments.

Electron energy loss spectrometer (EELS) revealed that the fibrous compound blocking the chimneys from the 2400°C runs incorporating SiC in the fuel channels are mostly SiC fibers. Graphite fibers were also identified, but they are believed to be in much smaller amounts.

An IFPT experiment incorporating silver in the fuel channels of a mock-up fuel element was conducted at 1500°C for 5 1/2 hrs. The filter did not collect any silver detectable by an EDAX. The chimney showed plated-out silver in a band of about 8 cm in length at a portion close to the susceptor.

The general problem of gas migration in a PCRV concrete during UCHA scenarios has been analyzed including the effect of water evaporating close to the heated surface and recondensing in cooler regions. Results for early phases of core heatup transients show that the water ingress into the core is much lower than previously estimated. Thus our previous estimates of containment building failure at about 10 days are even more conservative than we realized. However, the back pressure behind the liner could be higher than anticipated, if PCRV concrete is of low permeability, which would lead to liner failures earlier than anticipated.

SSC Development, Validation and Application

The Super System Code (SSC) Development, Validation and Application Program encompasses a series of three computer codes; (1) SSC-L for system tran-

sients in loop-type liquid metal-cooled reactors (LMRs); (2) SSC-P for system transients in pool-type LMRs and (3) SSC-S for long term shutdown transients. In addition to these code development and application efforts, validation of these codes is an ongoing task.

Under SSC-L activities, modeling extensions were developed for the sodium loop piping representation to account for the effects of radiative heat losses to the environment. As a test case, rock-wool was selected for the insulating material, as has been chosen for the SNR-300 plant. A total loss of heat sink at the IHXs was utilized as an example transient. For the FFTF design, this transient has been carried out to 80 hours of simulation time. Work proceeded on the model development to include the effects of inter-assembly heat transfer.

Efforts on the SSC-P version continued to center on the eventual utilization of the EBR-II tests data, which will be forthcoming from a series of transients presently being conducted at that facility. Some model enhancements and modification of the input data set were accomplished.

Work on the SSC-S code concentrated on the investigation of potential problem areas attendant with the usage of large timesteps for slow, long-term transients. Numerical instabilities were found to occur only in the IHX representation. When these calculations were artificially disabled, stable timesteps of up to 32 seconds were achieved in the remainder of the sodium loop hydraulic, loop energy, in-vessel hydraulic, in-vessel energy and fuel heat conduction computational modules.

CRBR Balance of Plant Modeling

The Generic Balance of Plant (BOP) Modeling Program deals with the development of safety analysis tools for system simulation of nuclear power plants. It provides for the developent and validation of models to represent and link together BOP components (e.g., steam generator components, feedwater heaters, turbine/generator, condensers) that are generic to all types of nuclear power plants. This system transient analysis package is designated MINET to reflect the generality of the models and methods, which are based on a momentum integral network method. The code is to be fast-running and capable of operating as a self-standing code or to be easily interfaced to other system codes.

Under MINET model development, a new mechanical rotor designated interface module was introduced. This will allow representation of a turbine-driven pump. Work on the development of a generic control system package continued with the design of twenty-four basic control modules. Details regarding user input requirements and interfacing were begun. The incorporation of a plotfile option into MINET neared completion. To accommodate larger data sets, some data storage areas were moved from small core memory to large core memory.

The initial interface between the RAMONA code and the MINET code has been completed. The composite code uses RAMONA as the host driver. To minimize confusion in error investigation, a simplified MINET input deck was used, and a steady-state (null) transient was executed. After further testing, BWR ATWS transients will be run using the RAMONA/MINET code in support of the SASA Program.

Complete code documentation of Version 1 of MINET has been made available, and copies have been distributed. A MINET computer code workshop has been planned to establish an initial group of external users.

Thermal-Hydraulic Reactor Safety Experiments

The data from the BNL debris bed quench experiments and simple heat transfer calculations strongly suggest that steam produced within a particle bed which is being quenched has a strong potential for being superheated. An analysis of the influence of this steam superheat (and hence of the initial debris bed temperature) on debris bed heat removal rate is presented. The predicted effect of steam superheat on the quenching process and bed heat removal rate is seen to be appreciable, especially for large superheats.

The simplified transient debris bed quenching model developed earlier has been extended to include the fluid momentum equations explicitly. It predicts the time history of solid temperature, fluid velocities, void fraction, and pressure at various points within the debris bed. Numerical computations show that the results are very sensitive to the choice of various adjustable parameters governing the modeling of local solid-fluid heat transfer coefficients and solid-fluid interfacial drag terms. A few sample results are presented.

Re-examination of the liquid-liquid film boiling data reduction and analysis procedure revealed that the magnitude of the R11/liquid metal film boiling data reported in the last Quarterly Progress Report were overestimated. Three of the experiments that were reanalyzed are discussed. R11/Bismuth Run 132 with J_G = 0 cm/s exceed the Berenson film boiling model by 25%. Runs 212 and 219, with J_G = 0.77 and 5.0 cm/s, respectively, were found to exceed the Berenson model on the average by a factor of 1.6 and 2.9, respectively. The enhancement to the film boiling heat flux by a noncondensable gas flux through the boiling interface is believed due to an increase in the interfacial contact area by the rising bubbles.

Development of Plant Analyzer

The LWR Plant Analyzer Program is being conducted to develop an engineering plant analyzer capable of performing accurate, real-time and faster than real-time simulations of plant transients and Small-Break Loss of Coolant

Accidents (SBLOCAs) in LWR power plants. The first program phase was carried out earlier to establish the feasibility of achieving faster than real-time simulations and faster than mainframe, general-purpose computer (CDC-7600) simulations through the use of modern, interactive, high-speed, special-purpose minicomputers, which are specifically designed for interactive time-critical systems simulations. It has been successfully demonstrated that special-purpose minicomputers can compete with, and outperform, mainframe computers in reactor simulations. The current program phase is being carried out to provide a complete BWR simulation capability, including on-line, multi-color graphic display of safety-related parameters.

The plant analyzer program is directed primarily toward reactor safety analyses, but it is also useful for on-line plant monitoring and accident diagnosis, for accident mitigation, further for developing operator training programs and for assessing and improving existing and future training simulators. Major assets of the simulator under development are its low cost, unsurpassed convenience of operation and high speed of simulation. Major achievements of the program are summarized below.

Existing training simulator capabilities and limitations regarding their representation of the Nuclear Steam Supply System have been assessed previously. Simulators reviewed at the time have been found to be limited to steady-state simulations and to restricted quasi-steady transients within the range of normal operating conditions.

A special-purpose, high-speed peripheral processor had been selected for the plant analyzer, which is specifically designed for efficient systems simulations at real-time or faster computing speeds. The processor is the AD10 from Applied Dynamics International (ADI) of Ann Arbor, Michigan. A PDP-11/34 Minicomputer serves as the host computer to program and control the AD10 peripheral processor. Both the host computer and the peripheral processor have been operating at BNL since March 15, 1982.

A four-equation model for nonequilibrium, nonhomogeneous two-phase flow in a typical BWR/4 had been implemented on the AD10 processor. It is called HIPA-BWR/4 for High-Speed Interactive Plant Analysis of a BWR/4 power plant. The implementation of HIPA-BWR/4 had been carried out in the high-level language MPS10 of the AD10.

It had been demonstrated during the last quarter of 1982 that the AD10 special-purpose peripheral processor can produce accurate simulations of a BWR design base transient at computing speeds up to ten times faster than real-time and 110 times faster than the CDC-7600 mainframe computer carrying out the same simulation.

After the successful completion of the feasibility demonstration, work has continued to expand the simulation capability to simulate the dynamics of the entire nuclear steam supply system as well as the entire balance of plant (steam lines, turbines, condensers and feedwater trains).

Models have been developed and implemented for point neutron kinetics with seven feedback mechanisms and seven automatic scram trip initiations, for thermal conduction in fuel elements, for steam line dynamics capable of simulating acoustical effects from sudden valve actions, for turbines, condensers, feedwater preheaters and feedwater pumps and for emergency cooling systems.

The software systems of both the PDP-11/34 host computer and the AD10 special-purpose peripheral processor have been upgraded to achieve greater computing speed and a larger number of analog input/output channels. Two AD10s are coupled via a direct bus-to-bus interface to compute in parallel.

Models had been developed and implemented for the feedwater controller, the pressure regulator and the recirculation flow controller. Twenty-eight parameters for initiating control systems and valve failures and for selecting set points can be changed on-line from a 32-channel control panel. Sixteen dedicated analog output lines are provided for the simultaneous display of 15 selected parameters versus time. All input-output channels are addressed approximately 200 times per second.

All program modules have been combined into the HIPA-BWR/4 code. The entire BWR power plant simulation, including the nuclear steam supply system, the steam lines with all valves, the turbines, condensers, feedwater preheater and pumps, and the control and plant protection systems, has been executed. Fifteen selected parameters can be stored simultaneously in the IBM Personal Computer and then displayed as functions of time in labelled diagrams. A silent movie has been produced to show how the plant analyzer is operated and how it responds to on-line analog signals.

During the previous reporting period, we presented the comparison of plant analyzer results with published results from GE for 10 different ATWS events as a part of developmental assessment. The assessment showed that the plant analyzer is capable of simulating ATWS. The plant analyzer has been generalized to simulate any BWR-4 power plant in response to input data changes from the keyboard. A draft report has been completed to document the plant analyzer.

During the current reporting period, we continued the developmental assessment of the plant analyzer by further comparisons against GE, TRAC-BD1, RELAP-5, and RAMONA-3B. Selected comparisons are presented in this report. The results show that the plant analyzer is capable of realistically simulating a large class of plant transients efficiently at very low cost.

The interest in the Plant Analyzer Development Program continues to be high, both in domestic and foreign institutions. Four presentations with demonstrations were given at BNL to foreign visitors, and two invited papers have been presented and submitted for publication during the current reporting period. Five presentations were given during March and April 1984 in laboratories and institutions abroad.

Code Assessment and Application (Transient and LOCA Analyses)

The TRAC-BD1/MOD1 (Version 22) code has been successfully implemented on the BNL CDC-7600 computer. Significant progress has been made in developing a TRAC-BD1/MOD1 input deck for simulating the BWR Full Integral Simulation Test (FIST) facility.

In addition, the thermal-hydraulic program of the BWR stability analysis code, NUFREQ-NP, developed at Rensselaer Polytechnic Institute has been implemented on the BNL CDC-7600 computer. However, the neutronic program may have to be implemented on the BNL VAX computer because of the very large central memory requirements.

Thermal Reactor Code Development (RAMONA-3B)

Several improvements and corrections have been made to the RAMONA-3B code. They are: (1) an improved recirculation pump model, (2) corrections in void fraction used in the reactivity calculation, and (3) correction in the static head calculation. A two-day RAMONA-3B seminar was held at BNL for the benefit of the RAMONA-3B users. Eleven persons from seven U.S. organizations attended the seminar.

Significant progress has been made in the generation of 3-D neutronic cross sections for the Browns Ferry Cycle 5 reactor core. This task is being performed under joint sponsorship between this and another NRC program (FIN A-3273, Application of RAMONA to BWR ATWS).

Calculational Quality Assurance in Support of PTS

Preliminary review of the RELAP5/MOD1.6 calculations and extrapolations of all the eleven transients for the H. B. Robinson-2 PTS study has been completed. The calculations performed at INEL seem to be reasonable. However, there are uncertainties due to the pressurizer model, structure stored energy and multidimensionality of some of the transients. Some of these transients are being reviewed in-depth using the simple method developed at BNL.

1. High Temperature Reactor Research

1.1 Graphite and Ceramics (B. S. Lee, J. H. Heiser, III, and D. R. Wales)

1.1.1 Nondestructive Measurements

Three (samples 1, 2 and 4) of the four oxidized medium sized Stackpole 2020 samples were taken to the Oak Ridge National Laboratory for nondestructive measurements. Eddy current responses were measured at different positions of the samples to see the density changes on the surface. Elastic moduli were estimated through ultrasonic wave velocity measurements. X-ray radiographs were also made on the samples.

1.1.1.1 Eddy Current Measurements

By measuring the eddy current response, the surface (<~1/4 inches, depending on the frequency used) conductivity can be estimated. This conductivity is a function of density of the graphite. When eddy current response was measured as a function of bulk density, a linear relationship was observed. Thus, it is believed that eddy current response is very sensitive to density changes (C. R. Kennedy, 1984).

The eddy current responses on three oxidized samples (samples 1, 2 and 4) and on control sample with same dimensions were measured. The measured values were converted to densities using the relationship between eddy current response and density developed by C. R. Kennedy of the Oak Ridge National Laboratory. It should be mentioned that these estimated densities should be used as relative values. The absolute densities may be different from these.

For example, the average density of the control sample estimated from the eddy current response measurements is about 1.74 g/cm^3, while the bulk density measured is 1.80 g/cm^3. This discrepancy may probably be due to the fact that the relationship used was obtained from a different batch of Stackpole 2020 (maximum density ~1.77 g/cm^3).

It should also be noted that some of the estimated densities in Tables 1.1.1 through 1.1.4 are extrapolated values.

However, these results are significant, because they give useful information on the oxidation gradient on the surface nondestructively.

These density values will be compared with the results from the density profile measurements using a destructive method in the near future.

As shown in Tables 1.1.2 - 1.1.4, there exists a very large oxidation gradient on the surface of each sample. It is obvious that these oxidation gradients are caused by the gas flow pattern inside the quartz reactor.

Thus, from the eddy current measurement results, we have learned two things. First, a sample holder with a proper design is needed to ensure the gas flow to be uniform around the samples. Secondly, the profiling technique

Table 1.1.1 The Estimated Densities for the Control Sample.

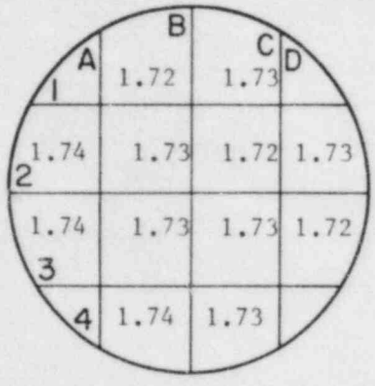

TOP

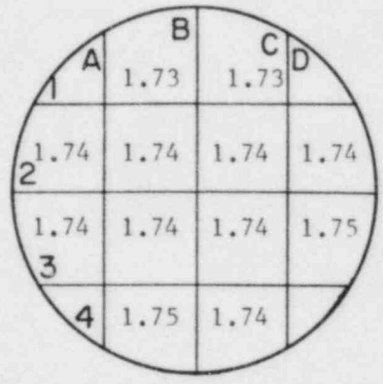

BOTTOM

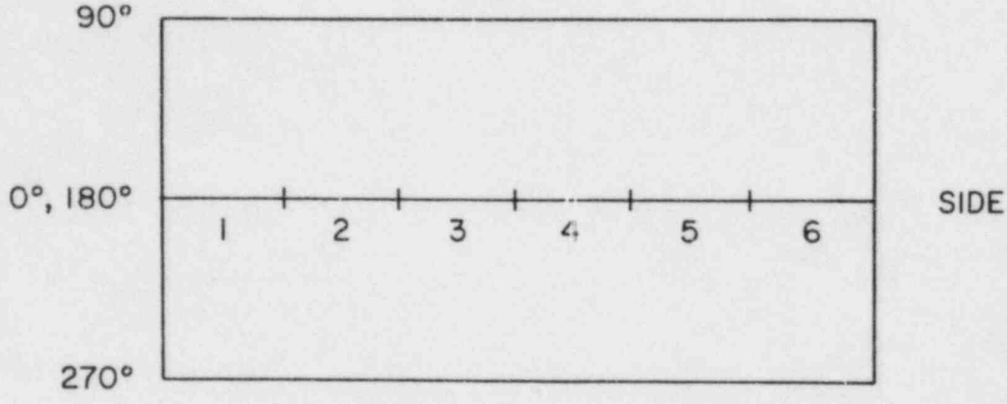

Position \ Angle	0	90	180	270
1	1.74	1.75	1.73	1.74
2	1.74	1.75	1.74	1.76
3	1.73	1.74	1.74	1.75
4	1.74	1.73	1.74	1.75
5	1.74	1.74	1.73	1.74
6	1.74	1.75	1.73	1.73

Table 1.1.2 The Estimated Densities for the Oxidized Sample No. 1.

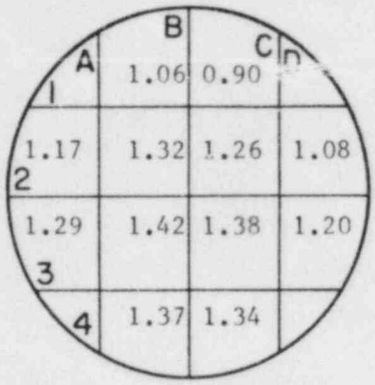

TOP

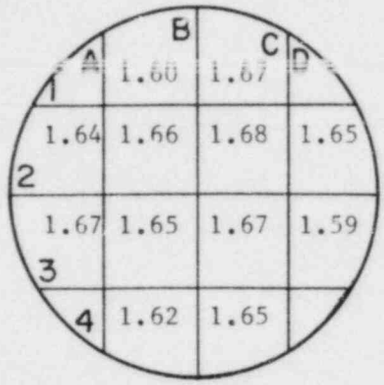

BOTTOM

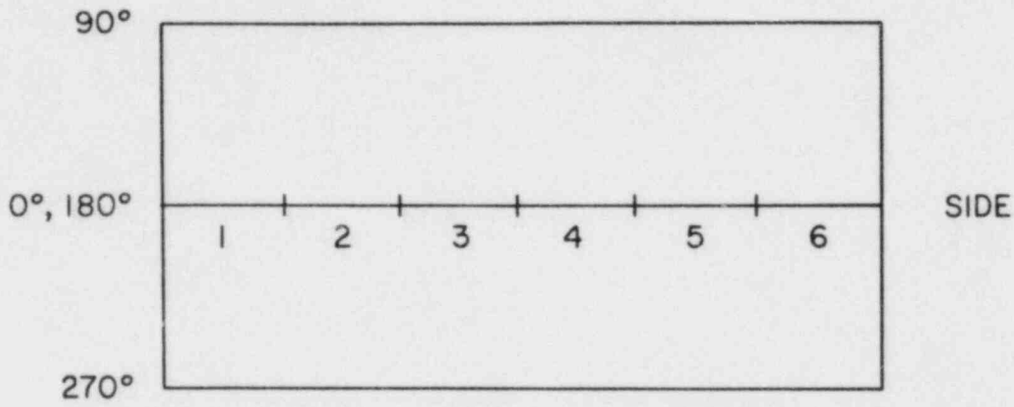

Position \ Angle	0	90	180	270
1	NR	NR	1.50	0.59
2	NR	NR	1.54	0.84
3	NR	0.41	1.53	1.00
4	NR	0.78	1.54	1.13
5	0.55	1.08	1.55	1.17
6	1.62	1.63	1.47	1.63

NR: No Reading

Table 1.1.3 The Estimated Densities for the Oxidized Sample No. 2.

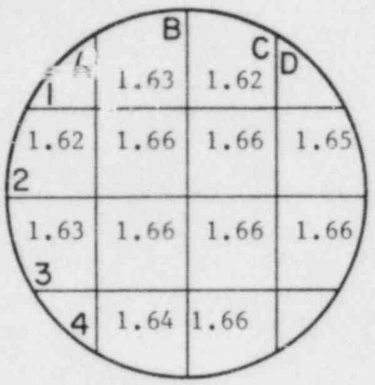

TOP

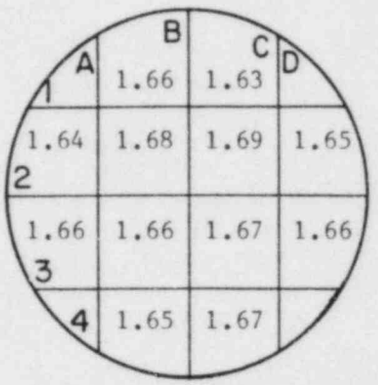

BOTTOM

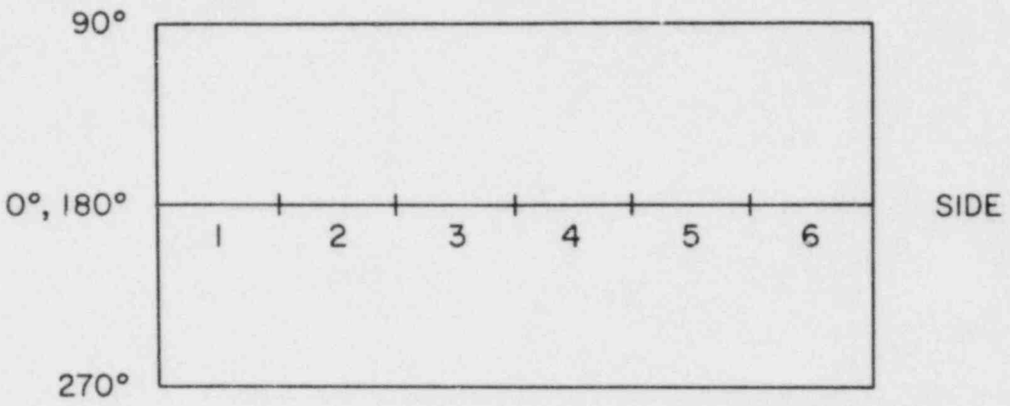

Position \ Angle	0	90	180	270
1	NR	0.39	1.55	0.93
2	NR	0.31	1.53	0.93
3	NR	0.44	1.55	0.97
4	NR	0.35	1.57	0.97
5	NR	0.35	1.57	1.00
6	NR	0.34	1.58	1.04

NR: No Reading

Table 1.1.4 The Estimated Densities for the Oxidized Sample No. 4.

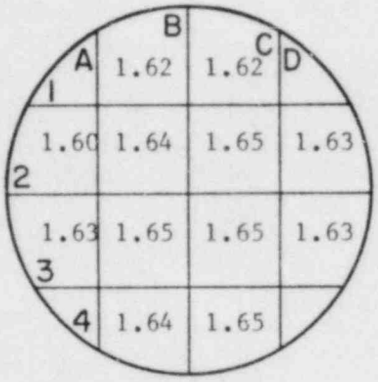

TOP

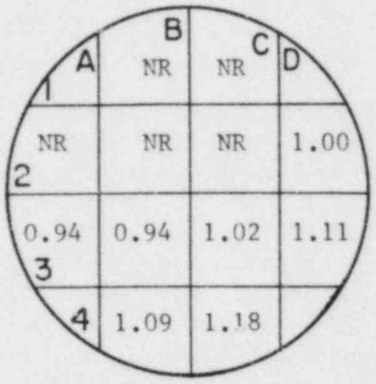

BOTTOM

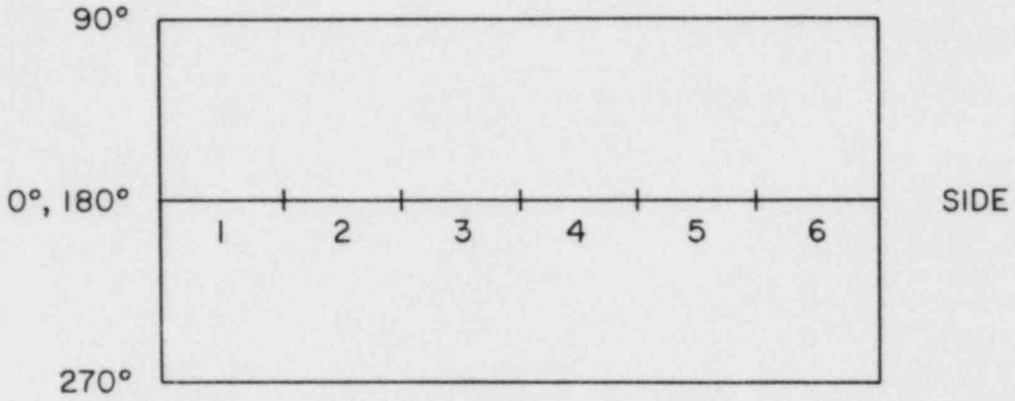

Position \ Angle	0	90	180	270
1	NR	NR	1.46	NR
2	NR	NR	1.50	NR
3	NR	NR	1.53	NR
4	NR	1.03	1.53	NR
5	NR	1.30	1.56	NR
6	NR	1.36	1.52	1.02

NR: No Reading

that has been used on small samples is not appropriate with the medium sized samples that show large surface oxidation gradient. Currently, designing a sample holder and a new profiling technique is in progress.

1.1.1.2 Sonic Testings

Ultrasonic wave velocity measurement methods utilizing longitudinal and shear waves were used to estimate the elastic moduli of the oxidized and control medium sized samples in the axial directions, and the results are shown in Tables 1.1.5 - 1.1.8.

The oxidized Sample No. 2 showed higher E value than the other samples, while it showed the highest weight loss, 8.61% compared to 5.87% and 6.12% for Sample No. 1 and No. 4, respectively. This is because the top and bottom of the Sample No. 2 were not oxidized extensively while the top of the Sample No. 1 and the bottom of the Sample No. 4 which were exposed to the gas flow were oxidized more heavily. (See Tables 1.1.2 - 1.1.4).

Due to the severely oxidized portions on the sides of the samples, the ultrasonic wave velocities could not be measured in the radial directions.

1.1.1.3 X-ray Radiography

The three oxidized medium sized samples and the control sample were x-ray radiographed utilizing the facility at the Oak Ridge National Laboratory. Radiography is used to show bulk density variations. However, the sample should have a thickness less than ~6 mm for this purpose, which is not possible until we finish the destructive test. Thus, the samples were radiographed as they were to check for any internal defects such as cracks. The radiographs showed that there exists no internal defects except a flow line in Sample No. 1 that is parallel to the top plane of the right cylinder.

1.1.2 Oxidation Kinetic Measurements on Stackpole 2020 and PGX Samples

It was reported previously that the experimental conditions for the medium term oxidation study will be modified for the next run when four PGX samples will be oxidized (B. S. Lee et al, 1984). This is necessary because the Stackpole 2020 samples showed higher oxidation rates than expected.

For this purpose, oxidation rate runs for Stackpole 2020 and PGX have been continuing in the helium impurity loop (HIL No. 1). Most of the planned experimental runs are completed at the present time. The results will be analyzed and reported in the next progress report.

These kinetic data are being compared with our earlier results from the small sample experiments and those from General Atomic Technology.

Table 1.1.5 The Estimated Moduli of Elasticity, E(GPa) for the Control Sample.

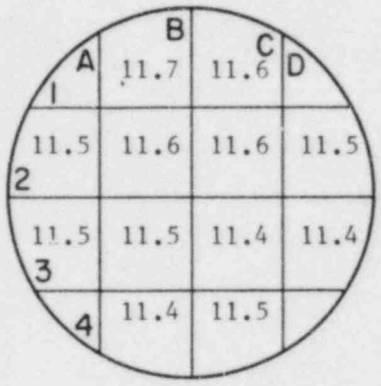

Table 1.1.6 The Estimated Moduli of Elasticity, E(GPa) for the Oxidized Sample No. 1.

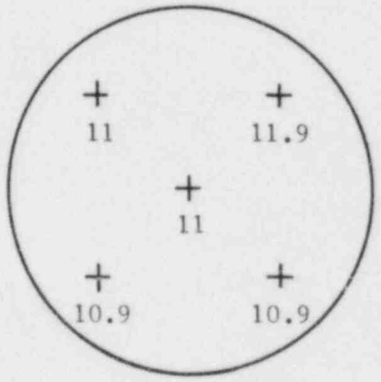

Table 1.1.7 The Estimated Moduli of Elasticity, E (GPa) for the Oxidized Sample No. 2.

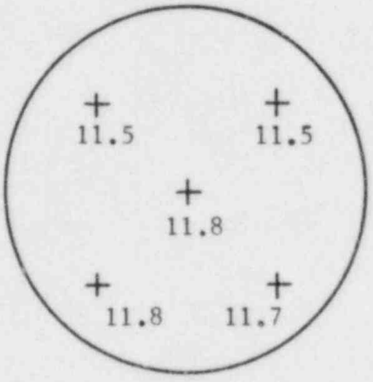

Table 1.1.8 The Estimated Moduli of Elasticity, E (GPa) for the Oxidized Sample No. 4.

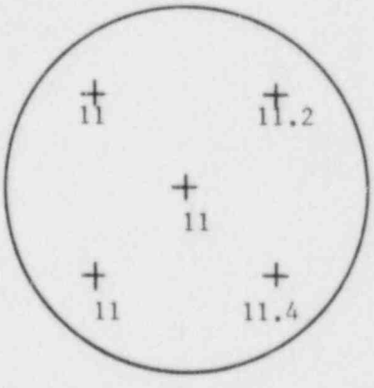

1.2 Fission Product Migration (B. S. Lee, J. H. Heiser, III, and C. C. Finfrock)

1.2.1 Integrated Fission Product Transport Experiments with SiC

The chimneys from the two IFPT experiments incorporating 3.7% (Run #3184) and 1.39% (Run #31384) SiC were split and examined with a SEM and a TEM.

Energy dispersive x-ray spectroscopy (EDAX) was used to identify the elements that plated out on the inner walls of the chimneys. The two chimneys showed an identical order of deposition of elements/compounds, which is shown in Figure 1.1.1. Figures 1.1.2. ~ 1.1.4 show the morphologies of the plated-out elements/compounds corresponding to positions 10 ~ 12 in Figure 1.1.1, respectively.

Electron energy loss spectrometer (EELS) revealed that most of the fibrous compound in Figure 1.1.2 is SiC. Graphite fibers were also identified, but they are believed to be in much smaller amounts.

We have proven that SiC and Si are playing a major role in blocking a chimney and in capturing aerosol particles when the susceptor temperature is higher than 2400°C. At lower temperatures (e.g., <2000°C), Si may not affect the fission product transport mechanism.

1.2.2 IFPT Experiments with Silver

An IFPT experiment incorporating 24 grams silver in the fuel channels was conducted at 1500°C for 5 1/2 hours (Run #51884). Silver was selected since data on silver are available from aerosols studies.

No visible amount of silver was observed in the filter after the experiment, and EDAX did not show the peak for silver. However, the filter will be analyzed for silver using a wet chemical analysis.

The chimney showed plated-out silver in a band of about 8 cm in length at a portion close to the susceptor. Figures 1.1.5(a) and (b) show the shapes of silver crystals plated out.

A wet chemical analysis will also be used to estimate the amount of silver plated out on the graphite chimney walls.

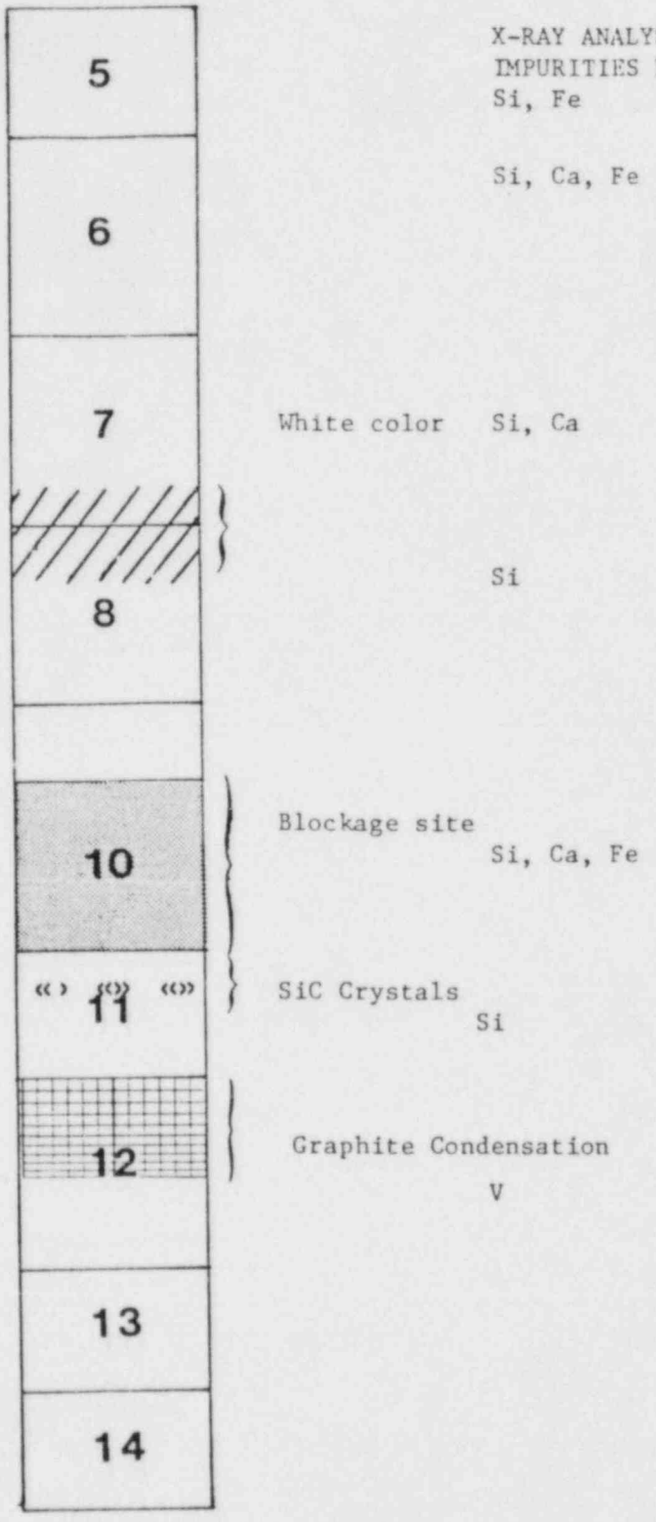

Figure 1.1.1 Split Section of a Chimney From the Run #31384 with SiC at 2400°C.

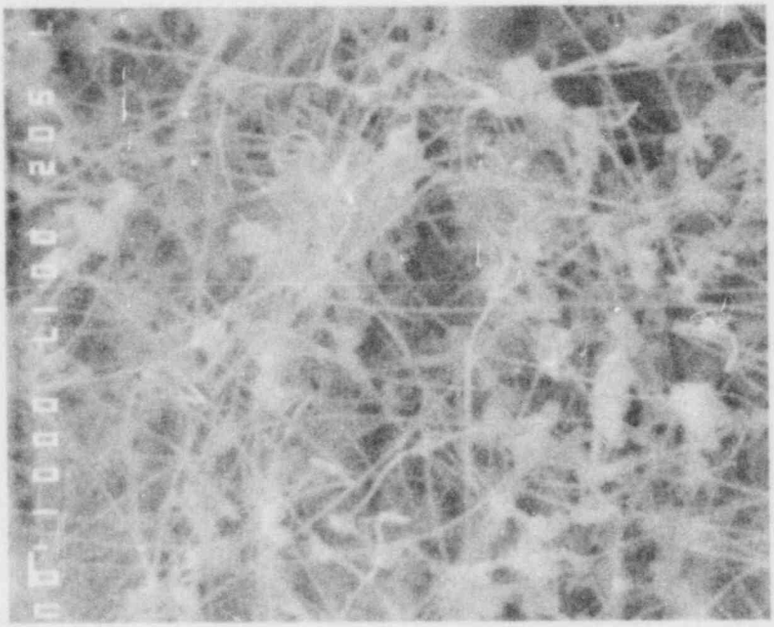

Figure 1.1.2 SiC and Graphite Fibers Formed in Section 10 in Figure 1.1.1 . Magn. 5000X.

Figure 1.1.3 SiC Formed in Section 11 in Figure 1.1.1. Magn. 10X.

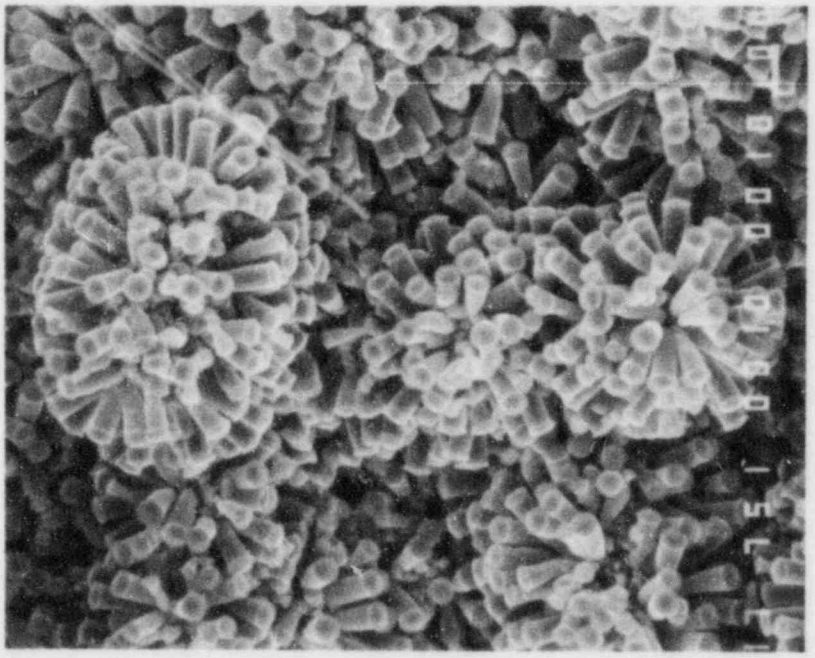

Figure 1.1.4 Graphite Formed in Section 12 in Figure 1.1.1. Magn. 750 X.

(a)

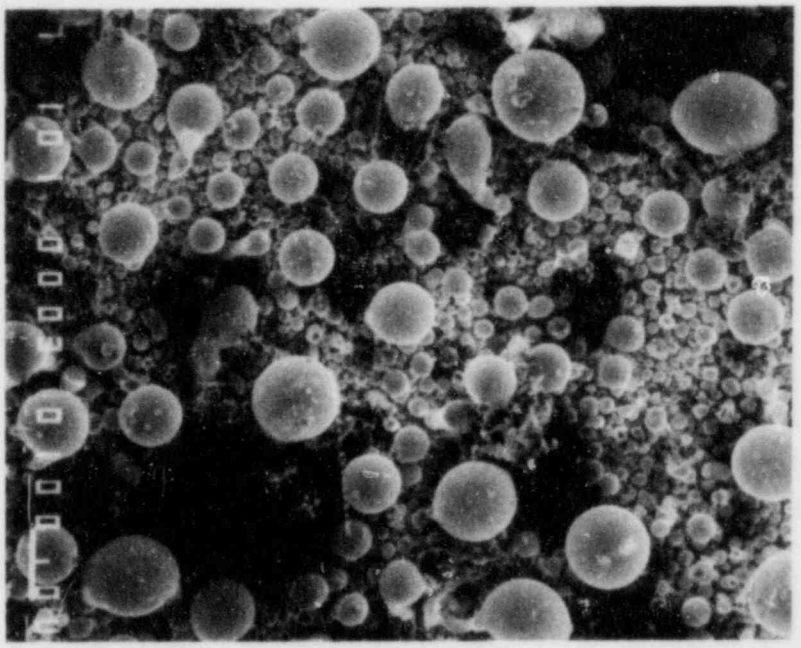

(b)

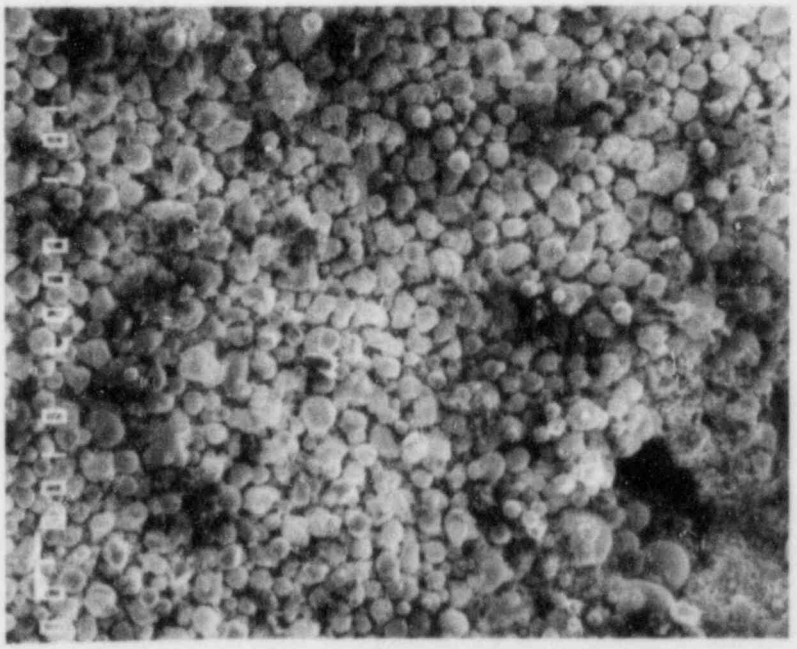

Figure 1.1.5 Silver Plated Out on the Inner Wall of the Chimney From Run # 51884.(a) is Closer to the Susceptor than (b).

1.3 Analytical

1.3.1 HTGR Code Library (J. Colman)

Table 1.3.1

HTGR Code Library - Alphabetic Code Order

Program	Origin/ Code Date	BNL Status	Function
BLAST	ORNL/ACC 8/76 (BNL 1/80)	OP	A dynamic simulation of the HTGR reheater-steam generator module.
BLOOST/ BLOOST-7	GA/SAI 1/70	OP	Performs zero-dimensional reactor kinetics calculations.
CHAP-1 (Jan.1978)	LASL 2/77	NOP	Simulates the overall HTGR plant with both steady state and transient solution capabilities.
CIRC (JETS)	BNL 4/78	OP	Calculates fluid dynamics in an HTGR containment vessel following a depressurization accident.
CNTB-7	GA 7/79	OP	Analysis of Partially mixed containment atmospheres during depressurization events.

CC = Argonne Code Center.
AW = Babcock and Wilcox.
NL = Brookhaven Nat. Lab.
PNW = Battelle Pacific N.W.
A = General Atomic.
ASL = Los Alamos Scientific Lab.
OP = Non-Operational.
P = Operational
RNL = Oak Ridge National Lab.
= Proprietary.
AI = Science Applications, Inc.

Program	Origin/ Code Date	BNL Status	Function
CONTEMP-G (CONTEMPT-G)	GA-BAW 2/74	OP (P)	Simulates temperature-pressure response of an HTGR containment atmosphere to postulated coolant circuit depressurization.
CORCON	GA 7/74	OP (P)	Computes the temperature history and fission product redistribution following a loss of all convective cooling of the core.
CORTAP	ORNL ACC 1/77 (BNL 1/80)	OP	A coupled neutron kinetics - heat transfer program for the dynamics simulation of the HTGR core.
DECAYREM	ORNL 5/74	OP	RSIC Data Library Collection.
DIFFTA	BNL 11/75	OP	Finite element method code for Steady State Heat Conduction, Fission Product Migration and Neutron Diffusion Calculations.
ENDFB and Satellite Codes	BNL	OP	Evaluated Nuclear Data File/B and file manipulation codes.
EVAP	BNL 5/78	OP	A model for the Migration of Fission Products along the coolant channels of an HTGR following a hypothetical accident of complete loss of cooling.
EXREM	ORNL 2/75	OP	Calculates external radiation doses.
FENG	LASL 2/77	OP	One of three codes which create or add to the reactions data library for QUIL and QUIC codes. Reactions added are of type Free Energy.
FEVER-7	GA	OP	Performs one-dimensional, diffusion theory, burnup and reload calculations.

Program	Origin/ Code Date	BNL Status	Function
FLAC	GA	OP	Calculates steady state flow distributions in arbitrary networks with heat addition.
FPPROD	BNL 3/78	OP	Performs simplified fission product production analysis.
FYSMOD	LASL 9/76	NOP	Calculates the two-dimensional solution of HTGR core blocks subjected to external motion.
GAKIT	GA 9/68	OP	Performs one-dimensional multigroup kinetics calculations with temperature feedback.
GAMBLE	GA	OP	A program for the solution of the multigroup neutron-diffusion equations in two dimensions, with arbitrary group scattering.
GGC4	GA/ACC	OP	Prepares broad thermal cross sections from the tape produced by WTFG and MAKE.
GOPTWO/ GOP-3	BPNW 6/75 BPNW 10/76	OP NOP	Graphite Oxidation Program. Analyzes the steady state graphite burnoff and the primary circuit levels of impurities.
HAZARD	BNL 3/77	OP	Analyzes gas layering and flammability in an HTGR containment vessel following a depressurization accident.
H-CON1	BNL 5/76	OP	Calculates one-dimensional heat conduction for an HTGR fuel pin by finite difference method.
HEATING5	ORNL 3/77	OP	Heat Conduction Code
HYDRA-1	BNL 5/76	OP	A program for calculating changes in enthalpy single phase liquid due to external heat source.
INREM	ORNL 2/75	OP	Calculates internal radiation doses.

Program	Origin/ Code Date	BNL Status	Function
INTERP	GA MICROX LIBRARY	OP	Prepares broad group cross sections from MICROX output data tapes.
JANAF	Dow Chemical Company 11/76	OP	JANAF Thermochemical Tables.
LARC-1	LASL 11/76	NOP	Calculates fission product release from BISO and TRISO fuel particles of an HTGR during the LOFC accident for single isotopes.
LARC-2	LASL	NOP	Similar to LARC-1; in addition, handles release from isotope chains.
LASAN-BNL LASAN-LASL	LASL/BNL 4/78	NOP	A general systems analysis code consisting of a model independent systems analysis framework with steady state, transient and frequency response solution capabilities. There are two versions of the code available - the original LASL version and the converted BNL version.
LEAF	LASL 11/76	NOP	Calculates fission product release from a reactor containment building.
MAKE	SAI	OP	Prepares fine group fast cross section tape from GFE2 for spectrum codes.
NONSAP-C	LASL 10/78	NOP	Calculates static and dynamic response of three-dimensional reinforced concrete structures, in addition to creep behavior.
ORECA-1	ORNL-ACC 4/76	OP	Simulates the dynamics of HTGR cores for emergency cooling analyses. (Ft. St. Vrain)

Program	Origin/ Code Date	BNL Status	Function
ORIGEN	ORNL 4/75	OP	Solves the equation of radioactive growth and decay for large numbers of isotopes with arbitrary coupling.
ORTAP	ORNL-ACC 9/77	OP	A nuclear steam supply system simulation for the dynamic analysis of HTGR transients.
OXIDE-3	GA 1/74	OP (P)	Analyzes the transient response of the HTGR fuel and moderator to an oxidizing environment.
POKE	GA 7/70	OP (P)	Calculates steady state 1-D flow distributions and fuel and coolant temperatures in a gas cooled reactor.
PREPRO	GA	OP (P)	Prepares input data and source code revisions for RECA code.
PRINT	SAI	OP	Reads the fast cross section tape produced by MAKE.
QUIC	LASL 2/77	OP	Solves complex equilibrium distribution in chemical environments.
QUIL	LASL 2/77	OP	Solves complex equilibrium distribution in chemical environments.
RATE	LASL 7/78	OP	One of three codes which create or add to the reactions data library for QUIL and QUIC codes. Reactions added are of type Rate.
RATSAM-6	GA 5/77	OP	Analyses the transient behavior of the HTGR primary coolant system during accidents.
RECA	GA 8/70	NOP (P)	Calculates time dependent flow distributions and fuel and coolant temperatures in the primary system.
RICE	LASL 3/75	OP	Solves transient Navier-Stokes equations in chemically reactive flows.

Program	Origin/ Code Date	BNL Status	Function
SODEMME	BNL 8/77	OP	Calculates transient thermal hydraulic aspects of circulating gas systems.
SOLGASMIX	ORNL 4/77	OP	Calculates equilibrium relationships in complex chemical systems.
SORS	GA 4/74	OP (P)	
SORSD	GA	OP (P)	Computes the release of volatile fission products from an HTGR core during thermal transients.
SORSG	GA	OP (P)	Computes the release of non-volatile gaseous fission products from an HTGR core during thermal transients.
SPRINT	GA/SAI	OP	Reads the thermal cross section tape produced by WTFG.
SURF	LASL 2/77	OP	One of three codes which create or add to the reactions data library for QUIL and QUIC codes. Reactions added are of type Surface.
SUVIUS	LASL	NOP	Solves the behavior of fission gases in the primary coolant of a gas-cooled reactor.
TAC2D	GA 9/69	OP	Performs two-dimensional, transient conduction analyses.
TAP	GA	OP (P)	Calculates the transient behavior of the integrated HTGR power plant.
TEMCO/TEMCO7	GA	OP	Computes reactor temperature coefficients from input cross section data.

Program	Origin/ Code Date	BNL Status	Function
THGRAF	BNL 11/77	OP	Calculates position and velocity of the thermo-chromatograph as a function of time for various models.
WTFG	GA	OP	Prepares fine group thermal cross section tape from GAND2 or FLANGE for spectrum codes.
1-DX		OP	Performs one-dimensional, diffusion theory, steady state calculations.

1.3.2 Vapor Migration in Concrete (P. G. Kroeger)

INTRODUCTION

The objective of this effort is to assess the effect of vapor migration in PCRV concrete on the gas release from the concrete and an ultimate CB failure during in UCHA scenarios without LCS. It is based on core heatup transients for the 2240 MW th reactor (Kroeger et al, 1983, and Reilly et al, 1984). Most of the results apply at least qualitatively to all HTGR's with PCRVs.

The basic process of moisture migration during concrete heatup can be described as follows: As the porous medium is heated at its exposed surface, some of the water is vaporizes, causing a pressure increase and a flow of gas and liquid phase into cooler regions, where recondensation can occur. When concrete temperatures exceed the local vapor saturation temperature, a "dry region" is formed in which water only exists in the vapor phase. This dry region expands with an "evaporation front" moving into the concrete. Beyond the front, water exists as liquid and as vapor, in equilibrium. This region is called the "wet region". A further important aspect affecting the process significantly is the presence of a non-condensible gas (generally air) in the porous structure. The problem is essentially one of a phase change front motion with a thermally driven flow field, but with significant feed back from the flow field to the temperature field.

THE MODEL

The current work represents a finite difference solution of the full partial differential equations of mass and energy conservation with Darcy's momentum equation. Two separate regions are modeled, a "dry" region and a "wet" region, separated by a moving phase change front. As pointed out before (McCormack et al, 1979; Shiina and Kroeger, 1984) the motion of gas and liquid in concrete heated beyond 100°C is predominantly due to pressure gradients, and the vapor motion by molecular diffusion is therefore being neglected.

A semi-infinite (or finite) slab of concrete is being considered with no-flux boundary conditions at the far end. The dry region contains concrete and superheated vapor, while the wet region contains concrete, water in liquid as well as in saturated vapor form, and air. The absence of air from the dry region is a result of the gas flow from the evaporation front, (Shiina and Kroeger, 1984). Local thermodynamic equilibrium (equal temperature of all phases at any time and location) is assumed.The thermal boundary condition at the outer surface (z=0) is that of a prescribed time varying source temperature, and outside heat transfer coefficient. The flow boundary condition can either be that of an impermeable surface, which applies prior to liner failure, or that of outflow with prescribed surface pressure, which applies subsequent to liner failure.

The resulting conservation equations for the dry region are

vapor mass

$$\frac{\partial}{\partial t} m_v = - \frac{\partial}{\partial z} \rho_v u_g \tag{1}$$

mixture energy

$$\frac{\partial}{\partial t} E + \frac{\partial}{\partial z} \rho_v h_v u_g = \frac{\partial}{\partial z} k_D \frac{\partial \theta}{\partial z} \tag{2}$$

where the dry region mixture internal energy is

$$E = (1-\varepsilon) (\rho c)_S (\theta - \theta_{ref}) + m_v e_v \tag{3}$$

The vapor flow follows from Darcy's law as

$$u_g = - (\frac{K}{\mu})_g \frac{\partial p_T}{\partial z} \tag{4}$$

The current model uses spline functions of high accuracy for the water properties. In the dry region these are generally solved as

$$p_v = p_T = p (\rho_v, \theta) \tag{5}$$

where

$$\rho_v = \frac{m_v}{\varepsilon} \tag{6}$$

but solutions for $\rho = \rho (p,\theta)$ are also provided.

The conservation equations for the wet region are

water mass

$$\frac{\partial}{\partial t} m_w = - \frac{\partial}{\partial z} (\rho_v u_g + \rho_\ell u_\ell) \tag{7}$$

air mass

$$\frac{\partial}{\partial t} m_a = - \frac{\partial}{\partial z} \rho_a u_g \tag{8}$$

energy

$$\frac{\partial}{\partial t} E + \frac{\partial}{\partial z} \left[(\rho_v h_v + \rho_a h_a) u_g + \rho_\ell h_\ell u_\ell \right] = - \frac{\partial}{\partial z} k_W \frac{\partial \theta}{\partial z} \tag{9}$$

where the mixture internal energy is

$$E = (1-\varepsilon) (\rho c)_S (\theta - \theta_{ref}) + m_v e_v + m_\ell e_\ell + m_a e_a \tag{10}$$

and of course

$$m_w = m_v + m_\ell . \tag{11}$$

The wet region Darcy flow relationships are

$$u_g = - a_g \left(\frac{K}{\mu}\right)_g \frac{\partial p_T}{\partial z} \; ; \; u_\ell = - \left(\frac{K}{\mu}\right)_\ell \frac{\partial p_T}{\partial z} \tag{12}$$

Equation (12) allows for the use of separate liquid and vapor permeabilities, to simulate the effect of reduced liquid flow which has been suggested by some authors (Dayan and Gluekler, 1982; Min and Emmons, 1972). Furthermore, in particular for large liquid volume fractions an impairment of the gas flow has been suggested. To simulate that effect the factor a_g was added in the gas flow equation. Optionally this factor can be set to 1.0 (no gas flow reduction) or to $a_g = S_g = \alpha_g/\varepsilon$, where α_g is the volume fraction of gas in the porous structure.

The wet region state relationships for water are obtained from spline fits to the 1967 IFC formulation, except for the liquid density which was assumed as constant (1000 kg/m^3). Air was treated as an ideal gas. All phases were assumed to be locally in thermodynamic equilibrium. The total pressure is then the sum of the partial pressures

$$p_T = p_v + p_a . \tag{13}$$

At the vaporization front, mass and energy must be conserved. As shown by Shiina and Kroeger, 1984, if molecular diffusion is being neglected, the air concentration in the dry region is zero and mass conservation of air at the vaporization front does not have to be considered explicitly.

Mass conservation of water for a vaporization front moving with velocity U_{fr} requires

$$(m_{v1} - m_{w2}) U_{fr} = \rho_{v1} u_{g1} - \left[\rho_v u_g + \rho_\ell u_\ell \right]_2 \tag{14}$$

where subscripts 1 and 2 refer to front properties on the dry side and on the wet side respectively.

Energy conservation at the front requires

$$(E_1 - E_2) U_{fr} = \left[k \frac{\partial \theta}{\partial z} \right]_1 - \left[k \frac{\partial \theta}{\partial z} \right]_2 + (\rho_v h_v u_g)_1 - \left[\rho_v h_v u_g + \rho_\ell h_\ell u_\ell \right]_2 \tag{15}$$

where E_1 and E_2 follow from Equations 3 and 10 respectively. Note that the u_i in Equations 14 and 15 are superficial velocities while the front velocity U_{fr} is an actual velocity.

The concrete heatup begins from an originally almost isothermal state. As the heatup progresses over days gradually larger parts of the PCRV are affected. To model this process efficiently, the current work solves the above equations in a moving coordinate system.

The dry region non-dimensional space coordinate is

$$\zeta = z/z_{fr}\,(t). \tag{16}$$

The wet region width was defined as

$$\Delta z_W = \text{const}\,\sqrt{\kappa_W t} \tag{17}$$

where the constant for the thermal analysis only could be taken as about 5 to 8. However, for the prevailing concrete data to be used below, it was found that the flow field extended deeper into the semi-infinite concrete than the temperature field and a constant of 18 was used for all computations reported here.

The wet region non-dimensional space coordinate was then defined as

$$\zeta = 1 + \frac{z - z_{fr}(t)}{\Delta z_W(t)} \tag{18}$$

In this coordinate system the dry region extends from $0<\zeta<1$, and the wet region from $1<\zeta<2$.

The equations were solved in a completely conservative finite difference formulation for ζ and t as independent variables. Details regarding this formulation and the experience obtained with it will be documented in a future report.

RESULTS

For the application to PCRV heatup transients, two flow boundary conditions at the heated surface are of interest (the thermal boundary condition used at all times is one of prescribed time varying source temperature and heat transfer coefficient). Up to the time of liner failure, the heated surface is impermeable to flow, and the boundary condition is

$$u = \frac{\partial p}{\partial z} = 0;\ z = 0 \tag{19}$$

Subsequent to liner failure, vapor can flow into the core cavity and the core inside pressure will provide the pressure boundary condition at the outside surface of the concrete, thus:

$$p = p_{core}\ ;\ \ z = 0 \tag{20}$$

At first, a general application of the model was considered, to facilitate comparison with previous work. Considering impermeable wall boundary conditions, a step change in temperature to 250°C was imposed at the outer surface of a semi-infinite slab, assuming an initial liquid fraction of $S_{\ell o}$=0.2. The other input data used for this case correspond to those of Shiina and Kroeger, 1984 and are summarized in Table 1.3.2.

Table 1.3.2

Properties and Input Data for Case of Step Change in Wall Temperature

k_D = 0.35 W/mK

k_W = 1.60 W/mK

$(\rho c)_S$ = 1.7×10^6 m^3K

θ_∞ = 20°C

p_∞ = 1 bar

$(\frac{K}{\mu})_g$ = 2.4×10^{-6} $\frac{m^2}{bar\ s}$

$(\frac{K}{\mu})_\ell$ = $10^{-4}(\frac{K}{\mu})_g$

ϵ = 0.32

The resulting vaporization front velocity and the front pressures and temperatures are shown in Figure 1.3.1. The results show that the previous approximations assuming a constant front temperature for the case of a step change in wall temperature was well justified. Also the approximate front progression of

$$z_{fr} \propto \sqrt{t}$$

is confirmed by Figure 1.3.1 to be accurate within 1% over the time range from 60 s to 4 hr. Figure 1.3.2 shows typical temperature, pressure and liquid fraction distributions. The front temperatures and pressures shown are slightly lower than the previous ones which is apparently due to the improved-latent heat relationships being used here. Altogether, the close agreement with the previous results confirms the validity of the simplified model, which is of value for rapid parametric evaluations, and it establishes confidence in this new and more general model.

As a further applications, the model was applied to the early phases of PCRV heatup under UCHA conditions. The thermal barrier core side temperatures were taken from core heatup transients of Kroeger et al, 1983 and Reilly et al, 1984. At the center location of the side barrel they ranged from about 300°C to 1000°C over the period of 0 - 80 hr when thermal barrier failure began. For such a transient source temperature and a thermal barrier of kao-wool insulation the transient heatup and moisture migration in a semi-infinite slab of concrete were analyzed. A summary of the properties being used for this application is given in Table 1.3.3. (Please note that the code does provide for temperature dependent properties, and that constant values were applied here only to keep the demonstration cases as simple as possible). The concrete thermal properties are representative of those of Appendix E of the Fort St. Vrain Safety Analysis Report (Final Safety Analysis Report), while the assumed best estimate permeabilities are based on referenced data (General Atomic Company, April 1978).

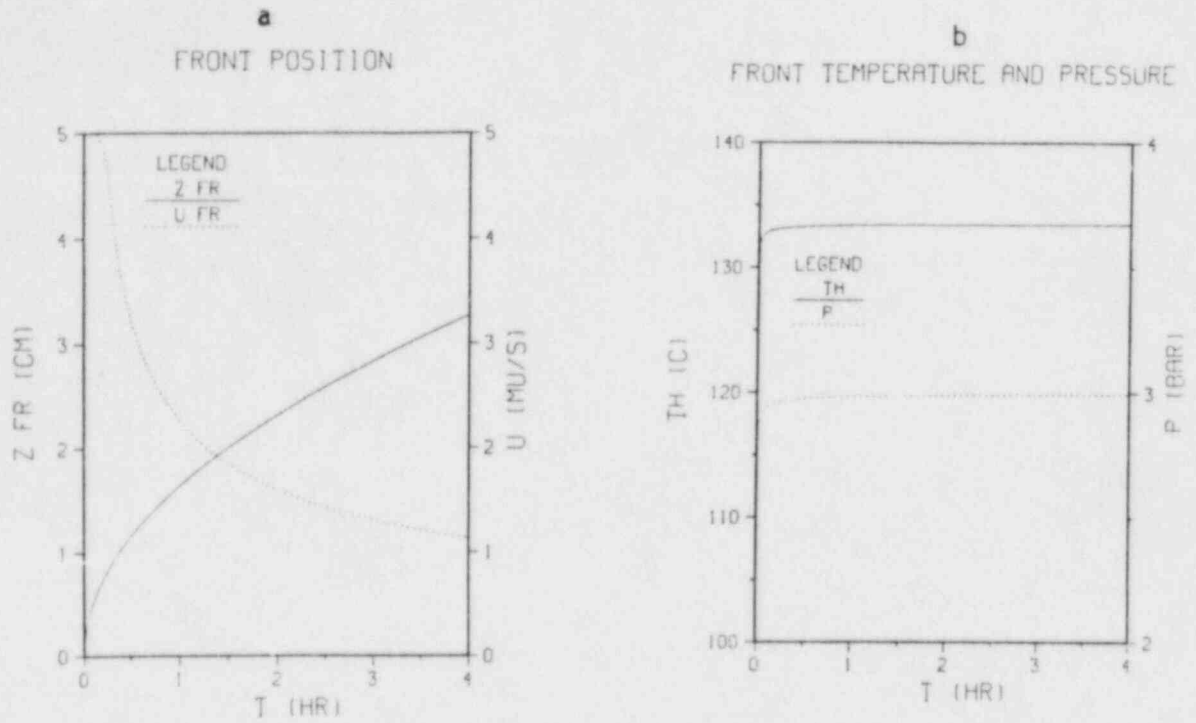

Figure 1.3.1 Front Position, Temperature and Pressure During Transient Heatup With Step Change in Surface Temperature.

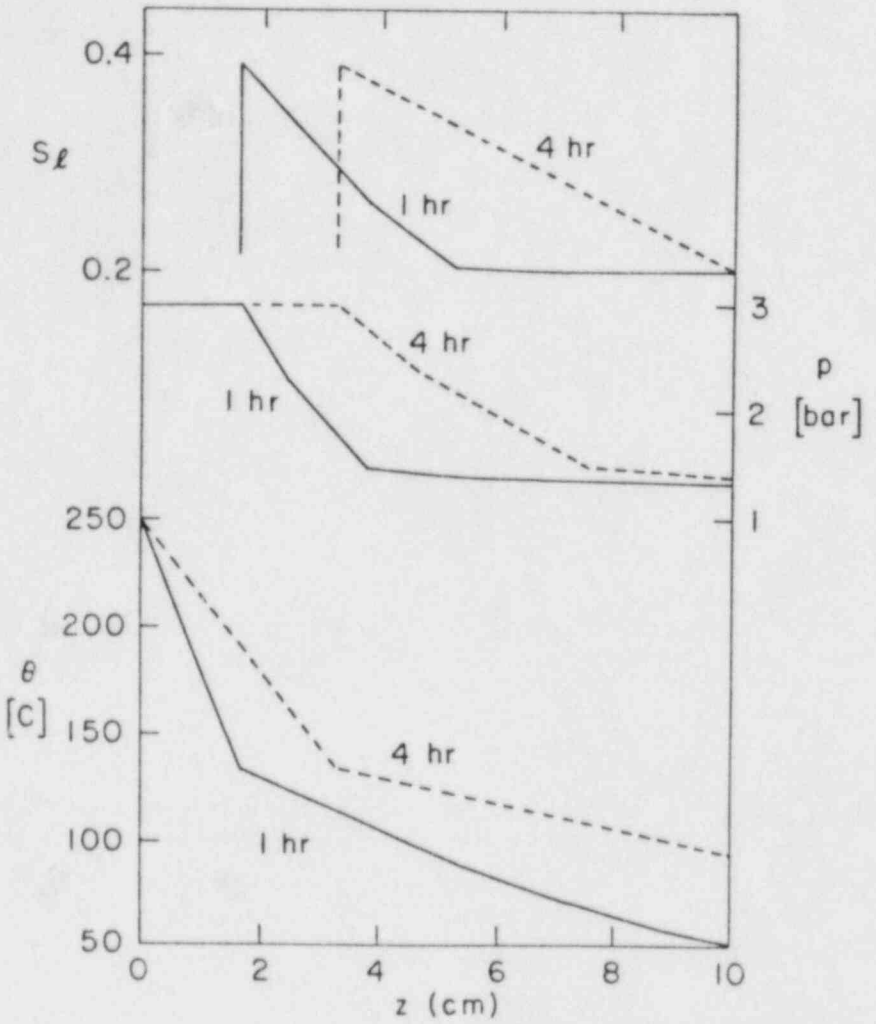

Figure 1.3.2 Temperature, Pressure, and Liquid Fraction Spatial Distribution During Transient Heatup with Step Change in Surface Temperature.

Results for the initial PCRV heatup prior to liner failure are shown in Figure 1.3.3. The core side thermal barrier temperature which is the source temperature in the current simulation is included in Frame (a). Two cases are are being considered: The best estimate permeabilities for concrete were used in the first case (BE PERM). In the other case, following a frequently suggested assumption that the liquid phase is immobile or moves at a much reduced rate (Min and Emmons, 1972, or Dayan and Gluecker, 1982) the liquid permeability was reduced by two orders (LL PERM). In this second case the evaporation front will be slowed down as all liquid must essentially be evaporated first to then move as vapor into colder regions of the concrete, while in the first case a significant part of the mass transfer into cooler regions is due to liquid flow.

Table 1.3.3

Properties and Input Data for Case of Simulated PCRV Heatup

Thermal Conductivities

kaowool	0.54 W/mK
concrete dry	2.8 W/mK
concrete wet	3.2 W/mK

Permeability

gas $\left(\frac{K}{\mu}\right)_g = 1 \times 10^{-5} \quad \frac{m^2}{bar\ s}$

liquid $\left(\frac{K}{\mu}\right)_\ell = \left(\frac{\mu_G}{\mu_\ell}\right)_{200°C} \times \left(\frac{K}{\mu}\right)_g = .05 \times \left(\frac{K}{\mu}\right)_g$

$(\rho c)_s = 1.92 \times 10^6 \ \frac{J}{m^3 K}$ (w/o voids)

$p_\infty = 1$ bar; $\theta_\infty = 20°C$

$\varepsilon = 0.35$; $S_{\ell\infty} = 0.4$

kaowool insulation thickness 67 mm

Frame (b) shows the front progression for both cases, indicating that the dry region forms at about 3 hrs, and is of substantial width in either case at the time of currently anticipated liner failure (about 60 to 80 hrs). At that time the dry region temperatures (Frame (a)) extend up to about 600°C which could result in further release of some of the chemically bound water with further pressure increases and flow towards the wet region. While this effect can be included in the VAPMIG code, it was not part of the current sample application, which only considered the physically bound water.

Frame (c) shows that for typical concrete permeabilities of Table 1.3.3 (BE PERM) the dry region pressures only build up to about 2 bars with a front temperature of about 120°C. (Similar to the above case of a step change in surface temperatures, Figure 1.3.2, with an impermeable outer surfaces the pressure remains virtually constant across the dry region). As shown in Frame (d), in the wet region adjacent to the front the pore volume is practically completely filled with liquid.

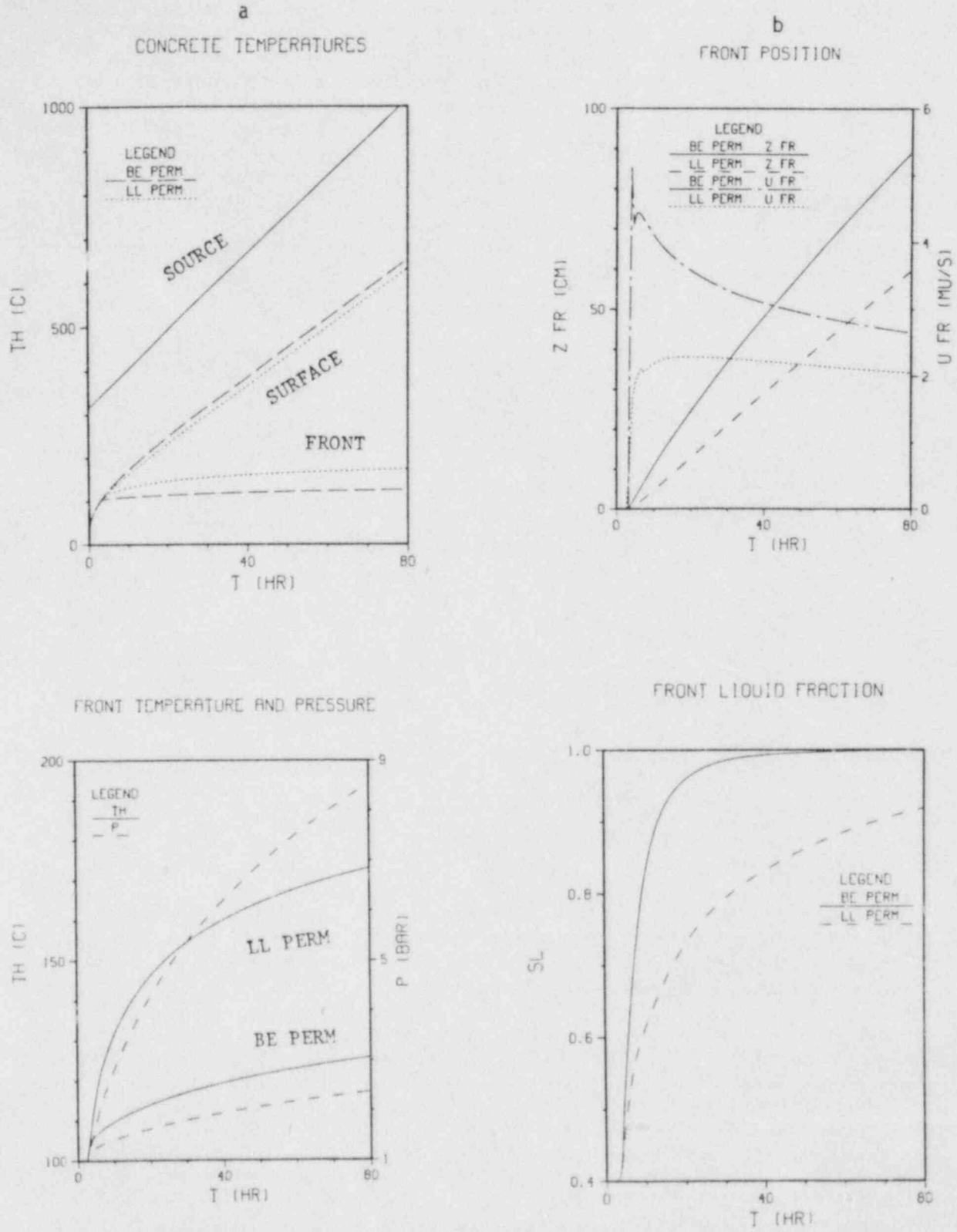

Figure 1.3.3 Simulated PCRV Heatup Prior to Liner Failure for Cases of Best-Estimate Concrete Permeabilities (BE PERM) and for Case of Reduced Liquid (LL PERM).

In the extreme case of reduced liquid mobility (LL PERM) the dry region pressures become quite significant and exceed 8 bars at 80 hrs. If these permeabilities should be representative of actual PCRV heatup conditions, it may cause earlier liner failure. The liner anchoring to the PCRV is generally designed for fluid pressures on the PCRV side of about 6 bars, to accommodate potential leaks of the LCS which operates at that pressure. However, the design pressure corresponds to LCS temperature levels of 30 to 50°C. Whether the liner and its anchors can accommodate these back pressures at 300 to 600°C is questionable. It, therefore, appears that earlier thermal barrier failure could possibly be initiated by liner failure due to excessive back pressure at 40 to 60 hrs, rather than by failure of the coverplate anchors due to excessive core side surface temperatures, which is the currently assumed failure mechanism. Further, more detailed investigations of PCRV concrete permeabilities, and a sensitivity study on the input data of this analysis would be required to confirm or reject this potential earlier failure mechanism.

Currently liner failure during UCHA scenarios without LCS is generally anticipated to occur not too long after thermal barrier (coverplate) failure, at about 60 to 80 hrs, both failures being due to excessive temperatures. Of crucial effect on the further accident progression is the water ingress from the PCRV moisture into the core cavity subsequent to liner failure. The simulations of Figure 1.3.3 were therefore extended, assuming liner failure and a corresponding flow boundary condition at $z = 0$ subsequent to failure. Some of the results are shown in Figure 1.3.4. There was virtually no change in the evaporation front velocity at failure time and the front progression into cooler regions continued undisturbed. In the case of best estimate permeabilities (BE PERM) front temperatures and pressures did not change visibly and continued there very slight upward trend. However, for the case of reduced liquid mobility (LL PERM) the liner failure essentially terminated the upward trend of front temperature and pressure, which dropped slightly at failure time and then remained roughly constant. The resulting mass flows of vapor into the core cavity are shown in Frame (b). For the best estimate case the actual ingress settles out at a value of about 0.035 kg/m^2hr while for the case of reduced liquid mobility it remains about an order higher at 0.5 kg/m^2 hr. It should be noted that the PCRV heatup rates used here correspond to the severest area, the center of the core side barrel. Thus either of these values is significantly lower than previously assumed values of about constant ingress of 1 kg/m^2hr averaged over the total core cavity surface (Reilly et al, 1984 and General Atomic Co., 1978). Such reduced water ingress could significantly extend the estimates for CB failure time beyond the current estimate of 10 days.

In the case of reduced liquid mobility significant dry region pressures were developed, and earlier liner failures from overpressure in the PCRV are not impossible. Therefore, earlier liner failure at 40 hr was considered as an additional case. The resulting water ingress for that case is included in Frame (b) of Figure 1.3.4. It is quantitatively about equal to the outflow at later liner failure, except that this flow now arises 40 hr earlier. But again, the water ingress rates remain much lower than previously estimated, and our current CB failure estimates appear to be even more conservative than

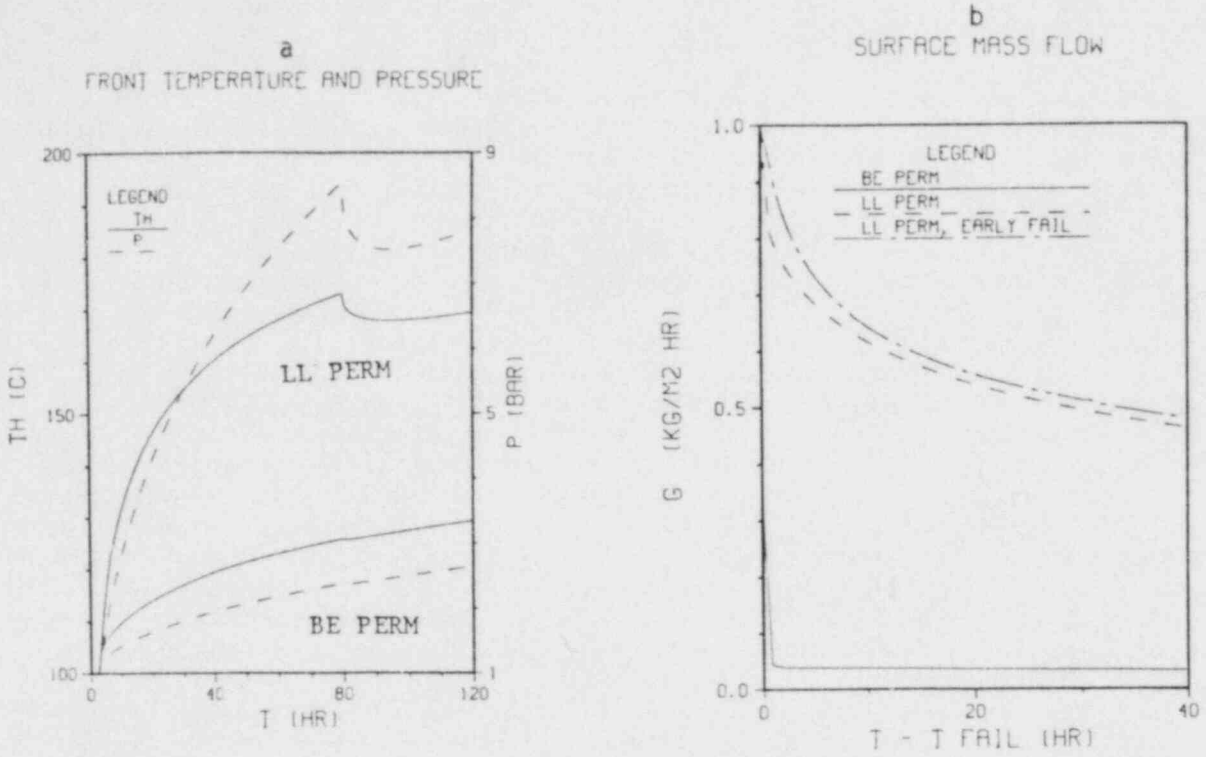

Figure 1.3.4 Simulated PCRV Heatup With Liner Failure for Case of Best-Estimate Concrete Permeabilities (BE PERM) and for Case of Reduced Liquid Mobility (LL PERM).

previously realized. The formation of a dry region and removal of most of the moisture beyond the evaporation front protects the core cavity from most of the original water in the concrete. As this front is driven by the heatup of the concrete, a reversal would only be possible with concrete cooldown, which cannot occur in this accident scenario.

It should further be noted, that our use of a one-dimensional cartesian geometry is conservative with regard to the actual PCRV heatup: At the core side barrel the radial divergence will provide more flow area and volume for the escaping water, resulting in a larger dry region and a lower pressure. The fact that the thermal barrier temperatures vary in axial direction, while we have used the highest temperatures which occur only at the center elevation further adds to this conservatism.

In the preceding simulations we assumed two different cases of concrete permeability and obtained significantly different results. The case of reduced liquid permeability can be considered as an upper limit for potential water ingress. Whether actual PCRV behavior would be closer to this limit or closer to the best estimate case would have to be determined by experimental efforts, since current available permeability data are not sufficiently detailed to provide sufficient inputs to the model. As special efforts are made to obtain high thermal conductivities in PCRV concretes (Fort St. Vrain, Appendix E) and since this requires dense structures, it could be that actual PCRV behavior might tend towards the case of reduced liquid mobility.

The exponential increase of concrete permeability with temperature, and the hysteresis effect (McCormack et al, 1979) will be included in future simulations. However, as we do not incur any cooldown over the time span of interest, the hysteresis effect should not affect our evaluations. The strong increase of permeability with temperature is only expected to effect the outer parts of the dry region which contain very little vapor. Thus, it is not expected that these future simulations will significantly alter our current conclusions.

CONCLUSION

A generalized model of vapor migration in porous concrete being heated at one side has been presented. A general application of the model agrees well with previous results, thus confirming some of the assumptions made in the previous work and establishing confidence in the new model.

Applying the model to PCRV heatup conditions it is found that significant pressures can possibly be generated in a large dry region close to the liner, potentially leading to earlier liner and thermal barrier failure. However, due to the significant thickness of the dry region of 40 to 80 cm, the previously used estimates of water ingress into the core after liner failure appear to have been excessive. With significantly reduced water ingress rates the estimated time of containment building failure could increase significantly beyond the current estimate of 10 days.

Further work is suggested, to obtain improved PCRV concrete permeability data and to consider such effects as the observed significant increase in concrete permeability with temperature as well as the increase in containment building pressure with time.

NOTATION

c	specific heat
E_i	internal energy of species i per unit volume of porous medium
e_i	internal energy of species i per unit mass of species i
h	enthalpy
k	thermal conductivity (D=dry region; W=wet region)
K	permeability
m_i	mass of species i per unit volume of porous medium
p	pressure
S_i	fraction of pore volume occupied by phase i (i=gas, or liquid) ($S_i=\alpha_i/\varepsilon$)
t	time
u_i	volumetric flow per unit area of species i (superficial velocity)
U_{fr}	evaporation front velocity
z	axial coordinate
z_{fr}	evaporation front position
α_i	volume fraction (for i = solid, liquid, gas)
ε	concrete porosity
ζ	dimensionless space coordinate (eqn's 16 and 18).
θ	temperature
θ_{ref}	reference temperature for zero internal energy (0°C used here).
κ	thermal diffusivity
ρ_i	density of species i

Subscripts

a	air		
D	dry	T	total
fr	at evaporation front	v	vapor
g	gas	W	wet
ℓ	liquid	w	water
S	solid	∞	initial uniform value

REFERENCES

DAYAN, A. and GLUEKLER, E. L., Heat and Mass Transfer Within an Intensely Heated Concrete Slab, Int. J. Heat Mass Transfer, 25, pp. 1461 (1982).

Final Safety Analysis Report, Fort St. Vrain HTGR, Appendix E.

"HTGR Accident Initiation and Progression Analysis Status Report - Phase II Risk Assessment," Report No. GA-A15000, General Atomic Company, April 1978.

KENNEDY C.R., Oak Ridge National Laboratory, private conversation, 1984.

KROEGER, P. G., COLMAN, J., and ARAJ, K., "Thermohydraulics in a High Temperature Gas Cooled Reactor Prestressed Concrete Reactor Vessel During Unrestricted Core Heatup Accidents," First Proceedings of Nuclear Thermal Hydraulics, ANS, p. 123, 1983.

LEE, B. S., HEISER, J. H, III, and WALES, D. R., Quarterly Progress Report, Brookhaven National Laboratory, Jan - April 1984.

McCORMACK, J.D., POSTAM, A. K., SCHUR, J. A., "Water Evolution from Heated Concrete," Hanford Engineering Development Laboratory, HEDL-TME-78-87, February 1979.

MIN, K., and EMMONS, H. W., "The Drying of Porous Media," Proc. of 1972 Heat Transfer and Fluid Mechanics Institute, Stamford University, 1972.

REILLY, H. J. et al, "Preliminary Evaluation of HTGR Severe Accident Source Terms," Appendix F, EGG-REP-6565, EG&G Idaho, April 1984.

SHIINA, Y., and KROEGER, P. G., "Transient Moisture Migration and Phase Change Front Propagation in Porous Media," ASME-AICHE National Heat Transfer Conference, ASME Paper No. 84-HT-7, Buffalo, N.Y., August 1984. (also BNL-NUREG-34280, Brookhaven National Laboratory, December 1983.)

2. SSC Development, Validation and Application (J. G. Guppy)

The Super System Code (SSC) Development, Validation and Application Program deals with advanced thermohydraulic codes to simulate transients in liquid metal-cooled reactors (LMRs). During this reporting period, work continued on three codes in the SSC series. These codes are: (1) SSC-L for simulating short-term transients in loop-type LMRs; (2) SSC-P which is analogous to SSC-L except that it is applicable to pool-type designs and (3) SSC-S for long-term (shutdown) transients occurring in either loop- or pool-type LMRs. In addition to these code development and application efforts, validation of these codes is an ongoing task. Reference is made to the previous quarterly progress report (Guppy, 1984) for a summary of accomplishments prior to the start of the current period.

2.1 SSC-L Code (W. C. Horak)

2.1.1 Pipe Insulation Test (W. C. Horak, R. J. Kennett)

A long term transient is now being run to determine the effect of rock wool insulation on a complete loss-of-heat sink accident. In this transient, a reactor similar to FFTF was assumed to have a 0.152m (6") layer of rock wool insulation over the primary piping. At time t = 0, all heat transfer across the IHXs was stopped, followed by a reactor scram with pump trip at 0.6 (s). The reactor vessel is considered to be adiabatic. The only heat loss is through the piping to the reactor containment, which is assumed to be at 295.6K (72°F).

To model the effect of piping insulation losses, modifications were made to both the steady-state and transient models of SSC. In the steady-state, the piping temperature was calculated for each node, accounting for the loss through the insulation. This produces a temperature distribution in the pipe in contrast to the present uniform temperature that results from the assumption of an adiabatic pipe. In the transient, the effect of the piping insulation is accounted for as thermal resistance between the pipe and the environment. The heat capacity of the pipe insulation is not accounted for.

Results for the first 80 hours of simulation time have been plotted. Preliminary examination of the results show a low, but positive loop flow rate that varies between 1.0 to 5.0 kg/s (Fig. 2.1). This cycling of the flow is apparently caused by the collapse and later reformation of the ΔT across the IHX primary side (Fig. 2.2). The core average and outlet temperatures also decrease and increase due to the cyclic flow rate (Fig. 2.3). However at this time, they still exhibit a general upward trend, although the temperature remains more than 300°K below saturation. The power-to-flow ratio is less than one with both the normalized power and flow rates below 1% of their steady-state values (Fig. 2.4).

It is planned to follow this transient until the onset of sodium boiling or, if the coolant does not boil, an established downward trend in temperatures is established.

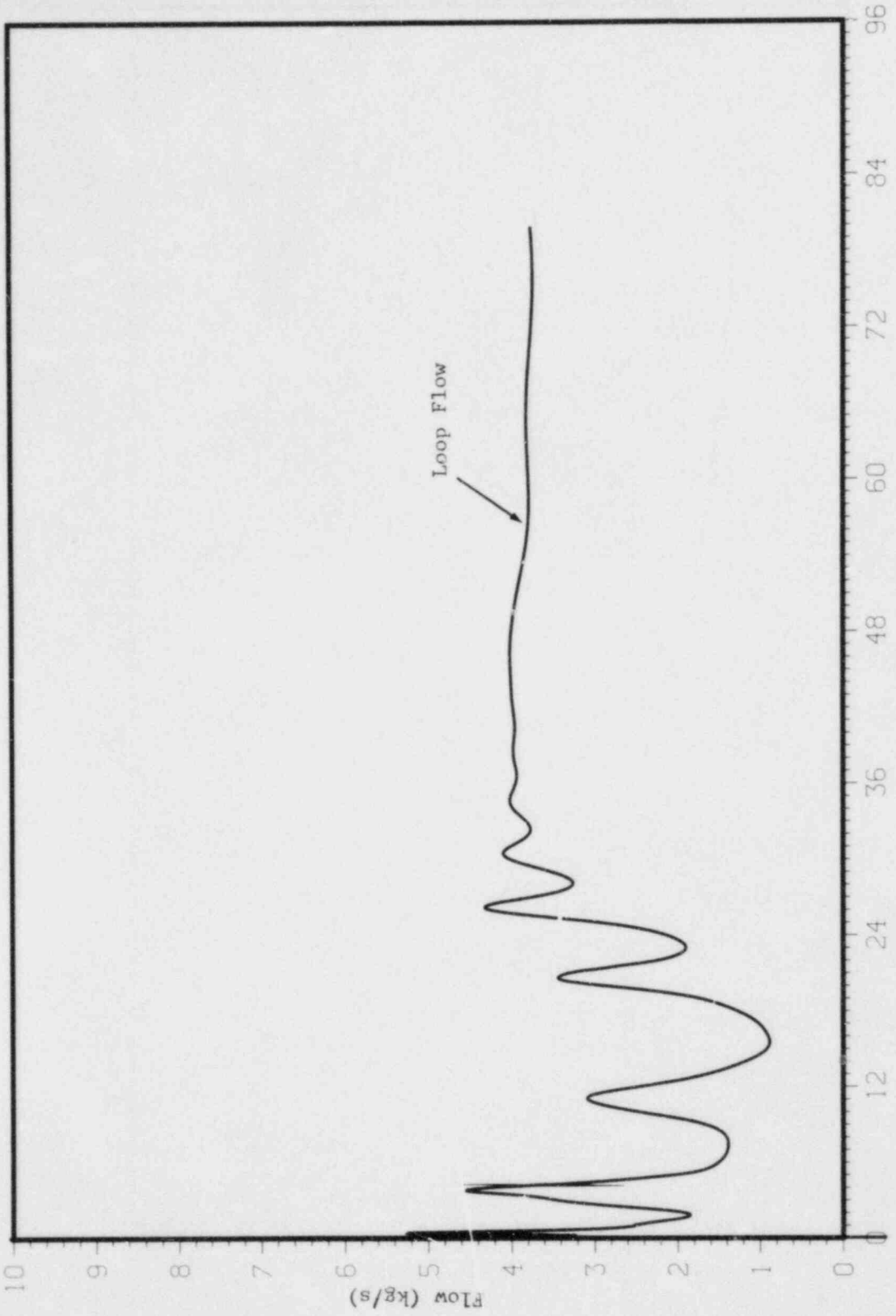

Fig. 2.1 Primary Loop Flow Rate

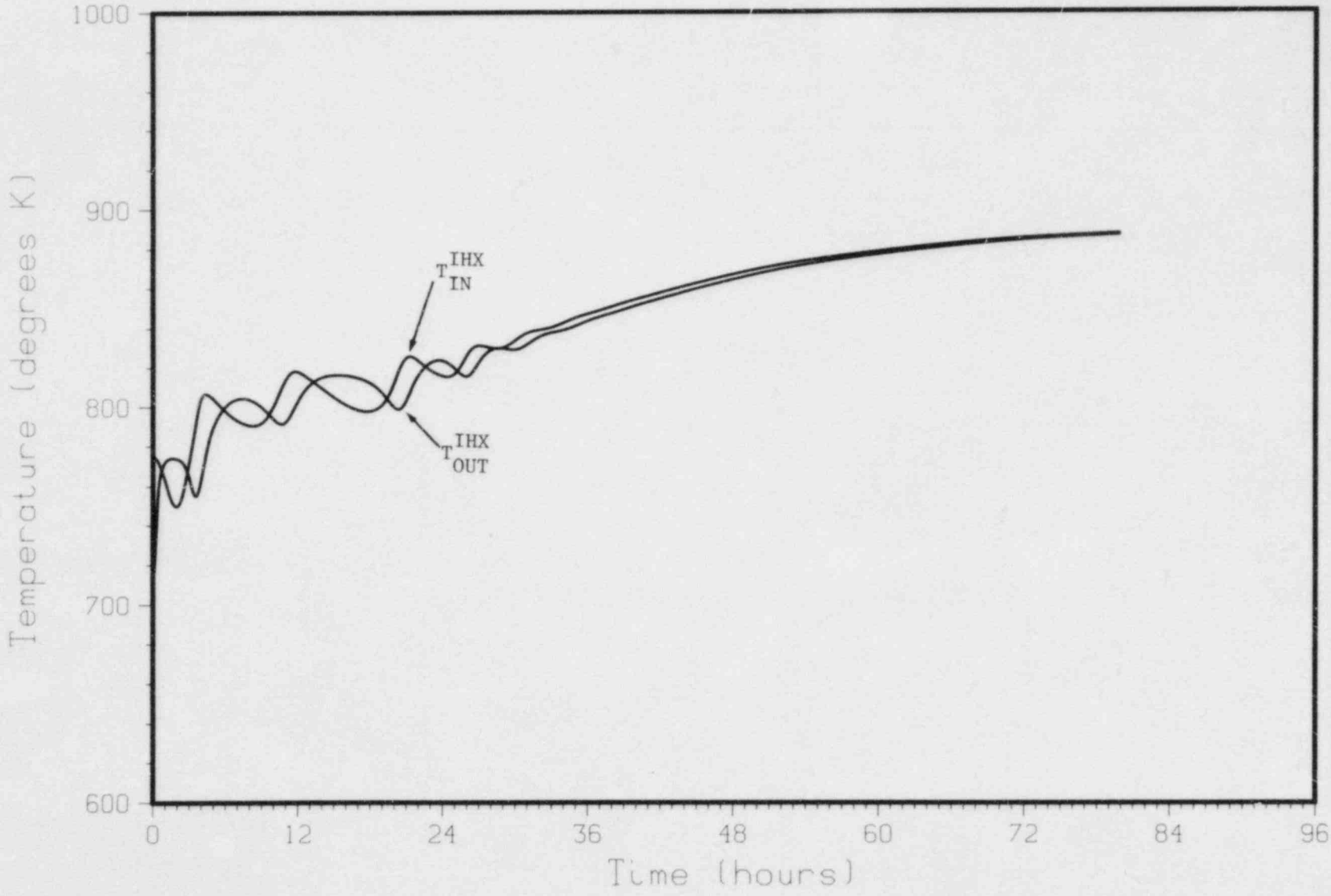

Fig. 2.2 Primary Side IHX Inlet and Outlet Temperatures

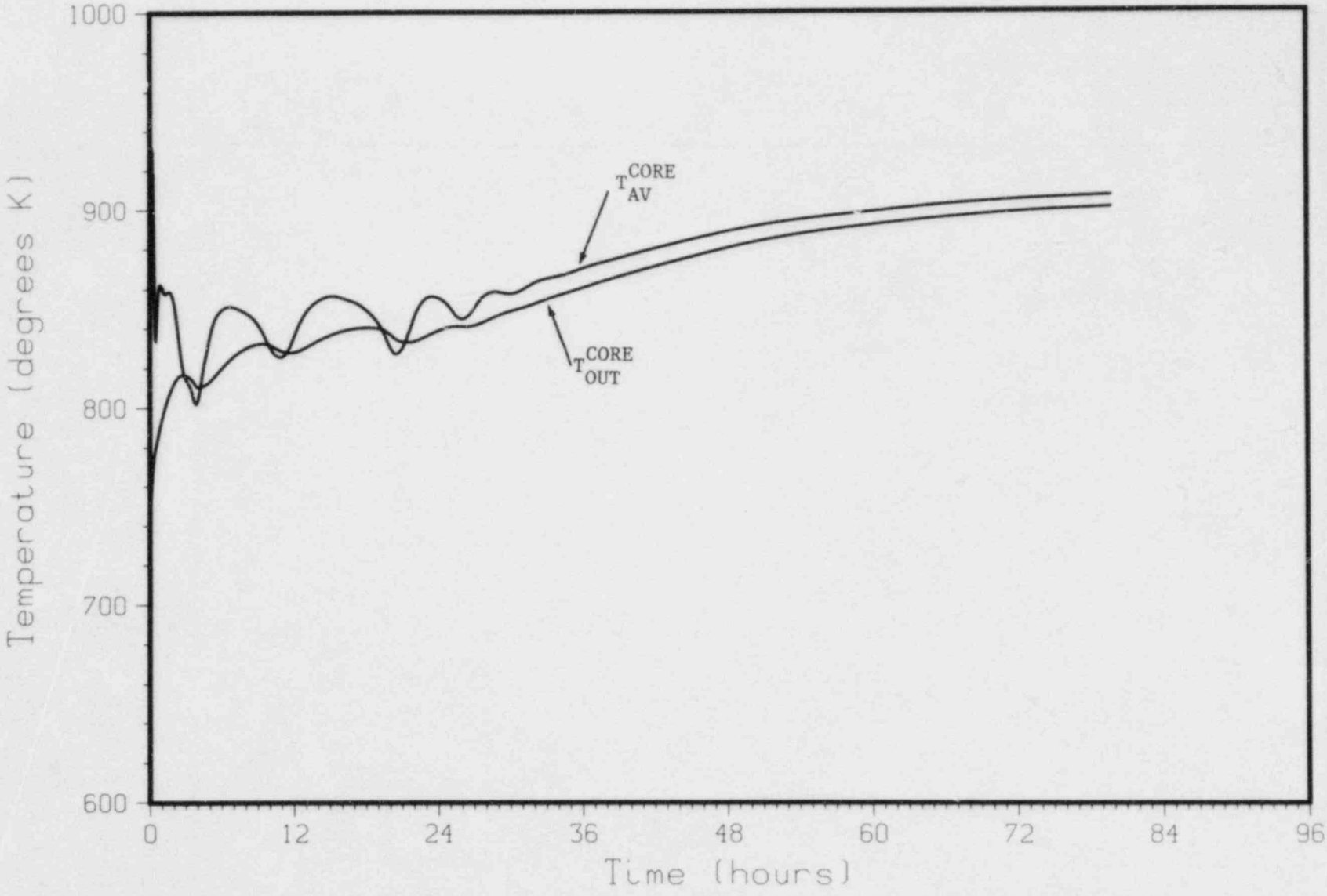

Fig. 2.3 Core Average and Outlet Temperatures

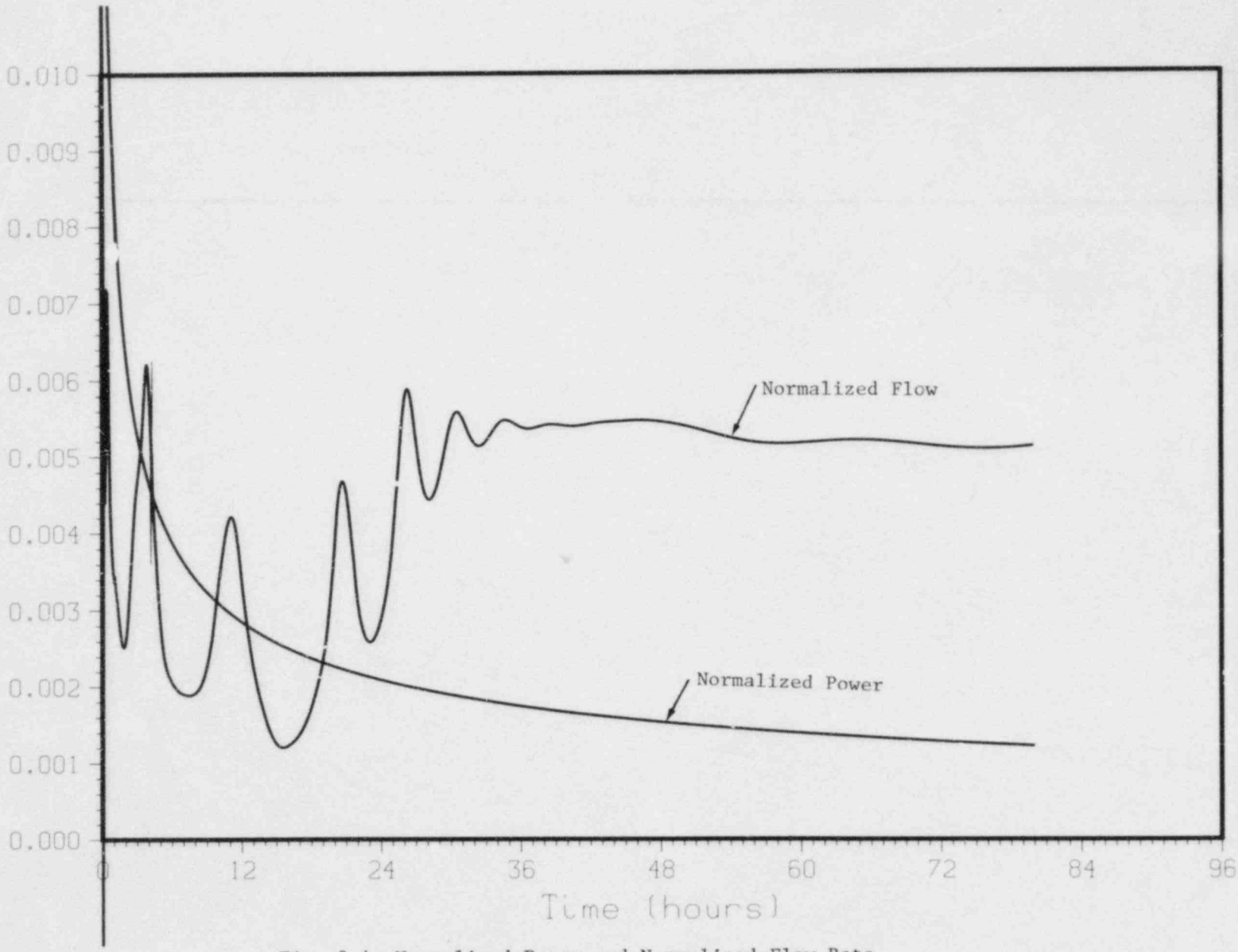

Fig. 2.4 Normalized Power and Normalized Flow Rate

2.1.2 Inter-Assembly Heat Transfer (W. C. Horak)

Preliminary nodalization studies using the previously developed intra-assembly heat transfer code have shown that the duct wall temperature is relatively insensitive to the degree of nodalization, even for sharply skewed power distributions. Nodalization studies on so-called "double-humped" distributions have not been done as yet.

Given these initial results, it has been decided to implement a full seven assembly cluster model, since the storage requirements should not be prohibitive. As a first step, a two-region duct wall temperature has been developed and is being coded. The degree of nodalization within the assembly has not yet been fixed, but initially an extremely coarse two-region model will be used.

Since the actual mechanisms of heat transfer between duct walls are modeled quite simply, most difficulties are expected to occur in the actual coding of the model. Given the systems nature of the SSC code, computational efficiency remains a priority.

Work is proceeding on the coding of this inter-assembly heat transfer model. In this first stage of the model development, the fluid temperature within the assemblies will be assumed to be known. The duct wall and interstitial sodium temperatures will be calculated on an axial level basis for steady-state conditions only. The model is for a seven-assembly cluster, with two duct wall temperatures per assembly. Initially, the temperature distribution within an assembly will be isothermal, but distributions obtained from the intra-assembly code will be used in the future. Although this testing will be done on a stand-alone basis, the coding will follow all SSC code standards and conventions in order to facilitate its subsequent incorporation into the main code.

Since the computational efficiency of the method will depend strongly on the bandwidth of the resulting matrices, consistent ordering schemes are being developed. Such a scheme will also reduce the overall storage requirements for the scheme, thus permitting the analysis of multiple, but independent, clusters.

A literature review is now under way to identify appropriate experiments for the validation of the method. Consideration is also being given to comparisons with core-analysis codes.

2.1.3 In-Vessel Review (W.C. Horak)

With the many changes that have occurred and the additional models that have been incorporated, a detailed review of the in-vessel energy calculations is being conducted. The purpose of this review is to streamline the present coding and provide for expansion of the upcoming intra- and inter-assembly heat transfer modules.

2.1.4 Interactive Computer Graphics (J. Brown)

An enhanced computer graphics output is now being developed. This extended capability is intended for use in an interactive version of SSC, but will initially be used to provide "snapshots" of the plant condition during various times of the transient. The FFTF plant will be the first design analyzed, with data provided from the long term simulations done earlier. The EBR-II plant will then be analyzed.

2.2 SSC-P Code (E. G. Cazzoli)

2.2.1 EBR-II Transient Analysis (J. G. Guppy)

To prepare for pre-test predictions of several of the upcoming test transients to be conducted at the EBR-II facility at INEL, SSC-P input decks and code modifications are being prepared. A base deck to simulate a null transient has been constructed and tested. Two further transients are being worked on: 1) a coastdown to natural circulation transient from full power, and 2) a reactor scram from full power, followed by pump trip being delayed out to 60 seconds. This latter transient will result in an almost isothermal temperature profile in the primary system. The purpose of this transient is to see if any flow stagnation/reversal occurs in the core under these conditions.

Using the recently updated EBR-II input deck, a plant trip and pump coastdown to natural circulation transient was conducted. The calculations were carried out to 180 seconds, by which time all in-vessel temperatures were exhibiting a downward trend. The changes made to the primary loop hydraulic calculations appear to be performing satisfactorily. The intermediate pump (which in the EBR-II plant is an EM pump, but which is currently being modeled in SSC as a centrifugal pump) is coasting down too slowly. An appropriate model extension to accommodate this is being investigated.

Attention is also being given to improving our comparisons to the Test 8A transient which was performed at the EBR-II facility in 1981. These test results will be used to "tune" the SSC simulation to the specific plant characteristics. Important here are loop and in-vessel pressure drops, initial pump speeds and loop temperatures, decay heat levels and primary and intermediate pump coastdown characteristics. Good progress is being made and this work is continuing.

2.2.2 Generic Pool Subroutine (W. C. Horak)

Work is continuing on the hydraulic modeling for a generic pool subroutine that can be incorporated directly into SSC. A review of various transient models is now being conducted to see which features are desirable for SSC.

2.2.3 Code Maintenance (E. G. Cazzoli)

The pool version of SSC is under review and is being modified in the latest cycle of the base program library, in order to take advantage of recent improvements in SSC-L. In order to ensure that the updated version of SSC-P incorporating the revisions is correct, previously simulated plant transients performed for Phenix will be repeated and comparisons made for consistency.

2.3 SSC-S Code (B. C. Chan)

2.3.1 Large Timesteps for Long Term Simulations (J. G. Guppy)

In order to determine and narrow down the potential problem areas attendant with the usage of large timesteps for slow, long-term transients, a previously developed and well-tested CRBR plant simulation was utilized as the test deck. A loss of electric power transient was assumed, and the simulation was carried out to 7,200 seconds (2 hours). At this point, the plant conditions are changing very slowly, although substantial ΔT's still exist across the core and heat exchangers.

The timesteps everywhere were then allowed to increase from their previously constrained maximum value of 1 second. Numerical difficulties were experienced only in the IHX. These are due to: 1) the explicit treatment utilized in the present version of SSC for the loop energy calculations, 2) the fact that the wall heat flux terms are lagged one timestep to enable a simple marching technique, which requires no iterations; and 3) the characteristic time constants, which are the smallest at the IHX.

As a test, the IHX temperatures were artificially prevented from changing. The result was that the remaining time constants are such that stable solutions were then obtained with timesteps up to 32 seconds. This encouraging situation has led us to give serious consideration to include an optional, implicit treatment of the IHX only, which could be automatically switched to during long-term simulations. We feel confident that total system timesteps of 30 seconds or perhaps larger could thus be achieved during these very long and slowly changing transients.

REFERENCE

GUPPY, J. G., et al., (1984), "SSC Development, Validation and Application," Safety Research Programs Sponsored by Office of Nuclear Regulatory Research Quarterly Progress Report, Jan. 1 - Mar. 31, 1984, Brookhaven National Laboratory Report to be published.

PUBLICATIONS

CHAN, B. C., "A Buoyancy-Dominated Model for LMFBR Upper Plenum Flows," Brookhaven National Laboratory Report to be published, 1984.

CHAN, B. C., KENNETT, R. J., GUPPY, J. G., "A Numerical Investigation of Buoyancy-Induced Flow Stratification in the LMFBR Upper Plenum," Brookhaven National Laboratory Report to be published, 1984.

GUPPY, J. G., et al., "Implementation of SNR-300 Controller Models Into SSC/MINET," Brookhaven National Laboratory Report to be published.

HORAK, W. C., KENNETT, R. J., GUPPY, J. G., "Long Term Post Test Simulation of the FFTF Natural Circulation Tests Using SSC," Trans. ANS, V. 46, p. 798, (1984).

MADNI, I. K., "Modeling Considerations for the Primary System of the Experimental Breeder Reactor - II, Brookhaven National Laboratory Report, NUREG/CR-3878, BNL-NUREG-51797, June 1984.

3. Generic Balance of Plant Modeling (J. G. Guppy)

The Generic Balance of Plant (BOP) Modeling Program deals with the development of safety analysis tools for system simulation of nuclear power plants. It provides for the development and validation of models to represent and link together BOP components (e.g., steam generator components, feedwater heaters, turbine/generator, condensers) that are generic to all types of nuclear power plants. This system transient analysis package is designated MINET to reflect the generality of the models and methods, which are based on a momentum integral network method. The code is to be fast-running and capable of operating as a self-standing code or to be easily interfaced to other system codes. Reference is made to the previous quarterly progress report (Guppy, 1984) for a summary of accomplishments prior to the start of the current period.

3.1 Balance of Plant Models (G. J. Van Tuyle)

Models for MINET Version 1 have been completed, incorporated in the code, and tested. Current model development is for Version 2 of MINET.

Models for pumps and turbines are currently available in MINET. In order to interface these modules so that a turbine-driven pump can be represented, a mechanical interface module called "rotor" is being introduced. A mechanical boundary module through which a torque or speed boundary condition can be specified is also being introduced. The modifications to the computational part of MINET have been developed and await testing. Modifications to the input processor, to process what amounts to a mechanical "network", are in the development stage.

A package of 24 control modules has been designed, and details regarding input and interfacing are being worked out. The goal here is to allow the user to input a control system using one or more control networks, built up from the basic MINET control modules. Among the more intricate modules are those for switches, summing points, take-off points, comparers, stores (for feedback), and the input and output modules, which interface with the MINET thermal-hydraulic networks. Several of these generic controller modules were adapted from the SNR-300 control system modeling effort.

An enhancement of the MINET volume module, to allow the user to specify a height-dependent cross-sectional area, is being planned.

3.2 MINET Code Improvements (G. J. Van Tuyle, T. C. Nepsee, E. G. Cazzoli)

At this stage, any alterations to the existing version of MINET, i.e., Version 1, are relatively minor and either a correction of some error revealed through testing or a straightforward extension of capabilities. On the other hand, far more extensive changes are planned for Version 2, in order to model turbine-pump interfaces and control systems. The modification sets for Version 2 will be kept in code update form until all planned changes have been developed and tested.

Several relatively minor adjustments and improvements are being made in preparation for exporting Version 1 of MINET. A plotfile option is being incorporated in order to output values for plotting. Since plot-support computer software tends to vary between systems, the program that reads data from the planned MINET plotfile and generates the time (t) vs. f(t) plots may not be generally exportable. Therefore, an effort is underway to purge the MINET program library of system dependent routines which were used in the testing process. Finally, further input verification is being incorporated to recognize unacceptable input values as they are being processed.

A new network processing algorithm has been developed to replace the BACKTRACK algorithm used in the input processor. This algorithm, called MOUSE, because of the way it "explores" the network, correctly processes certain classes of network which BACKTRACK cannot handle. As an additional benefit, code complexity and storage requirements are both reduced with the MOUSE algorithm.

Data storage areas used by the NODE Data Management Utility have been moved from CDC Small Core Memory to Large Core Memory in order to accommodate larger data sets, while still allowing the full set of Data Management Utilities to be globally available within the code. This was accomplished by introducing LEVEL 2 declarations in the FORTRAN source code. Because these declarations do not conform to ANSI standard FORTRAN, they have been bracketed by directives, allowing them to be suppressed in non-CDC versions of the code.

An updated version of MINET (Version 1.8) has been constructed.

Some initial work has been done to enhance the input processor to handle multiple network types (mechanical, electrical, and control) in addition to the flow networks which it now processes. Specific modifications are being made to accommodate ROTOR modules as part of a generalized rotational mechanical network. TURBINE and PUMP modules are also being extended to include rotational port connections for the mechanical network.

A successful RAMONA/MINET composite code has been constructed, using RAMONA as host driver. A steady-state calculation was performed by the composite, using a simplified MINET input deck representing a single pipe. Transient calculations are currently undergoing testing.

3.3 MINET Standard Input Decks (G. J. Van Tuyle, J. Guillen)

For MINET, Version 0, a standard input deck for EBR-II (E1) is being maintained, and a deck for the SNR-300 (S3) is kept readily available. Standard input decks for EBR-II (E1) and an example BOP deck (X2) are used to retest new cycles of MINET, Version 1.

Current development work is focused on the RAMONA/MINET interface, in support of the Severe Accident Sequence Analysis (SASA) program. A simple 1-node pipe deck is currently being used in testing the transient interface, so as to minimize any confusion in error investigation. MINET Standard Deck

BF1, which represents the latter part of the Browns Ferry feedwater train (with several approximations for unknown parameters), will be used in testing the combined RAMONA/MINET representation against startup test data from Browns Ferry. A more extensive deck, to be designated BF2, is under development, and will include representations for the High Pressure Coolant Injection System (HPCIS) and the Reactor Core Isolation Cooling System (RCICS). Some information has also been obtained for the Browns Ferry Residual Heat Removal System (RHRS), the Core Spray (CS), the Suppression Pool, and the plant control system, and may be incorporated in future decks (See Figures 3.1 - 3.3).

3.4 MINET Validations and Applications (G. J. Van Tuyle, E. G. Cazzoli, J. Guillen, T. C. Nepsee)

The current effort is focused on the RAMONA/MINET interface, and the BWR simulation capabilities that will result. The two codes were segmented so that both could be fit in CDC 7600 small core memory at the same time. Interfaces for the steady-state and transient segments were developed. A null transient case was accomplished, which used the RAMONA 3B 1/8 core Browns Ferry geometry and a very simplified MINET one-node pipe geometry representing the feedwater line.

3.5 User Support (G. J. Van Tuyle, J. G. Guppy)

Code documentation for Version 1 of MINET is now available, and several copies have been distributed, along with copies of some of our recent validation study reports. We have not yet released the code to external users, but will be prepared to do so late this summer.

A MINET computer code workshop has been scheduled for August 23 and 24, in order to establish and support an initial group of external users. Invitees include representatives from reactor vendors, utilities, universities, NRC, DOE, EPRI, national laboratories, and consulting firms. Topics of the workshop include balance of plant modeling; MINET code development, validation, and applications; interfacing MINET with other computer codes; and sample applications and test problems.

Two types of external applications are of particular interest to us, (1) those that provide some degree of code validation and (2) those in which MINET is to be interfaced with other computer codes. In each case, MINET would be further tested and improved in support of our primary goals of improved power plant modeling.

REFERENCES

GUPPY, J. G., et al., (1984), "Generic Balance of Plant Modeling,", Safety Research Programs Sponsored by Office of Nuclear Regulatory Research Quarterly Progress Report, Jan. 1 - Mar. 31, 1984, Brookhaven National Laboratory Report to be published.

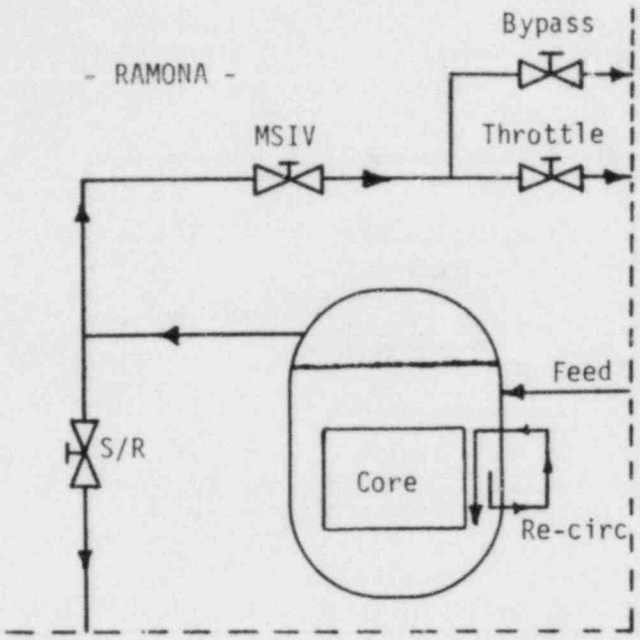

Fig. 3.1 RAMONA Representation of BWR System

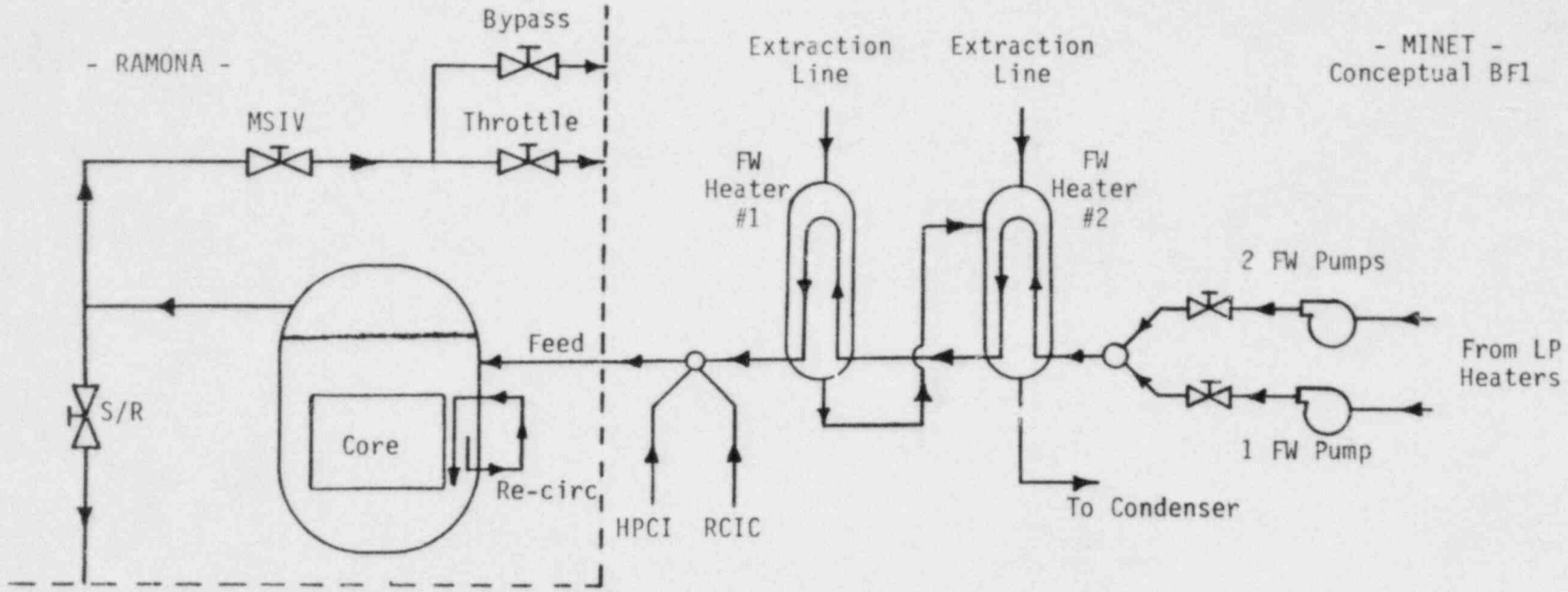

Fig. 3.2 Conceptual Drawing of RAMONA/MINET BWR Representation Using MINET Deck BF1

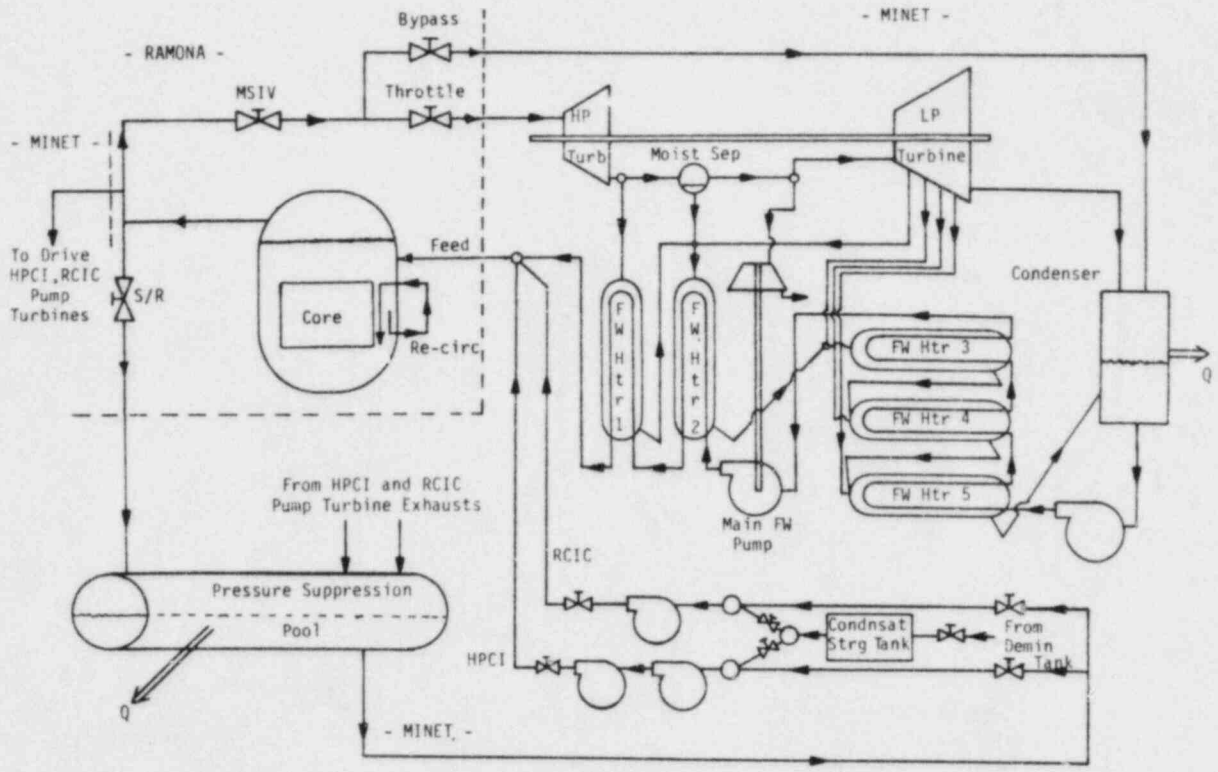

Fig. 3.3 RAMONA/MINET Representation of BWR System Currently in Planning Stage

PUBLICATIONS

VAN TUYLE, G. J., NEPSEE, T. C., GUPPY, J. G., "MINET Code Documentation, "Brookhaven National Laboratory, NUREG/CR-3668, BNL-NUREG-51742, February 1984.

VAN TUYLE, G. J., "Simulation of a Helical Coil Sodium/Water Steam Generator, Including Structural Effects," Brookhaven National Laboratory, NUREG/CR-3765, BNL-NUREG-51766, April 1984.

VAN TUYLE, G. J., "MINET Validation Study Using EBR-II Transient Data," Second Proceedings of Nuclear Thermal Hydraulics, 1984 ANS Annual Meeting, New Orleans, June 1984.

VAN TUYLE, G. J., et al., "Analysis of Postulated BWR ATWS for the Brown's Ferry Plant Using RAMONA/MINET," Brookhaven National Laboratory Report to be published.

VAN TUYLE, G. J., "MINET Validation Study Using Steam Generator Transient Data," Brookhaven National Laboratory , NUREG/CR-3813, BNL-NUREG-51775, May 1984.

4. Thermal-Hydraulic Reactor Safety Experiments

4.1 Core Debris Thermal-Hydraulic Phenomenology: Ex-Vessel Debris Quenching (T. Ginsberg, J. Klein, J. Klages, and C. E. Schwarz)

This task is directed towards development and experimental evaluation of analytical models for prediction of the rate of steam generation during quenching of core debris under postulated LWR core meltdown accident conditions. This program is designed to support development of LWR containment analysis computer codes.

4.1.1 Experimental Observations Relevant to the Potential for Steam Superheating During Debris Bed Quenching

BNL debris bed quenching experiments suggest that a superheated debris bed which is cooled by liquid supplied from an overlying pool of water is cooled in a two-stage quench front propagation process, represented schematically in Figure 4.1 (Ginsberg, 1983). Coolant is postulated to initially penetrate the bed, leaving dry regions of particles. If the bed were internally heated then the particles would continue to heat. Upon arrival of the downward front to the base of the bed, a final upward-directed front propagates up the bed, removing the remaining stored energy.

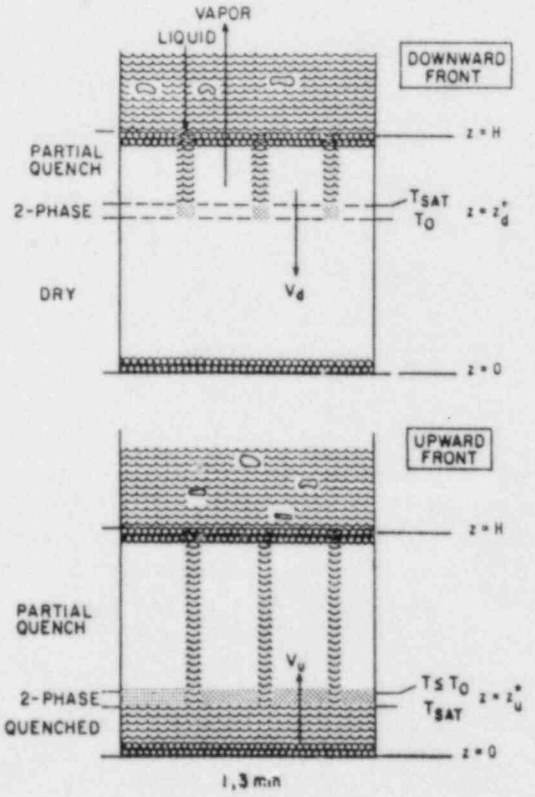

Figure 4.1. Schematic of Superheated Packed Bed Quench Process.

The data indicate that in the unquenched regions of the bed the particles may remain at their initial temperature for extended periods of time. During the extended dry periods, the dry channels are postulated to serve as flow channels through which steam, produced at the quench front, flows upwards along a path which leads to the overlying pool of water. Since the steam is generated at the water saturation temperature and the particles would be at some elevated temperature, perhaps close to their initial temperature, the potential exists for heat transfer between the steam and the particles. Steam-particle heat transfer calculations were performed using single-phase particle bed heat transfer data (Kuni and Levenspiel, 1969). These calculations indicate that, for particles in the millimeter diameter range, the steam would heat to nearly the particle temperature as it flows a distance of only millimeters or a few centimeters. These calculations strongly suggest that steam produced within a particle bed which is being quenched has a strong potential for being superheated as a result of heat transfer from the unquenched particulate in the dry channels or pockets of the bed.

4.1.2 Analysis: Influence of Steam Superheat on Debris Bed Heat Removal Rate

If the steam is indeed superheated as it leaves the particle bed, then the countercurrent flow mechanism which controls the global cooling rate of the bed, and the quench propagation rate, could be affected by the elevated temperature of the steam. Calculations were performed to study the effects of steam superheating on the bed heat removal processes. It is assumed that the Lipinski countercurrent hydrodynamics model (Lipinski, 1984) characterizes the debris bed heat removal rate during the bed quench process.

Consider the debris bed shown in Figure 4.1. The heat flux at the quench front is given by

$$\ddot{q}_{QF} = (\rho_g j_g)_{QF} h_{fg} \tag{4.1}$$

where ρ_g is the steam density, h_{fg} is the heat of vaporization, both evaluated at the water saturation temperature, and j_g is the steam superficial velocity at the quench front. At the top of the bed it is assumed that the steam exits at temperature T_g. The heat flux at the top of the bed is, therefore,

$$\ddot{q}_{TB} = (\rho_g j_g)_{TB} h_{fg} \left[1 + \frac{C_g (T_g - T_{SAT})}{h_{fg}} \right] \tag{4.2}$$

where T_{SAT} is the saturation temperature and C_g is the steam specific heat. The quantities ρ_g and j_g are evaluated at the top of the bed. The mass fluxes at the quench front and at the top of the bed are equal and, therefore,

$$(\rho_g j_g)_{QF} = (\rho_g j_g)_{TB} \cdot \tag{4.3}$$

In terms of the mass flux at the top of the bed, the heat fluxes at the quench front and at the top of the bed are

$$q''_{QF} = (\rho_g j_g)_{TB} h_{fg} \tag{4.4}$$

$$q''_{TB} = (\rho_g j_g)_{TB} h_{fg} \left[1 + \frac{C_g (T_g - T_{SAT})}{h_{fg}} \right] . \tag{4.5}$$

Both ρ_g and j_g are evaluated at the temperature of the steam leaving the bed, T_g.

The two-phase countercurrent flow conditions at the top of the bed are assumed to limit the bed heat removal rate, since this is the location of maximum volumetric flux of both liquid and vapor. The Lipinski model was used to compute the volume flux of vapor, j_g, leaving the bed, where it was assumed that all steam properties are evaluated at the specified steam temperature. The calculations indicate that j_g is a relatively weak function of steam temperature. The heat flux, therefore, is influenced most strongly by (i) the effect of temperature on the steam density and (ii) the superheating of the steam, as shown in Eqs. (4.4) and (4.5). The heat removal rate at the quench front, which influences the speed of quench front propagation, decreases monotonically with steam temperature, while the overall bed heat flux varies with temperature in a somewhat more complex manner.

4.1.3 Calculation Results

The calculation results are presented in Fig. 4.2. The heat flux is presented for particle beds of height H=1 m, porosity ε=0.4. The beds are assumed to be composed of spherical particles of uniform diameter. Results are presented for particle diameters 1, 3, and 12 mm.

Figure 4.2 indicates that, based on the above assumptions, the quench front heat flux (dashed curves) is, as discussed above, a strong function of steam superheating. The effect of steam superheating would be to reduce the rate of advance of the quench front during the bed quench process. The qualitative behavior of the overall bed heat flux with steam superheat is seen to depend on particle size. For the small particle diameters, the heat flux first decreases, then increases, with steam temperature. For the 12-mm particles the bed heat flux is seen to increase with steam temperature. This difference in behavior is attributable to the effect of temperature (although relatively small) on the computed superficial steam velocity j_g.

The predicted effect of steam superheat on the bed heat removal and quench processes is seen to be appreciable, especially for large superheats. The BNL bed quench data are now being examined to determine whether the predicted effect is observable.

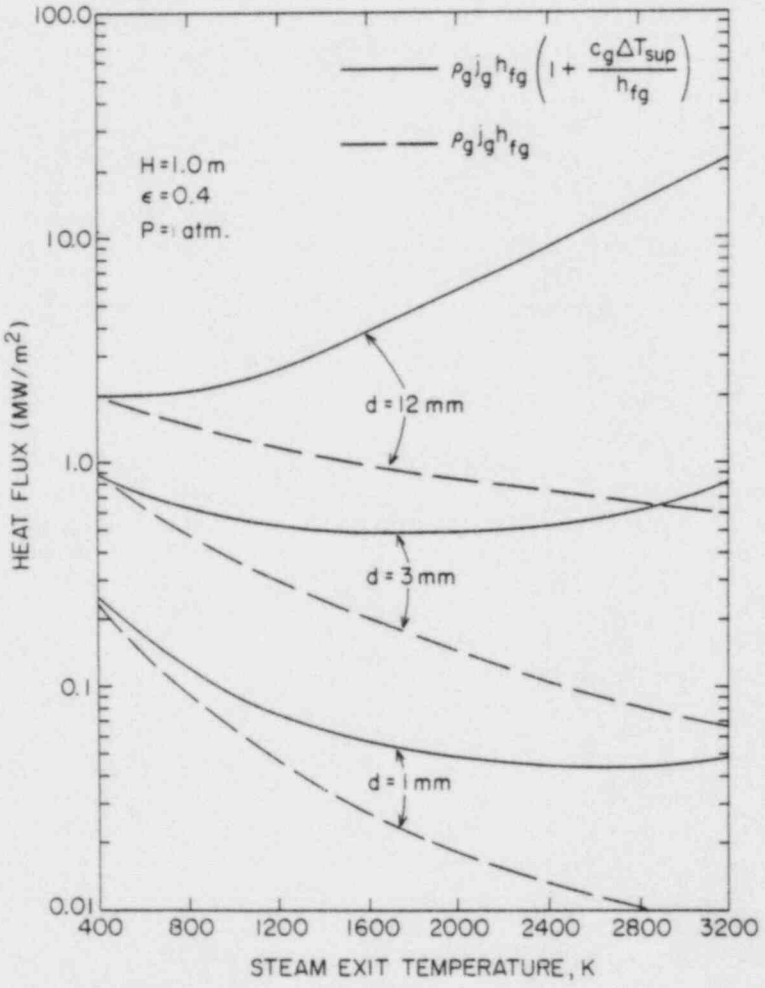

Figure 4.2 The Effect of Steam Temperature on Bed Quench Heat Flux.

4.2 Core Debris Thermal-Hydraulic Phenomenology: In-Vessel Debris Quenching

(N.K. Tutu, T. Ginsberg, J. Klein, J. Klages, and C.E. Schwarz)

The purpose of this task is to develop an understanding of the transient quenching of in-vessel debris beds (formed in the reactor core region) when the coolant is injected from below. The experimental results would, in addition, generate a data base for verifying the transient thermal-hydraulic models for the quenching process. The present experimental and model development effort is directed towards the case where the coolant is being injected at a constant rate.

4.2.1 Model Development

The simplified transient debris bed quenching model developed earlier (Tutu et al., 1984) assumes the absolute velocity of a liquid element within the debris bed to be a constant. Thus the quench behavior could be predicted without using the fluid momentum equations explicitly, and hence without the necessity of modeling the solid-fluid interfacial drag terms. The model served very well in illuminating the mechanics of the quench behavior. To make the model quantitatively more realistic, the transient model has been extended to include the fluid momentum equations explicitly. The model has been coded, debugged, and successfully run. It predicts the time history of solid temperature, fluid velocities, void fraction, and pressure at various points within the debris bed provided the local solid-fluid heat transfer coefficient and the interfacial solid-fluid drag terms are modeled in terms of the other dependent variables. At present there are no basic experimental data or theoretical models available for the local heat transfer coefficient during a two-phase flow through a porous medium. Similarly, the modeling of interfacial drag terms for two-phase flow through high permeability porous beds is yet to be placed on a solid empirical or theoretical foundation, although models for these terms are available (Lipinski, 1984). Therefore, our first goal is to find the sensitivity of the quench behavior to the choice of models for these terms. This task is still in progress. We model the heat transfer coefficient exactly as in the simplified transient model (Tutu et al., 1984). It has three parameters that can be varied to test the sensitivity of the solution to the heat transfer coefficient. To model the solid-fluid interfacial drag terms we used the Lipinski model with one modification; instead of using Lipinski's value for the exponent in the inertial relative permeability of the liquid phase, we treat it as a variable parameter. Numerical computations show that results are very sensitive to the choice of various adjustable parameters. As an example, Figures 4.3 and 4.4 show the computed values of instantaneous steam flux at the bed top for two different values of the set of parameters controlling the local heat transfer coefficient. In these figures, C_{tr} is the heat transfer coefficient multiplier during the transition boiling regime, C_{fm} is the heat transfer coefficient multiplier during the film boiling regime, and ΔT_{mf} is the particle superheat at minimum film boiling temperature. These calculations were performed for a 0.42 meter deep bed consisting of 3 mm stainless steel particles. Decreasing C_{fm} reduces the heat transfer coefficient during the film boiling regime, and hence slows down the rate of rise of the steam flux and delays the onset of transition boiling regime. For the case presented in Figure 4.4, the entire bed is filled with water approximately 10 seconds before the particles go into the transition boiling regime. As a result, a

large steam spike is generated upon the onset of transition boiling regime. Thus we can see that the quench characteristics are sensitive to the choice of heat transfer coefficients. Similarly, since the interfacial solid-fluid drag terms govern the local void fraction, and hence the local heat transfer coefficient, it can be shown that these terms also have an important influence upon the debris bed quench characteristics. Therefore, significant effort must be directed towards developing reliable models for the local solid fluid heat transfer coefficient and the interfacial solid-fluid drag terms.

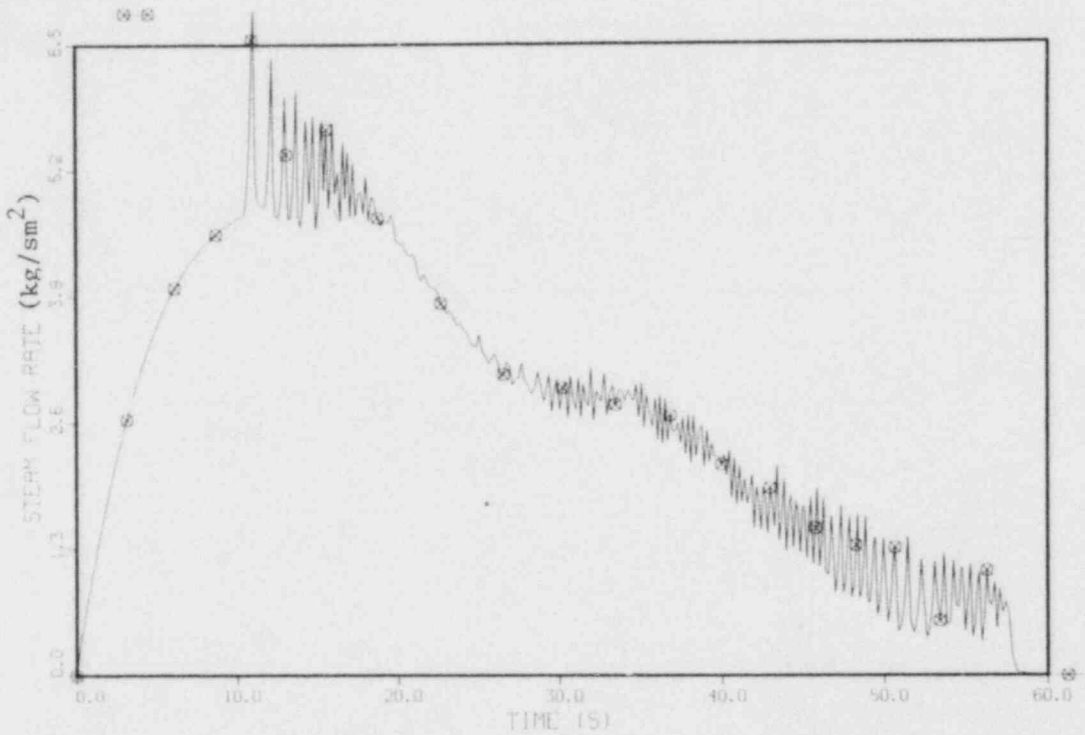

Figure 4.3 Calculated Instantaneous Heat Flux at Bed Top. Initial debris bed temperature = 775 K, inlet water superficial velocity = 7.4 mm/s, inlet water temperature = 373 K, C_{tr} = 1.0, C_{fm}= 1.0, ΔT_{mf} = 101 K.

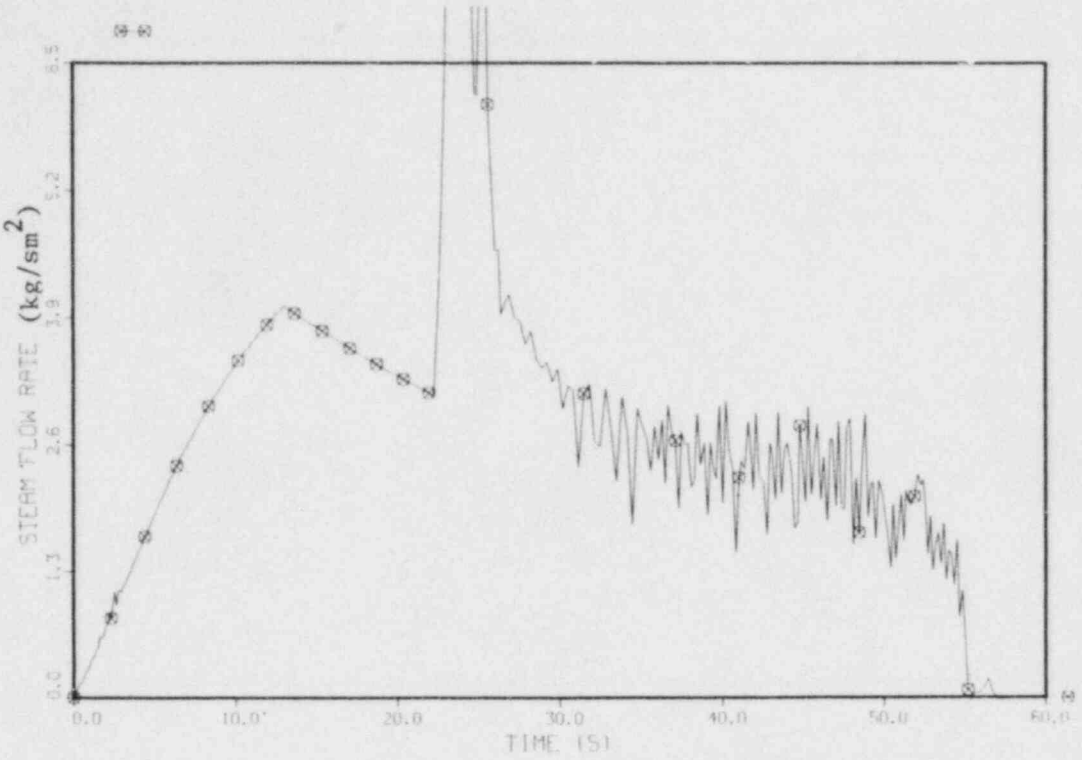

Figure 4.4 Calculated Instantaneous Heat Flux at Bed Top. C_{fm} = 0.16, ΔT_{mf} = 200 K, other parameters same as in Figure 4.3.

4.3 Core-Concrete Heat Transfer Studies: Coolant Layer Heat Transfer (G.A. Greene and T.F. Irvine, Jr. (SUSB))

The purpose of this task is to study the mechanisms of liquid-liquid boiling heat transfer and its effect on the ex-vessel attack of molten core debris on concrete. This effort is in support of the CORCON development program at Sandia National Laboratories.

4.3.1 Reanalysis of Experimental Data: R11/Liquid Metal Film Boiling

Reexamination of the liquid boiling data reduction revealed that the magnitude of the R11/liquid metal film boiling data reported in the last Quarterly Progress Report (Greene, 1984) were overestimated. The data analysis program was corrected and reanalysis of the liquid-liquid film boiling data with and without gas flux was initiated.

A sample of the results for three of the experiments that were reanalyzed is shown in Table 4.1. The graphical results for these three runs are shown in Figures 4.5 to 4.7. Shown are both the boiling heat flux as well as the boiling heat flux normalized by the prediction of the Berenson film boiling model as a function of the melt surface superheat.

Figure 4.5(a-b) presents the reanalyzed results of Bismuth/R11 Film Boil Run 132 without gas injection from below. The results are seen to lie very close to and slightly above the line indicating the Berenson film boiling result (Berenson, 1961). Figure 4.5(b) shows that the data, on the average, exceed Berenson by about 25%.

Figure 4.6(a-b) presents the results for Pb/R11 Film Boil Run 212 with an average superficial gas velocity of 0.77 cm/s. Recall that the gas injection was accomplished by bubbling through a submerged coil with discrete ports, approximately separated by the Taylor instability wavelength for R11. It is evident that the effect of the gas bubbling is to enhance the liquid-liquid boiling heat flux above the limit presented by the zero gas flux case. Figure 4.6(b) indicates that these data exceed the Berenson film boiling calculation by approximately 60%, as compared to 25% for the zero gas flux case. This is an increase in measured boiling heat flux of 30% over Run 132 ($J_G = 0$).

Finally, in Figure 4.7(a-b) are presented the results for Pb/R11 Film Boil Run 219 with superficial gas velocity equal to 5.0 cm/s. This represents the highest gas flux achieved in these tests. Here we see the measured heat flux exceeds the Berenson model by a considerable amount, on the average approaching a factor of three. This is an increase in measured boiling heat flux of a factor of 2.4 over Run 132. It is apparent that no upper limit to the gas bubbling enhancement to the film boiling heat flux has been reached within the range of superficial gas flux achieved in these tests.

Since no vapor explosions were induced in these tests by the interfacial disturbances created by the gas bubbling, it must be concluded at this time that R11 in film boiling on a pool of liquid metal (Bismuth, Lead, or Wood's metal) is always a stable mode of boiling, and that the enhancement to the measured boiling flux by the non-condensable gas bubbling is due to an increase in the surface area between the two fluids.

Table 4.1

R11/Liquid Metal Film Boiling

Run No.	132	212	219
Melt	Bismuth	Lead	Lead
Coolant	R11	R11	R11
Superficial Gas Flux (cm/s)	0.00	0.77	5.00
$\frac{q''_{Measured}}{q''_{Berenson}}$	1.24	1.61	2.94

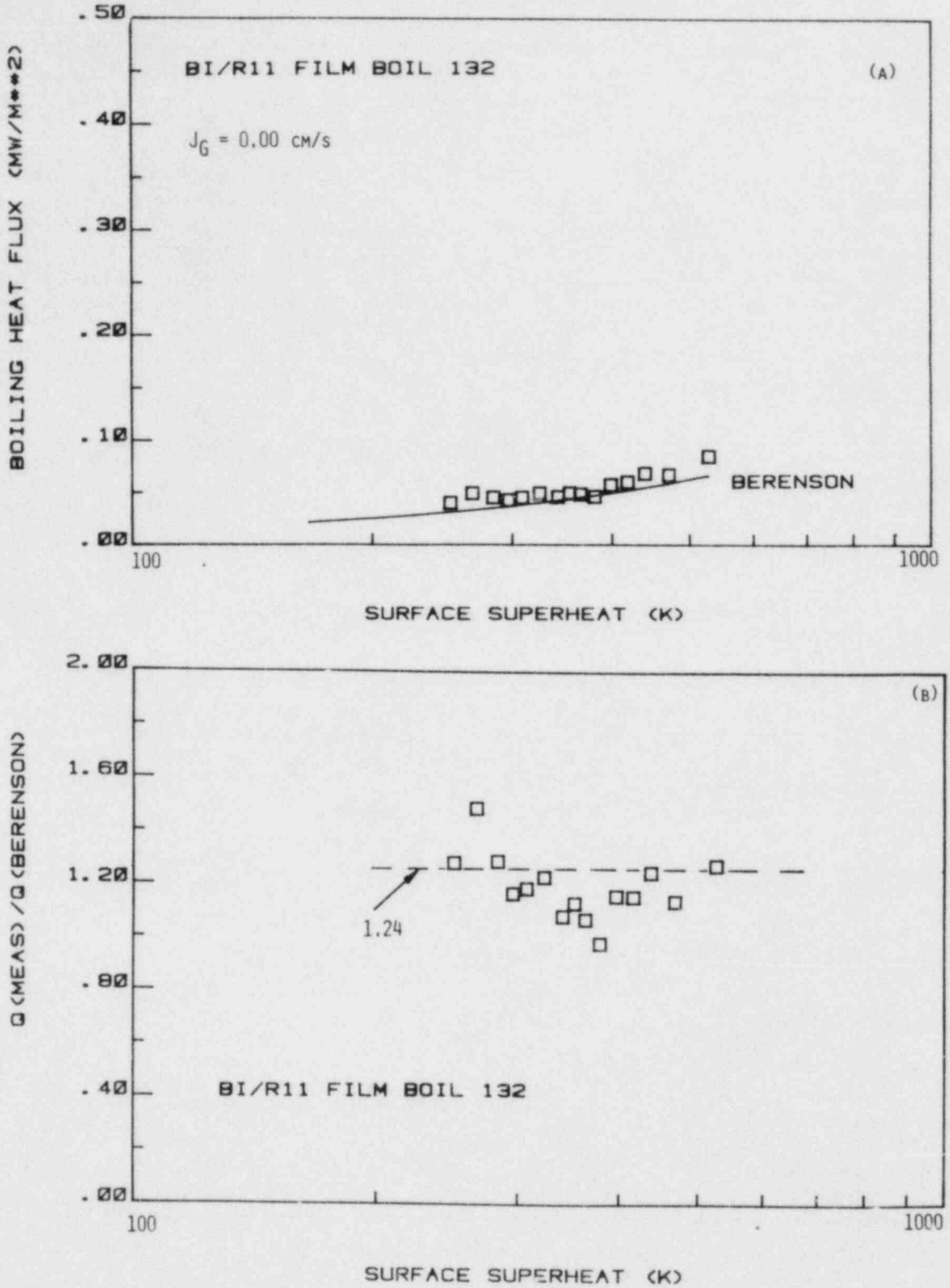

Figure 4.5 Liquid-Liquid Film Boiling Run 132: J_G = 0 cm/s.

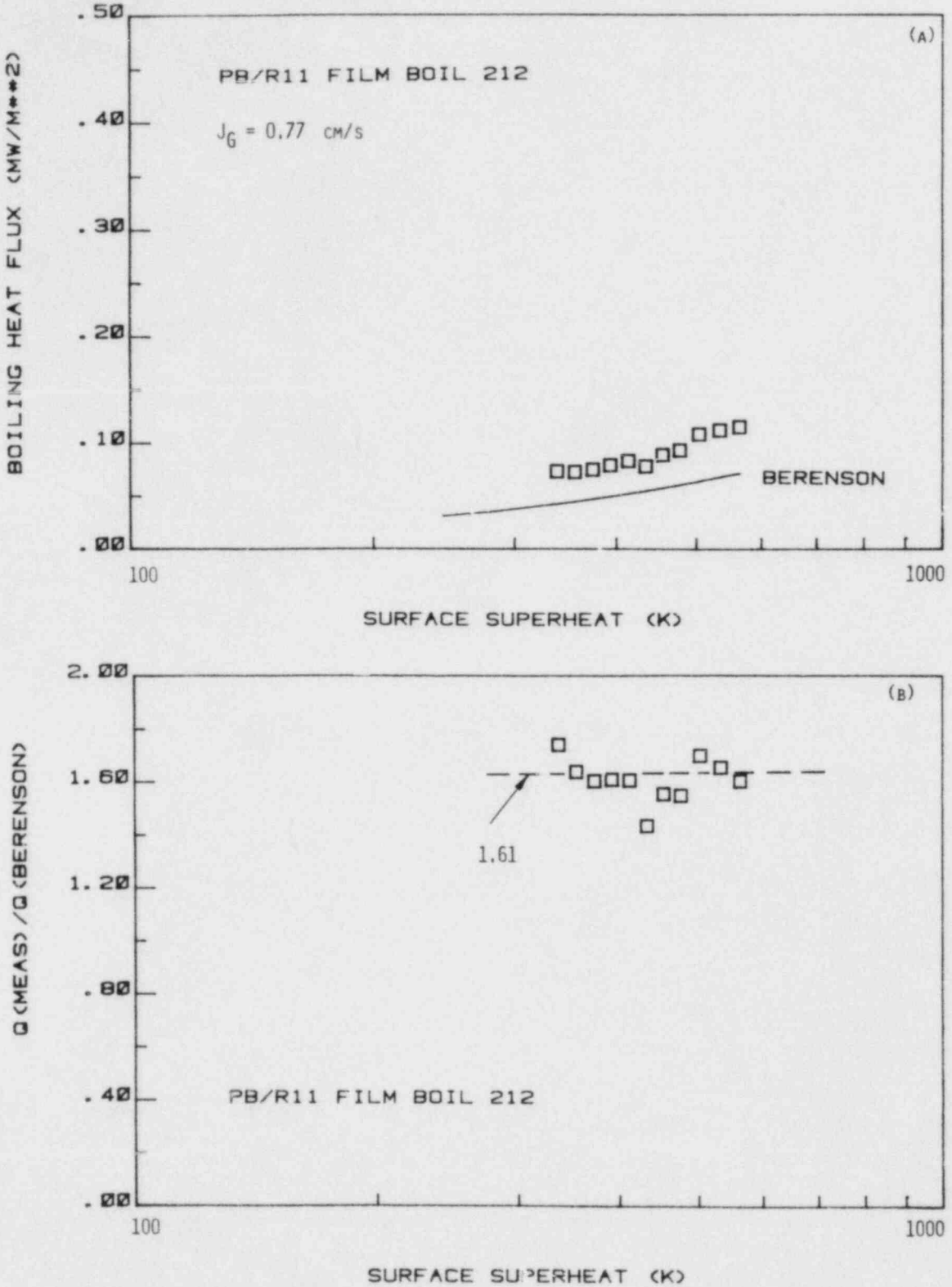

Figure 4.6 Liquid-Liquid Film Boiling Run 212: J_G = 0.77 cm/s.

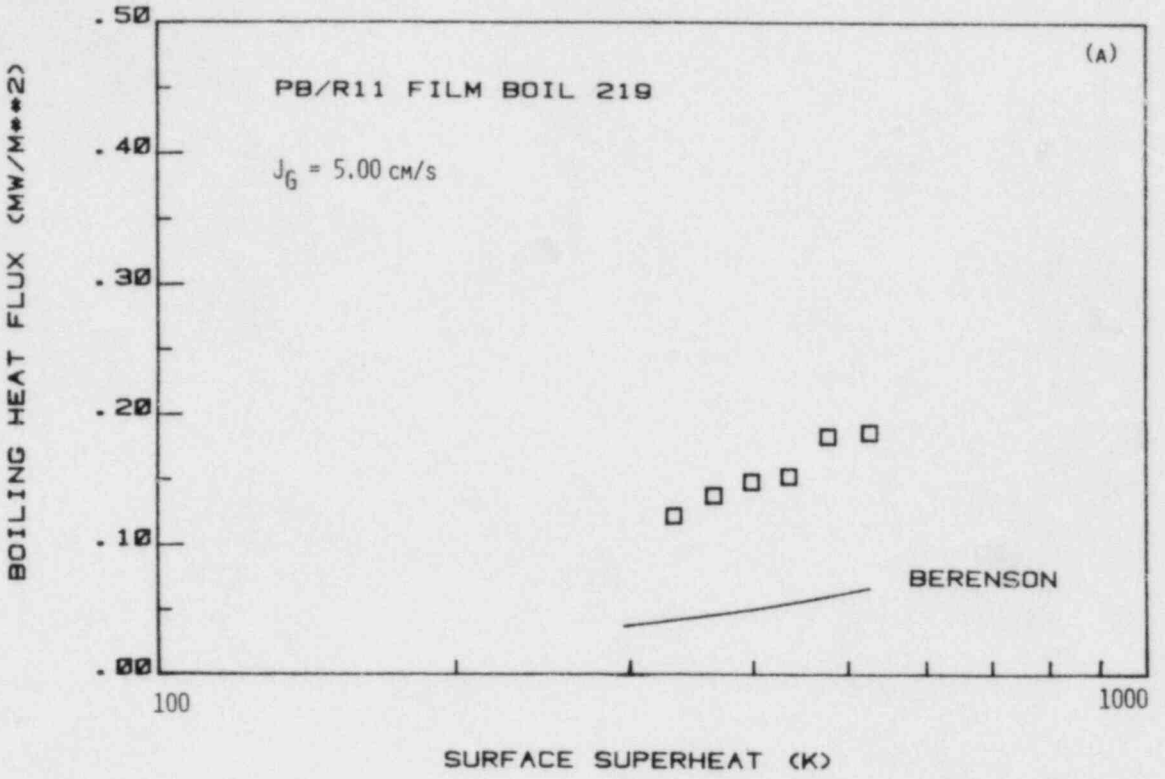

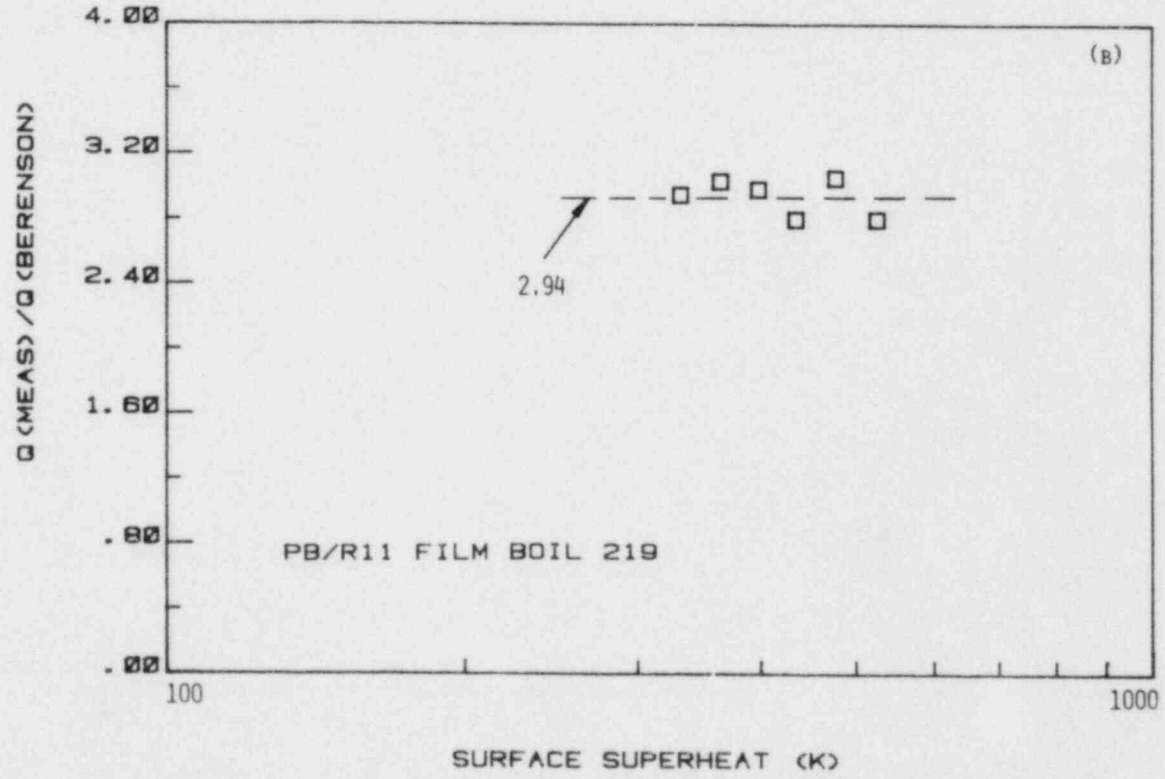

Figure 4.7 Liquid-Liquid Film Boiling Run 219: J_G = 5.0 cm/s.

REFERENCES

BERENSON, P.J., (1961), "Film Boiling Heat Transfer From a Horizontal Surface," J. Heat Transfer, 83, pp. 351-358 (1961).

GINSBERG, T., et al., (1983), "Thermal-Hydraulic Reactor Safety Experiments," Ch. 4 in Safety Research Programs Sponsored by Office of Nuclear Regulatory Research, Quarterly Progress Report, compiled by Allen J. Weiss, April 1 - June 30, 1983, NUREG/CR-2331, BNL-NUREG-51454, Vol. 3, No. 2 (1983).

GREENE, G.A., et al., (1984), "Thermal-Hydraulic Reactor Safety Experiments," Ch. 4 in Safety Research Programs Sponsored by Office of Nuclear Regulatory Research, Quarterly Progress Report, compiled by Allen J. Weiss, January 1 - March 31, 1984, NUREG/CR-2331, BNL-NUREG-51454, Vol. 4, No. 1 (1984).

KUNII, D. and Levenspiel, O. (1969), Fluidization Engineering, John Wiley and Sons, (1969).

LIPINSKI, R.J., (1984), "A Coolability Model for Postaccident Nuclear Reactor Debris," Nuclear Technology, Vol. 65, pp. 53-66, 1984.

TUTU, N.K., et al., (1984), "Debris Bed Quenching Under Bottom Flood Conditions (In-Vessel Degraded Core Cooling Phenomenology), NUREG/CR-3850, BNL-NUREG-51788, 1984.

5. Development of Plant Analyzer
(W. Wulff)

5.1 Introduction

This program is being conducted to develop an engineering plant analyzer, capable of performing accurate, real-time and faster than real-time simulations of plant transients and Small-Break Loss of Coolant Accidents (SBLOCAs) in LWR power plants. The engineering plant analyzer is being developed by utilizing a modern, interactive, high-speed, special-purpose peripheral processor, which is designed for time-critical systems simulations. The engineering plant analyzer supports primarily safety analyses, but it serves also as the basis of technology development for nuclear power plant monitoring, for on-line accident diagnosis and mitigation, and for upgrading operator training programs and existing training simulators.

There were three activities related to the LWR Plant Analyzer Development Program; namely, (1) the assessment of the capabilities and limitations of existing simulators for nuclear power plants, (2) the selection and acquisition of a special-purpose, high-speed peripheral processor suitable for real-time and faster than real-time simulation of power plant transients, and (3) the development of mathematical models and the software for this peripheral processor.

(1) One each of operating PWR and BWR power plants and their simulators had been selected to establish the status of current real-time simulations with respect to modeling fidelity for the thermohydraulics in the Nuclear Steam Supply System (NSSS). The assessment consisted of establishing the modeling assumptions in the process descriptions for the NSSS, and comparing NSSS-related simulator results with results from RETRAN calculations. The evaluation was performed to determine the current simulator capabilities and limitations of providing engineering predictions for operational transients and for transients caused by loss of coolant injection, by a loss of feedwater or feedwater heaters, by a loss of heat sink (steam generator failure), or by a mismatch between fission power and cooling rate.

(2) The AD10 of Applied Dynamics International (ADI) of Ann Arbor, Michigan, had been selected earlier as the special-purpose, high-speed peripheral processor on the basis of its capacity to execute faster and more efficiently the operations which are currently being performed in training simulators by general-purpose computers. Specifically, the AD10 was selected for efficient, high-speed integration of ordinary differential equations and for direct, on-line interactions with the user, with instrumentation, with both digital and analog signals from other computers and with graphic devices for continuous, on-line display of a large number of computed parameters.

(3) The software development for the new peripheral processor is carried out in two phases. The first phase was the implementation of an existing thermohydraulics model for the coolant dynamics of a BWR vessel to simulate operational transients on the new processor. This phase served to compare the

computing speed and accuracy of the AD10 processor with those of the CDC-7600 mainframe computer, and thereby demonstrated the feasibility of computing realistic transients at faster than real-time computing speeds. The second phase is the modeling of the primary loop outside of the vessel and its controls, neutron kinetics and thermal conduction for the complete BWR simulation, and the formulation and implementation of a thermohydraulic model for the faster than real-time analysis of operational and SBLOCA transients in PWR power plants. This is supplemented by implementation of multicolor graphics displays.

Below is a brief summary of previous results and a detailed summary of achievements during the current reporting period.

5.2 Assessment of Existing Simulators (W. Wulff and H. S. Cheng)

The assessment of current simulator capabilities consisted of evaluating qualitatively the thermohydraulic modeling assumptions in the training simulator and comparing quantitatively the predictions from the simulator with results from the detailed systems code RETRAN.

The results of the assessment have been published earlier in three reports (Wulff, 1980; Wulff, 1981a; Cheng and Wulff, 1981). It had been found that the reviewed training simulators were limited to the simulation of steady-state conditions and quasi-steady transients within the parameter range of normal operations. Most PWR simulators delivered before 1980 cannot simulate two-phase flow conditions in the primary reactor coolant loops, nor the motion of the two-phase mixture level beyond the narrow controls range in the steam generator secondary side. Most BWR simulators delivered before 1980 cannot simulate two-phase flow conditions in the recirculation loops or in the downcomer and lower plenum, nor can they simulate coolant level motions in the steam dome, the lower regions of the downcomer (below the separators), or in the riser and core regions. These limitations arise from the lack of thermohydraulic models for phase separation and mixture level tracking (Wulff, 1980; 1981a).

The comparison between PWR simulator and corresponding RETRAN results, carried out for a reactor scram from full power, showed significant discrepancies for primary and secondary system pressures and for mean coolant temperatures of the primary side. The discrepancies were found even after the elimination of differences in fission power, feedwater flow and rate of vapor discharge from the steam dome. Good agreement was obtained between simulator and RETRAN calculations for only the early part (narrow control range) of the water level motion in the steam generator. The differences between simulator and RETRAN calculations have been explained in terms of modeling differences (Cheng and Wulff, 1981).

5.3 Acquisition of Special-Purpose Peripheral Processor (A. N. Mallen and R. J. Cerbone)

The AD10 had been selected earlier as the special-purpose peripheral processor for high-speed, interactive systems simulation. A brief description of

the processor has been published in a previous Quarterly Progress Report (Wulff, 1981b). A PDP-11/34 DEC computer serves as the host computer.

Two AD10 units, coupled directly to each other by a bus-to-bus interface and equipped with a total of one megaword of memory, have been installed with the PDP-11/34 host computer, two 67 megabyte disc drives, a tape drive and a line printer. On-line access is facilitated by a model 4012 Tektronix oscilloscope terminal and a 28-channel signal generator. The system is accessed remotely via four ADDS CRT terminals and two DEC Writer terminals, one also equipped with a line printer. An IBM Personal Computer will also be used to access the PDP-11/34 host computer, but is now used primarily to generate labelled, multicolored graphs from AD10 results. An advanced multicolor graphics terminal is needed, however, for extensive on-line display of simulated parameters generated by the AD10 at real-time or faster computing speeds.

5.4 Software Implementation on AD10 Processor

A four-equation model for nonhomogeneous, nonequilibrium two-phase flow had been formulated and supplemented by constitutive relations from an existing BWR reference code, then scaled and adapted to the AD10 processor to simulate the Peach Bottom-2 BWR power plant (Wulff, 1982a). The resulting High-Speed Interactive Plant Analyzer code (HIPA-PB2) has been programmed in the high-level language MPS10 (Modular Programming System) of the AD10. After implementing the thermohydraulics of HIPA-PB2 on the AD10, we compared the computed results and the computing speed of the AD10 with those of the CDC-7600 mainframe computer, to demonstrate the feasibility of achieving engineering accuracy at high simulation speeds with the low-cost AD10 minicomputer (Wulff, 1982b).

It has been demonstrated (Wulff, 1982b) that (i) the high-level, state equation-oriented systems simulation language MPS10 compressed 9,950 active FORTRAN statements into 1,555 calling statements to MPS10 modules, (ii) the hydraulics simulation occupies one-fourth of available program memory, (iii) the difference between AD10 and CDC-7600 results is only approximately $\pm$ 5% of total parameter variations during the simulation of a severe licensing base transient, (iv) the AD10 is 110 times faster than the CDC-7600 for the same transient, and (v) the AD10 simulates the BWR hydraulics transients up to ten times faster than real-time process speed. It has been demonstrated now that even after the inclusion of models for neutron kinetics, conduction, balance of plant dynamics and controls, the AD10 still achieves ten times real-time simulation speed for all transients reported earlier (Wulff, 1983c).

The HIPA-PB2 hydraulics program used earlier for the feasibility demonstration has been expanded to simulate neutron kinetics (point kinetics), thermal conduction in fuel elements and the thermohydraulics of the components of the balance of plant shown in Figure 5.1. The expanded version is called HIPA-BWR/4.

The stand-alone program modules for neutron kinetics with reactivity feedback and reactor trip, for thermal conduction in fuel elements, for compressible flows in the steam line and for the control logic for operating the

safety and relief valves tested earlier (Wulff, 1982c; 1983a) have been implemented in HIPA-BWR/4. Models had been formulated and tested separately for the control and plant protection systems and the plant components forming the loop through turbines, condensers and the feedwater trains. They have been implemented during the previous reporting period.

Specific accomplishments of the current reporting period are described below.

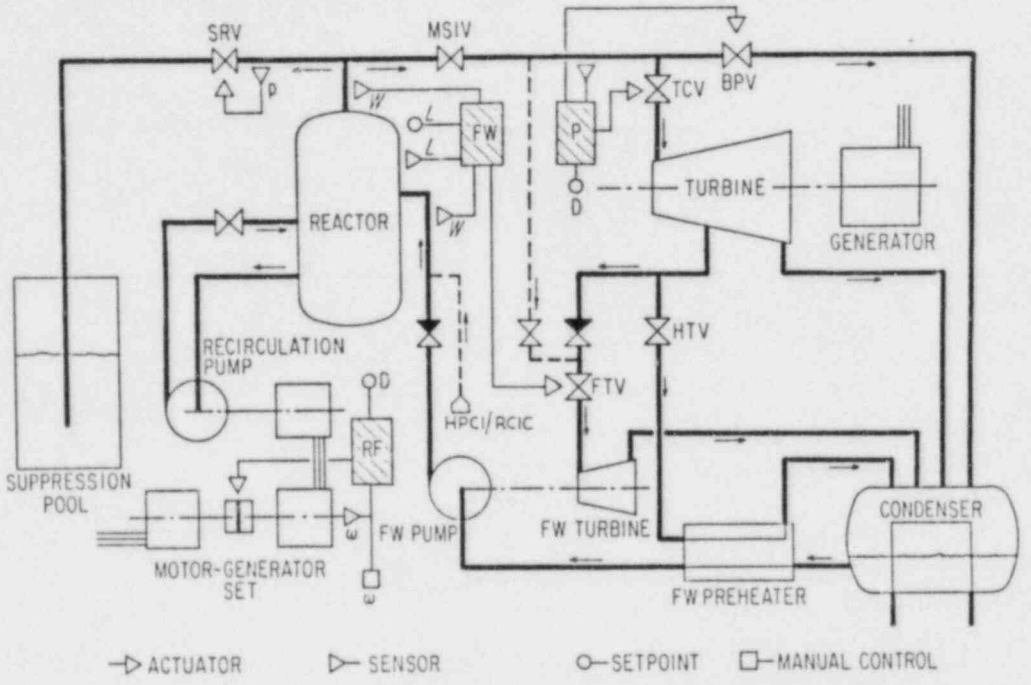

Figure 5.1 Flow Schematic and Control Blocks for BWR Simulation; FW - Feedwater Controller, P - Pressure Controller, RF - Recirculation Flow Controller.

5.4.1 Program Improvements (A. N. Mallen and A. Stritar)

During the course of developmental assessment, we observed that, for some transients, the noise in the core flow was excessive. The source of the noise has been found to be due to the improper procedure used to compute the local vapor generation rate. An improved procedure was developed and implemented, which removed the excessive noise observed for those transients.

5.4.2 Implementation of Boron Tracking (H. S. Cheng)

A boron transport model had been developed and reported in the last quarterly progress report (Wulff, 1983d). In the current reporting period, the

boron transport model was implemented first as a stand-alone module to test the model validity. The testing was performed using the natural circulation condition encountered in a MSIV-ATWS event. Figure 5.2 shows the results obtained for a 2000-second transient in which boron injection was initiated at 200 seconds with 43 gallons-per-minute capacity and 75% mixing efficiency. It is seen that it will take about 30 minutes to shut down the reactor under these conditions. This is consistent with the GE estimate based on their testing. The tested stand-alone module is being implemented into the HIPA-BWR/4 code.

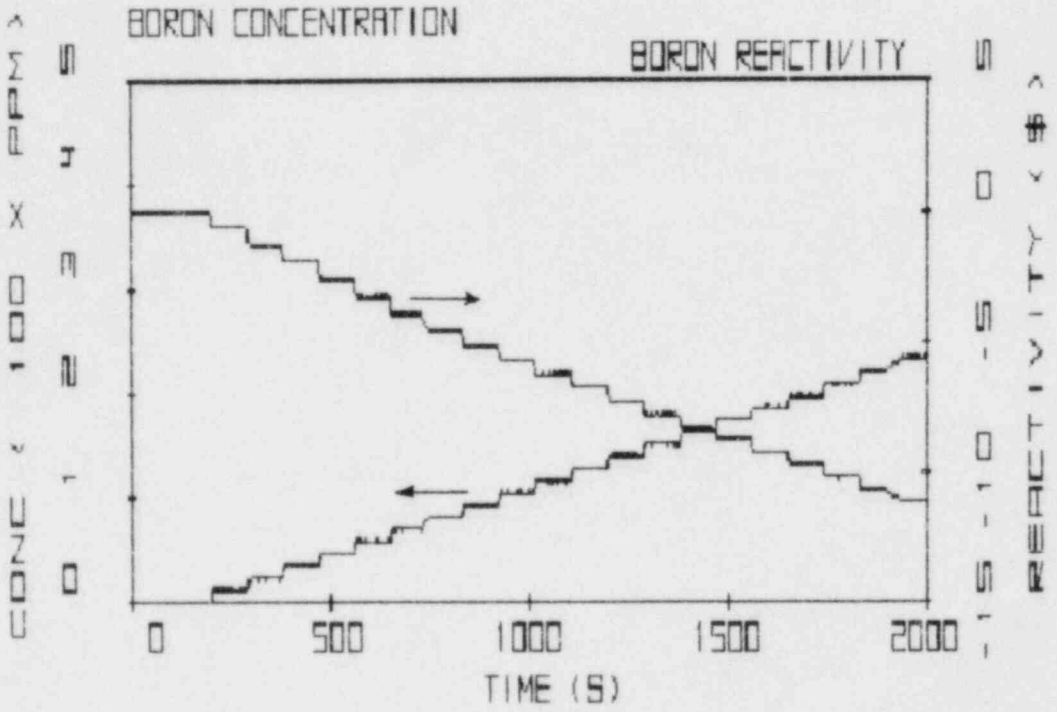

Figure 5.2 Boron Concentration and Boron Reactivity During Natural Circulation Conditions of a MSIV-ATWS Event (43 GPM and 75% Mixing Efficiency)

5.4.3 Graphics Display System (S. V. Lekach)

The current graphics display capability in the plant analyzer project consists of an IBM PC/XT with a 10-megabyte hard disk and a color bit-mapped display monitor. The two AD10s are linked to the PC/XT with 16 analog lines. The PC/XT contains an analog-to-digital converter board (12-bit accuracy for 16 channels). During an AD10 simulation, the two machines are sending 16 analog voltages to the PC/XT. One of the voltage channels is always the time in the problem, and the other 15 can be any of the variables being calculated by the AD10s. The PC/XT receives the information, translates it into screen

coordinates and displays it while simultaneously storing the 16 variables on the hard disk for future re-display.

One major improvement during this past quarter has been the performance speedup, so that up to two variables can be displayed on-line with the AD10s on the multicolor screen, with axes and labels in the appropriate physical units. At the same time, all 16 variables are being stored on disk for future replay. This improvement in performance is due to the software having been rewritten into the C language and the use of more efficient graphics display software.

If so desired, any of the 15 variables can be replayed as soon as the transient is over for further examination. The histories can also be plotted on the graphics dot matrix printer attached to the PC/XT to obtain hard copy. The transients shown in this report have all been recorded with the PC/XT and the figures were created using the convenient hard copy feature.

Another achievement during this quarter has been the organization of a Local Area Network (LAN) to display the AD10-simulated results remotely. A presentation was made by the Plant Analyzer Development Group in May 1984 to a group of nuclear industry vendors on the performance of the AD10s. Due to the size of the audience, it had to be held in a conference room about 600 feet away from the HIPA simulation laboratory. In order to show the AD10 results, the primary PC/XT was linked via a LAN to another PC in that conference room. The second PC drove two large color monitors that displayed the AD10 curves as captured and immediately relayed through the network's cables. It was necessary to use a LAN, rather than the usual telephone connections, because of the amount of information that had to be relayed in a short time (about 200 Kbytes/second).

5.5 Developmental Assessment (H. S. Cheng, S. V. Lekach and W. Wulff)

In the last quarterly progress report, we presented the results of the first series of developmental assessment for ten ATWS events (Wulff, 1984). We have since carried out further assessment of the plant analyzer against GE predictions for 20 more plant transients, as listed in the FSAR of the Peach Bottom 2 BWR (Philadelphia Electric Co., 1971), against TRAC-BD1 results for an ATWS event induced by MSIV closure, against RAMONA-3B for this same MSIV-ATWS event, and against RELAP-5 simulations for a feedwater controller failure at maximum demand, a MSIV closure event, and a loss of feedwater transient, all with scram permissible.

5.5.1 Plant Analyzer Vs. GE

We present in Figures 5.3 through 5.14 the results of those transients in the FSAR for which the corresponding GE results are available for comparison. It should be mentioned that the GE calculations, done in 1971 with conservative assumptions, are commonly known as evaluation models, in contrast to the best-estimate models of the plant analyzer. For this reason, we do not expect to obtain good quantitative agreement throughout. Rather, the purpose of such comparisons is to assure that the plant analyzer predicts the proper trend for

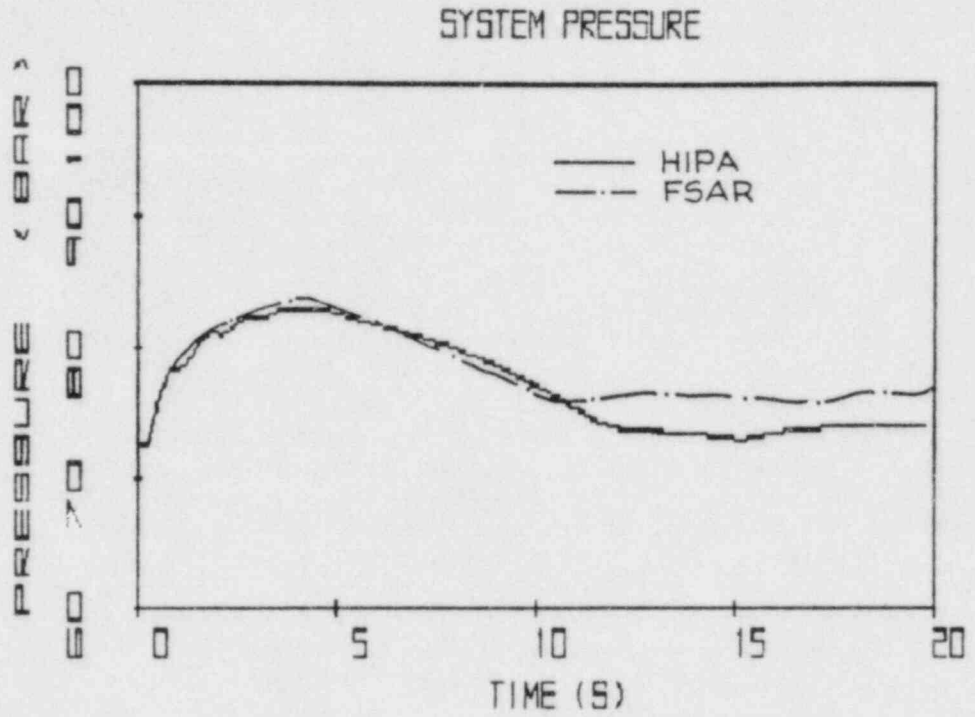

Figure 5.3 Turbine Trip Without Bypass, Comparison for System Pressure

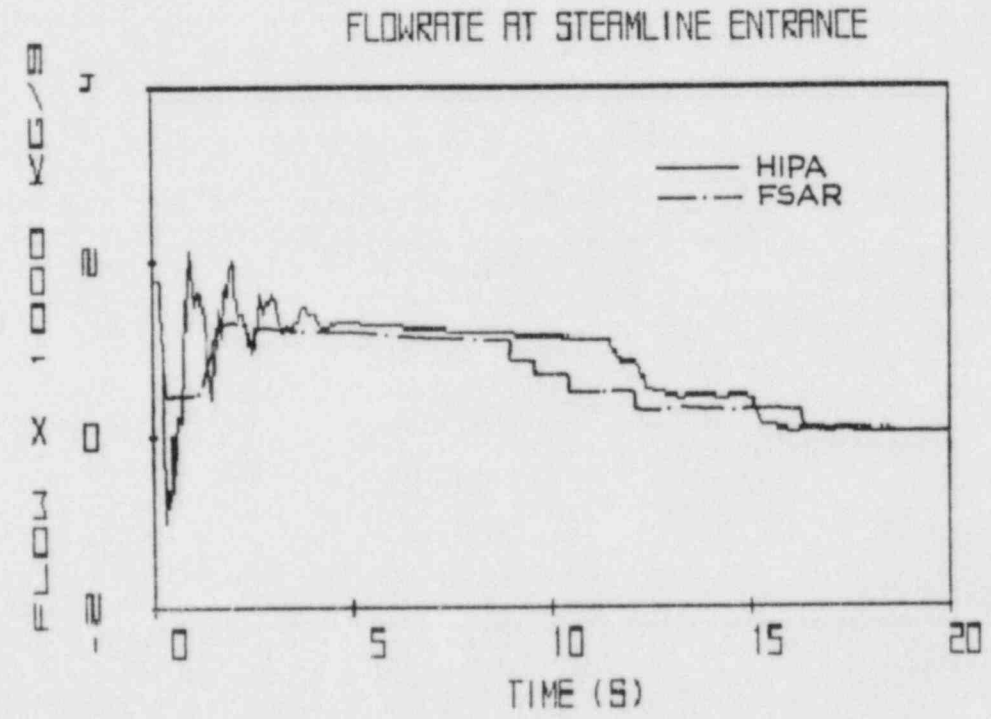

Figure 5.4 Turbine Trip Without Bypass, Comparison for Steam Mass Flow Rate at Steam Line Entrance

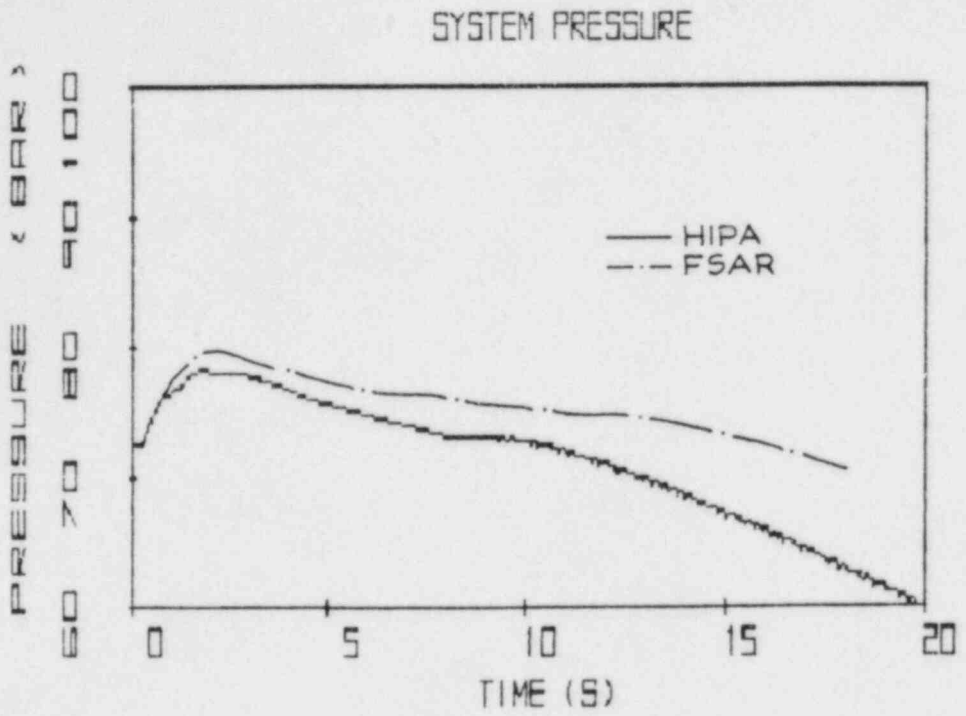

Figure 5.5 Turbine Trip With Bypass, Comparison for System Pressure

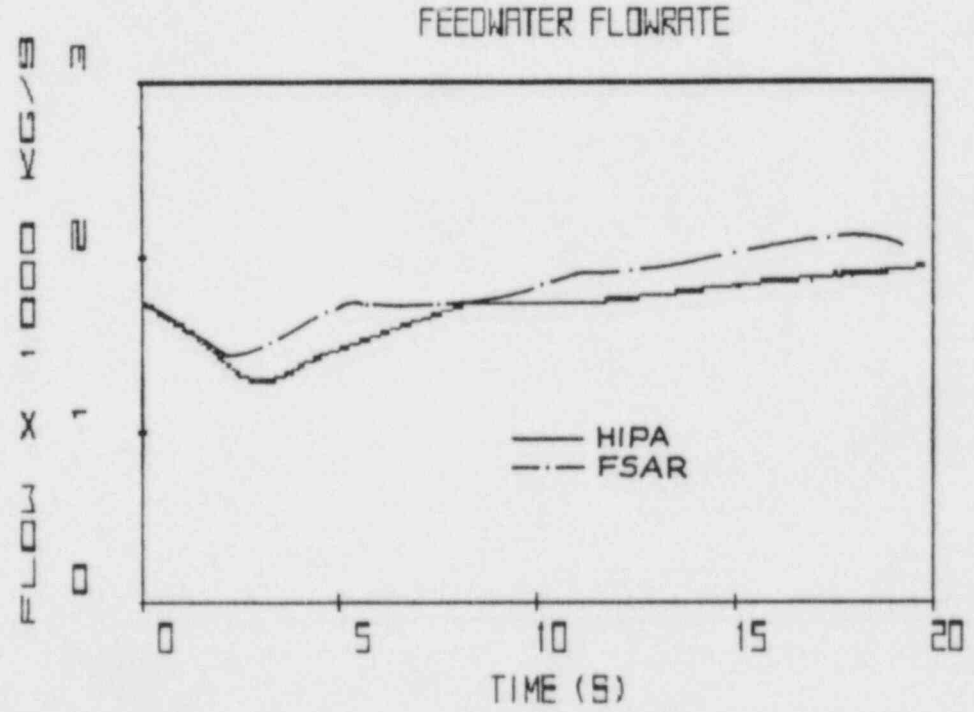

Figure 5.6 Turbine Trip With Bypass, Comparison for Feedwater Mass Flow Rate

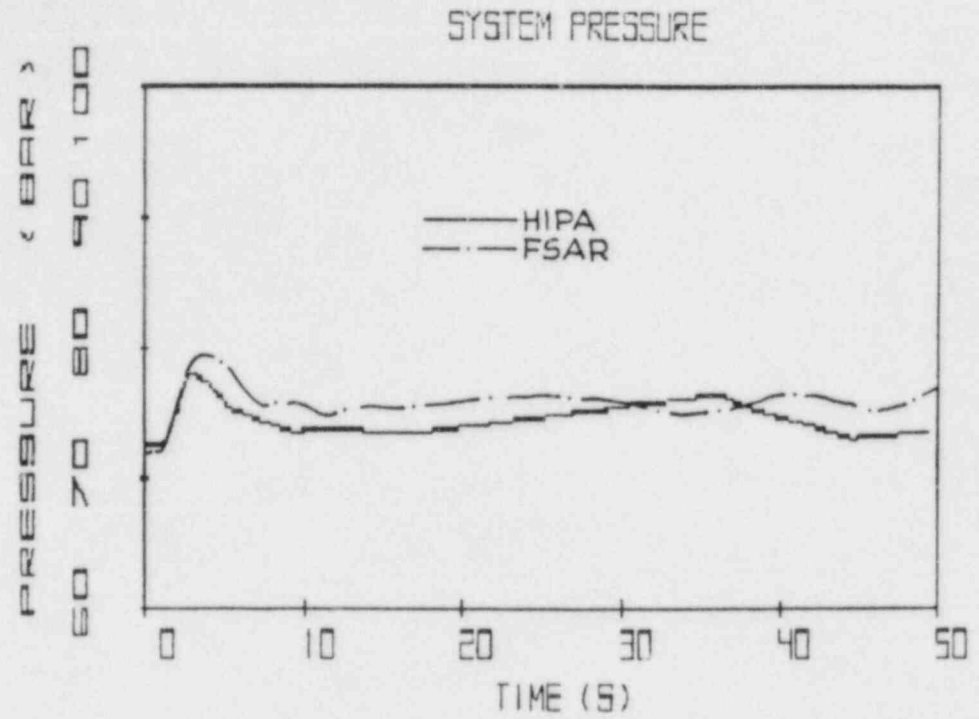

Figure 5.7 Main Steam Isolation Valve Closure, Comparison for System Pressure

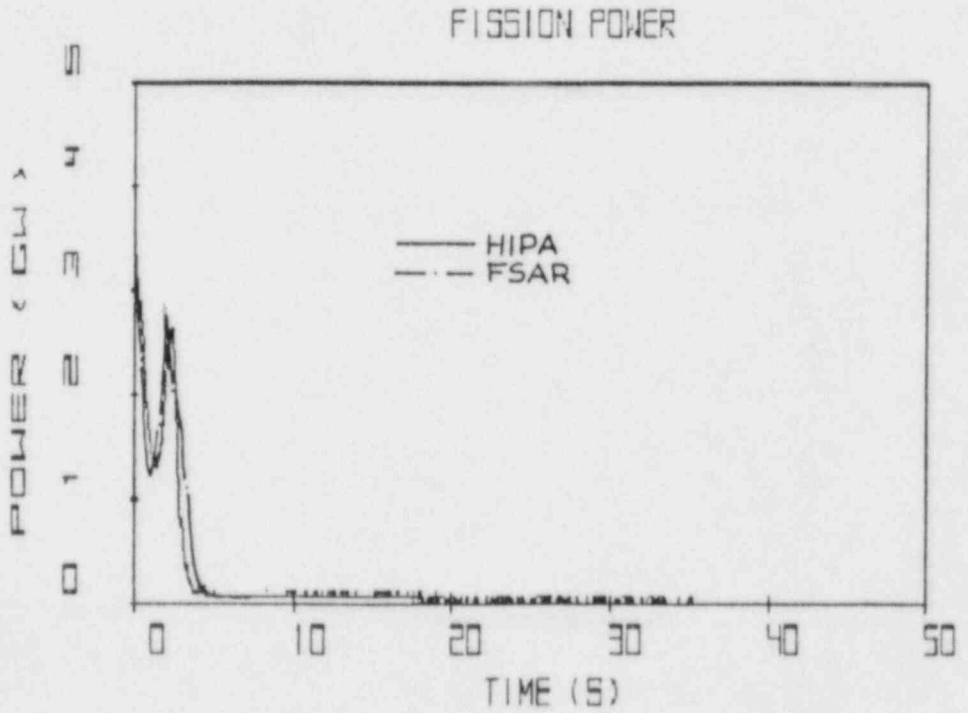

Figure 5.8 Main Steam Isolation Valve Closure, Comparison for Fission Power

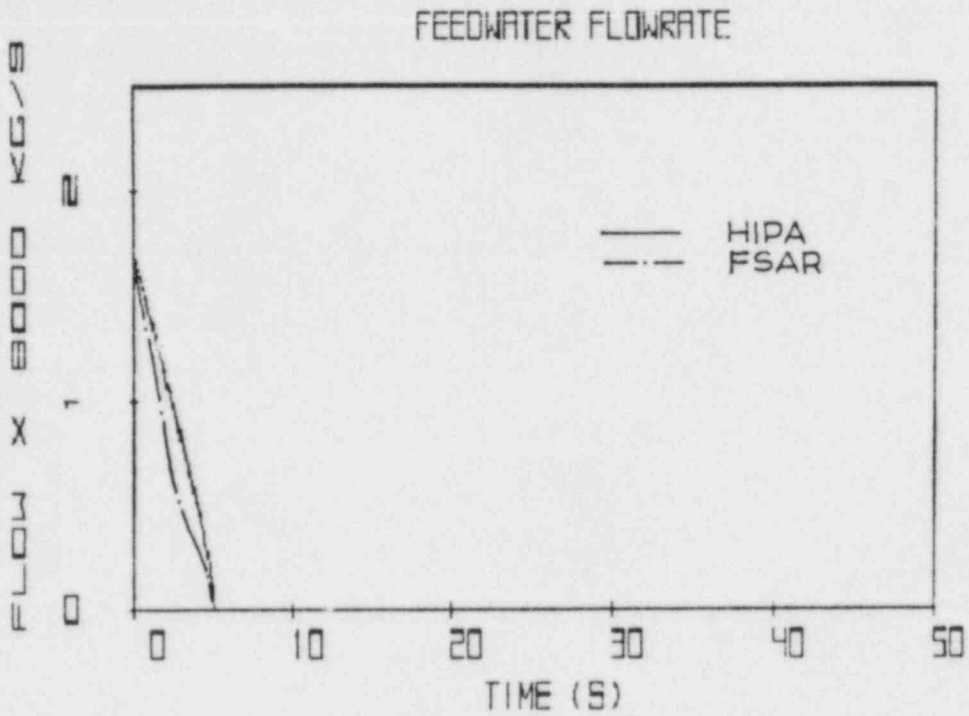

Figure 5.9 Loss of Feedwater Flow, Comparison for Feedwater Flow Rate

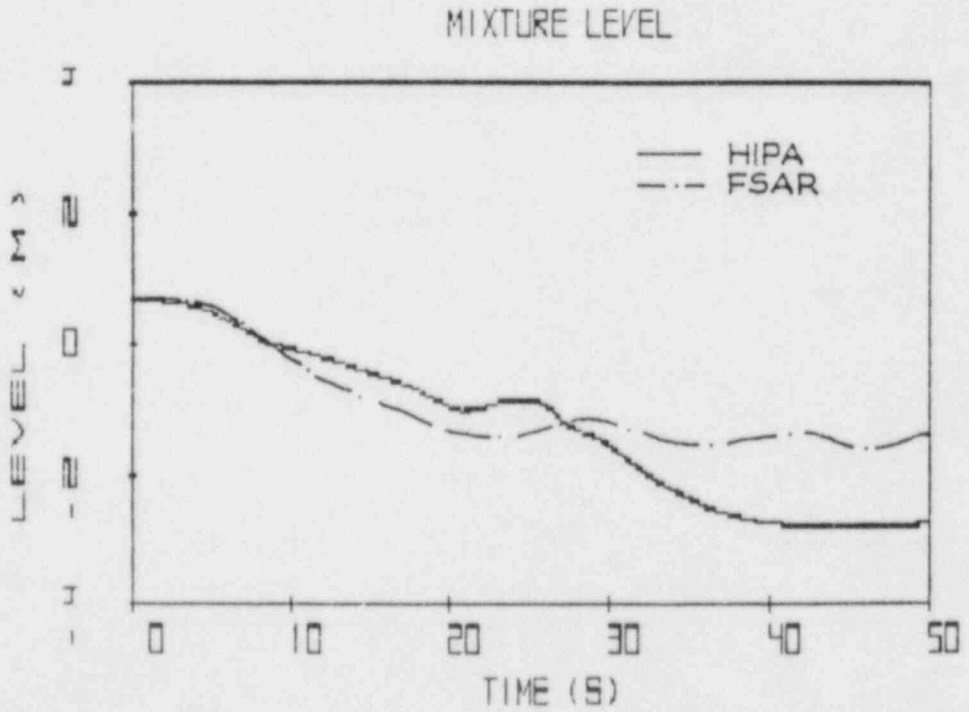

Figure 5.10 Loss of Feedwater Flow, Comparison for Mixture Level in Downcomer

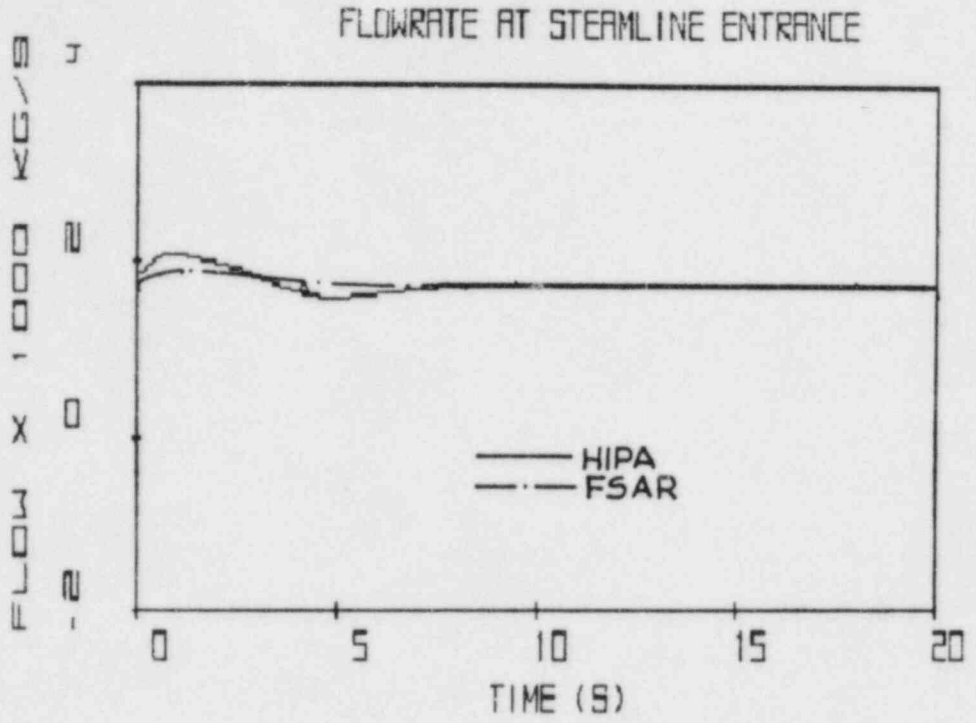

Figure 5.11 Relief Valve Stuck Open (First Bank), Comparison for Steam Line Mass Flow Rate

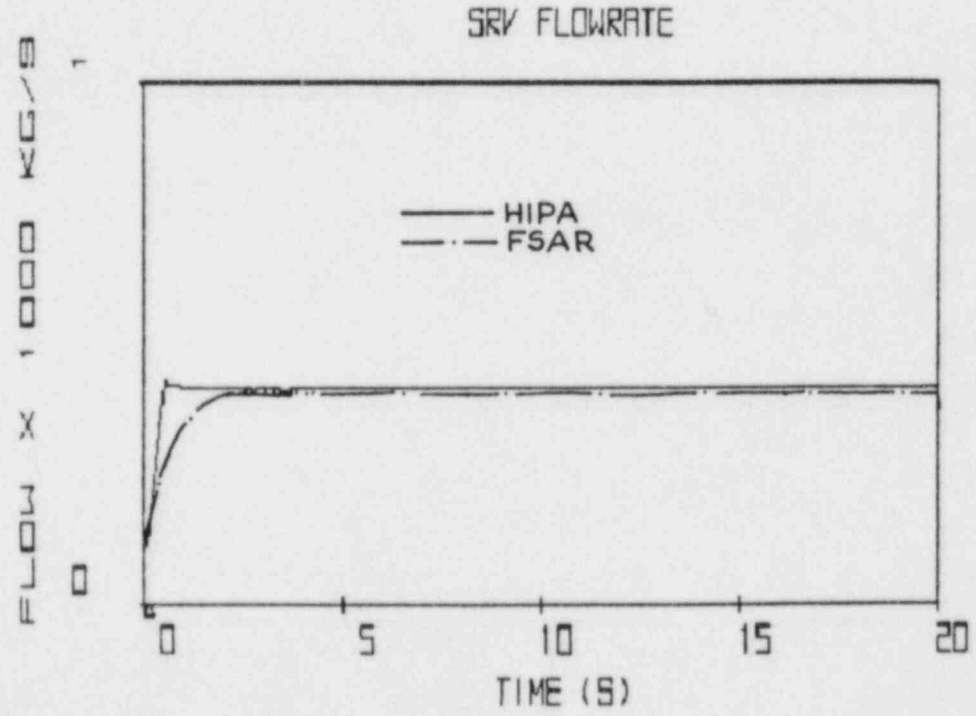

Figure 5.12 Relief Valve Stuck Open (First Bank), Comparison for Mass Flow Rate Through Safety and Relief Valves

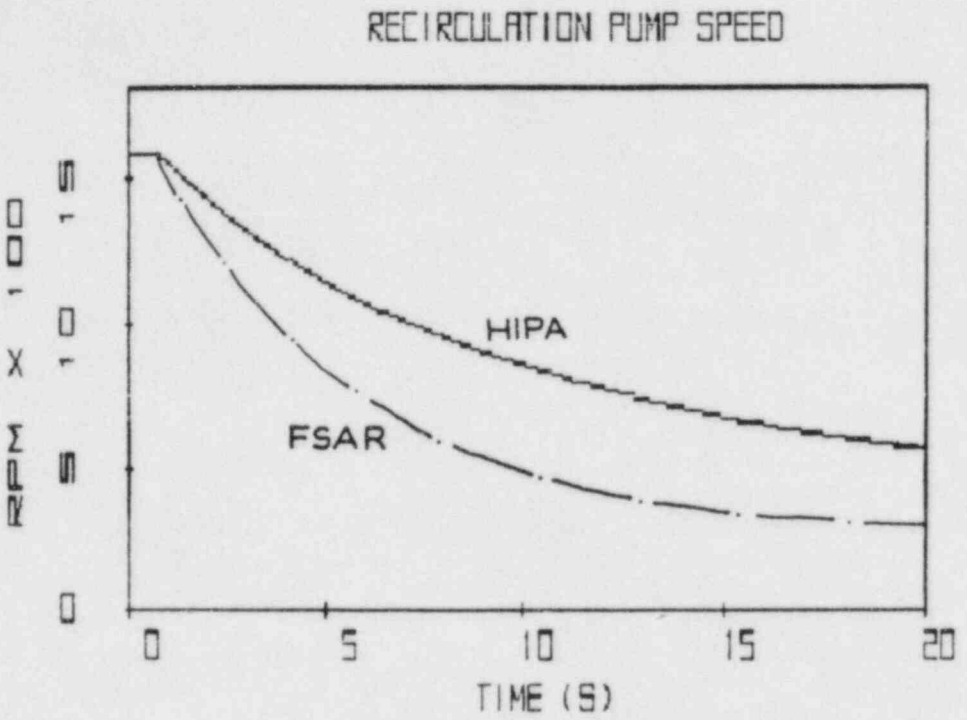

Figure 5.13 Motor-Generator Trip, Comparison for Recirculation Loop Flow

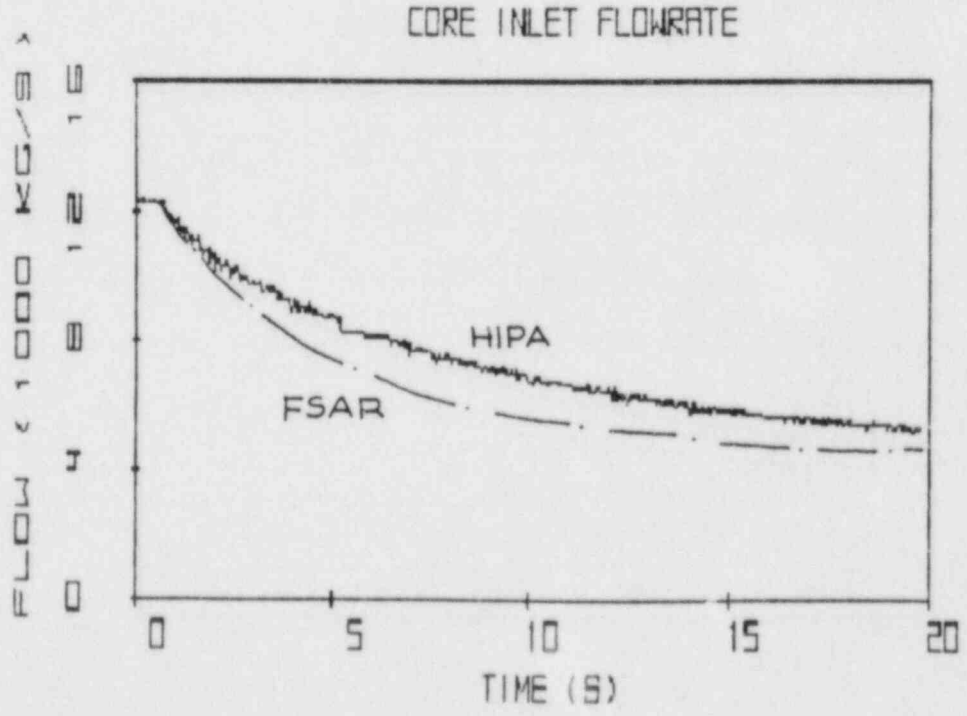

Figure 5.14 Motor-Generator Trip, Comparison for Core Inlet Mass Flow Rate

these plant transients. In general, the qualitative agreement between the plant analyzer and GE predictions is good. One noticeable difference is the coastdown rate of the recirculation pump speed, which can be attributed to the different pump inertia used. Another potential difference is the scram characteristic curve used. The plant analyzer used an end-of-cycle (EOC) scram curve, which is significantly less effective than a beginning-of-life (BOL) scram curve. We suspected that GE had probably used a BOL scram curve in their calculations. To confirm this, we calculated the MSIV closure event with the plant analyzer using a BOL scram curve. The results, presented in Figures 5.7 and 5.8, show a very good agreement between the plant analyzer and GE for this transient.

5.5.2 Plant Analyzer Vs. TRAC-BD1

Hsu, Neymotin and Saha (1984) computed an ATWS event induced by MSIV closure using the TRAC-BD1 code. Two calculations have been completed, one with the time-dependent fission power computed by the point kinetics in TRAC-BD1, the other with the fission power first computed with RAMONA-3B and then imposed as a boundary condition on the TRAC-BD1 simulation.

Figures 5.15 and 5.16 show the comparisons between the plant analyzer and TRAC-BD1 predictions for the system pressure and fission power, respectively. The TRAC-BD1 prediction with point kinetics appears to be too high for both the peak pressure and peak power. The plant analyzer results agree reasonably well with those of TRAC-BD1 using the imposed RAMONA-3B power history.

5.5.3 Plant Analyzer Vs. RAMONA-3B

The same MSIV closure-induced ATWS event has also been calculated by Hsu et al. (1984) with the RAMONA-3B code using the 3-D neutron kinetics option. Figures 5.17 and 5.18 show the pressure and power history comparisons between the plant analyzer and RAMONA-3B. The agreement is generally good.

5.5.4 Plant Analyzer Vs. RELAP-5

RELAP-5/MOD1 calculations have been carried out for a Feedwater Regulator Failure at Maximum Demand and a Main Steam Isolation Valve Closure with Scram on high pressure (Lu and Shier, 1983), and for a Loss of Feedwater Flow transient (Lu, Levine and Shier, 1982). These calculations were performed after slight modifications to the code as originally received from Idaho National Engineering Laboratory.

Figures 5.19 and 5.20 show the comparisons of the system pressure and fission power history predicted by the plant analyzer and RELAP-5 for the Feedwater Regulator Failure event. The agreement is good except for some shift in timing, which may be caused by a higher core flow or a faster response of the actuator of the plant analyzer.

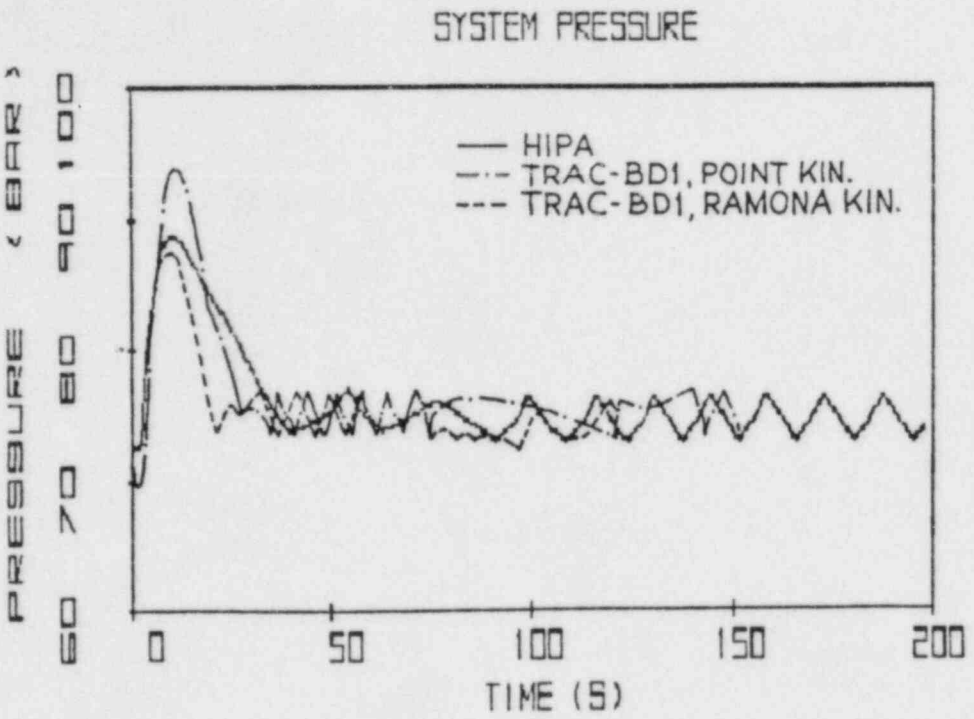

Figure 5.15 Comparison of System Pressure Predictions by Plant Analyzer and TRAC-BD1 for the MSIV-ATWS

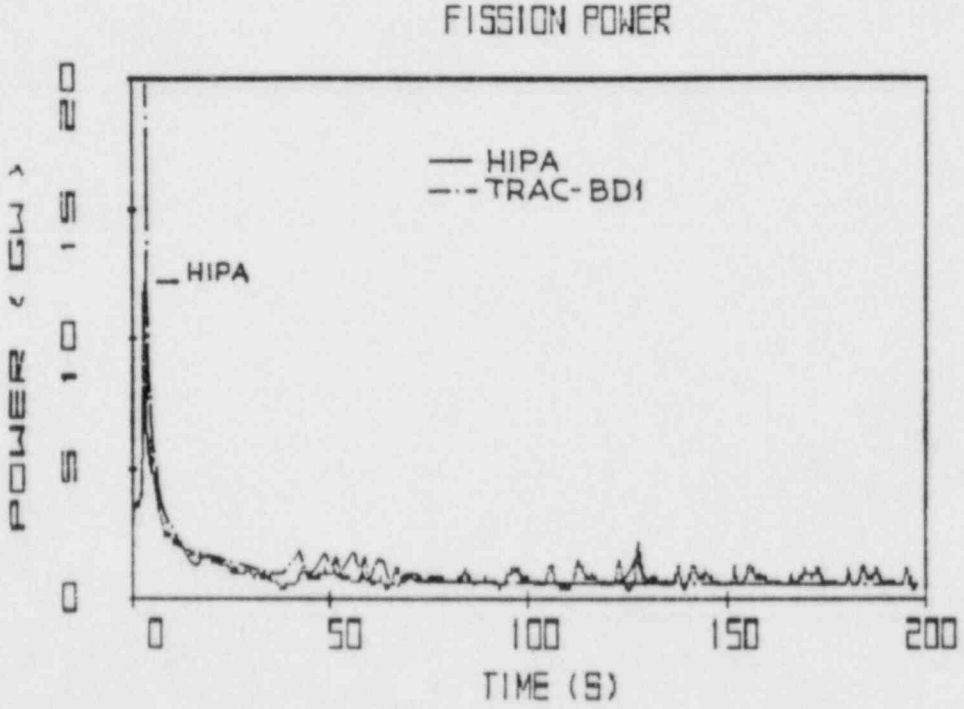

Figure 5.16 Comparison of Fission Power Predictions by Plant Analyzer and TRAC-BD1 for the MSIV-ATWS

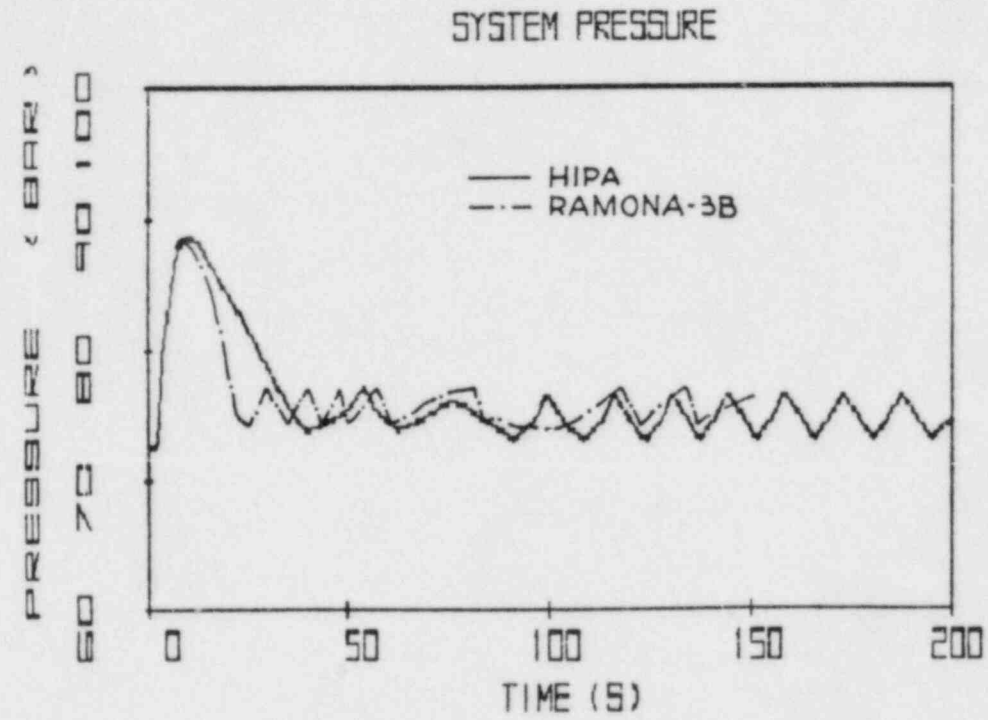

Figure 5.17 Comparison of System Pressure Predictions by Plant Analyzer and RAMONA-3B for the MSIV-ATWS

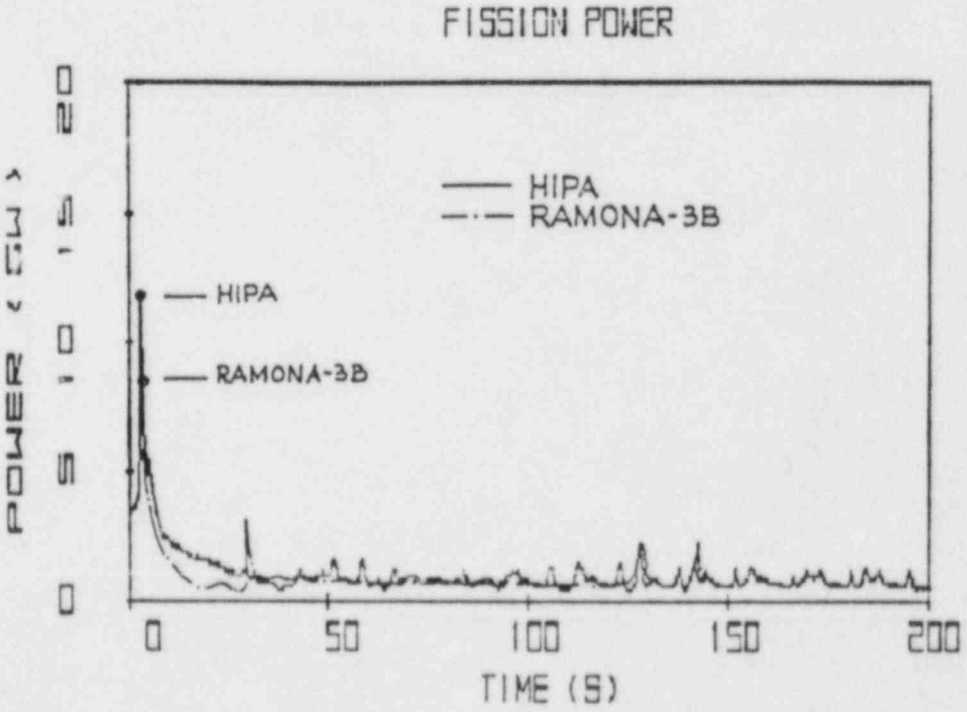

Figure 5.18 Comparison of Fission Power Predictions by Plant Analyzer and RAMONA-3B for the MSIV-ATWS

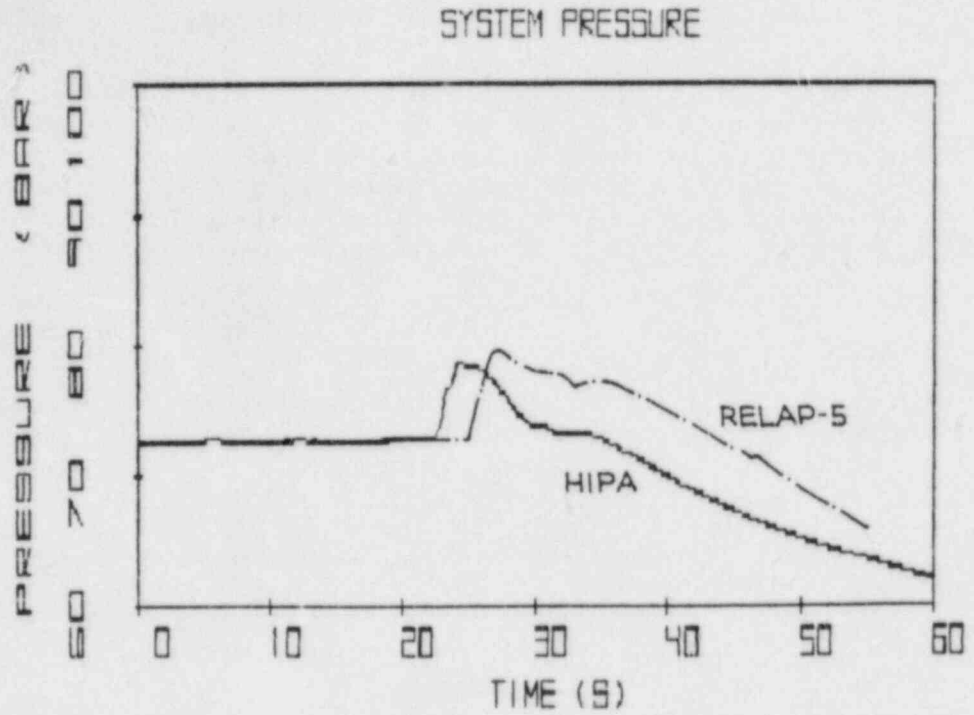

Figure 5.19 Comparison of System Pressure Predictions by Plant Analyzer and RELAP-5 for the Feedwater Regulator Failure Event

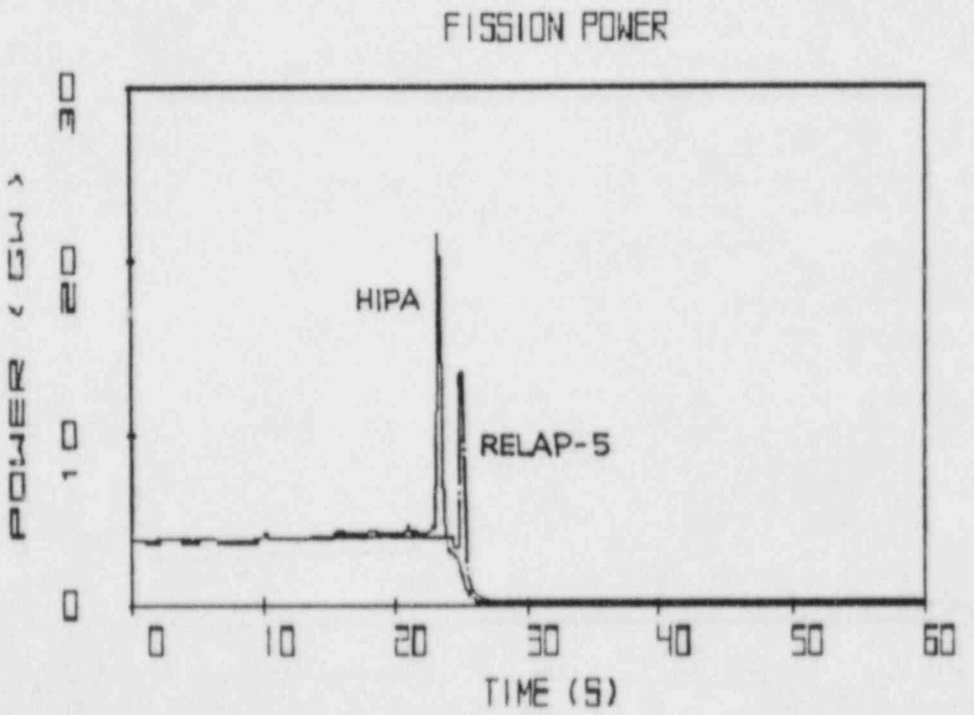

Figure 5.20 Comparison of Fission Power Predictions by Plant Analyzer and RELAP-5 for the Feedwater Regulator Event

Conclusions

The assessment carried out so far shows that the plant analyzer can carry out realistic and accurate simulations of transients in BWR-4 power plants if the correct specifications for the plant control system and the engineered safety systems are used. The plant analyzer has not yet been shown to simulate conditions of flow reversal and departure from nucleate boiling (DNB). All comparisons presented here were produced without any change in system parameters.

5.6 Future Plans

Assessment work will continue with comparisons against the turbine trip test data of the Peach Bottom 2 BWR. The BWR simulation capability will be expanded to accommodate flow reversal, phase separation via the drift flux model instead of the present slip flow model, and DNB conditions.

The plant analyzer will be presented and demonstrated to domestic industries and foreign institutions interested in nuclear power plant simulation for the purpose of developing cooperative programs directed toward PWR simulations.

REFERENCES

CHENG, H. S. and WULFF, W., (1981), "A PWR Training Simulator Comparison with RETRAN for a Reactor Trip from Full Power," Informal Report, BNL-NUREG-30602, Brookhaven National Laboratory, September 1981.

GE, NEDO-24222 (1981), Assessment of BWR Mitigation of ATWS, Vol. II, NUREG-0460, Alternate No. 3.

Hsu, C. J., Neymotin, L. and Saha P., (1984), "Analysis of a Typical BWR/4 MSIV Closure ATWS Using RAMONA-3B and TRAC-BD1 Codes," Joint ASME/ANS Conference on Design, Construction and Operation of Nuclear Power Plants, Portland, Oregon; ASME Paper No. 84-NE-10.

Lu, M. S. and Shier, W. G., (1983), "Analysis of Three Rapid Transients for a BWR/4 with the RELAP-5 Code," Informal Report, BNL-NUREG-34507.

Lu, M. S., Levine, M. M. and Shier, W. G., (1982), "BWR Loss of Feedwater Transient Analysis," Informal Report, BNL-NUREG-32396.

PHILADELPHIA ELECTRIC COMPANY (1981), "Final Safety Analysis Report, Peach Bottom Atomic Power Station Units 1 and 2."

MILTON, J. D. (1982) "TRAC-BWR Control System Model Developmental Assessment," Interim Technical Report, EG&G, Idaho, Inc., WR-CD-82-073.

WULFF, W., (1980), "PWR Training Simulator, An Evaluation of the Thermohydraulic Models for its Main Steam Supply System," Informal Report, BNL-NUREG-28955, September 1980.

WULFF, W., (1981a), "BWR Training Simulator, An Evaluation of the Thermohydraulic Models for its Main Steam Supply System," Informal Report, BNL-NUREG-29815, Brookhaven National Laboratory, July 1981.

WULFF, W., (1981b), "LWR Plant Analyzer Development Program," Ch. 6 in Safety Research Programs Sponsored by the Office of Nuclear Regulatory Research, Quarterly Progress Report, April 1-June 30, 1981; A. J. Romano, Editor, NUREG/CR-2231, BNL-NUREG-51454, Vol. 1, No. 1-2, 1980.

WULFF, W., CHENG, H. S., DIAMOND, D. J. and KHATIB-RAHBAR, M., (1981c), "A Description and Assessment of RAMONA-3B MOD.0 CYCLE4: A Computer Code with Three-Dimensional Neutron Kinetics for BWR Systems Transients," NUREG/CR-3664, BNL-NUREG-51746, Manuscript completed 1981, published 1984.

WULFF, W., (1982a), "LWR Plant Analyzer Development Program," Ch. 5 in Safety Research Programs Sponsored by the Office of Nuclear Regulatory Research, Quarterly Progress Report, January 1-March 31, 1982; A. J. Romano, Editor, NUREG/CR-2331, BNL-NUREG-51454, Vol. 2, No. 1, 1982.

WULFF, W., (1982b), "LWR Plant Analyzer Development Program," Ch. 5 in Safety Research Programs Sponsored by the Office of Nuclear Regulatory Research, Quarterly Progress Report, July 1-September 30, 1982; compiled by Allen J. Weiss, NUREG/CR-2331, BNL-NUREG-51454, Vol. 2, No. 3, 1982.

WULFF, W. (1982c), "LWR Plant Analyzer Development Program," Ch. 5 in Safety Research Programs Sponsored by the Office of Nuclear Regulatory Research, Quarterly Progress Report, October 1-December 31, 1982; compiled by Allen J. Weiss, NUREG/CR-2331, BNL-NUREG-51454, Vol. 2, No. 4, 1982.

WULFF, W., (1983a), "LWR Plant Analyzer Development Program," Ch. 5 in Safety Research Programs Sponsored by the Office of Nuclear Regulatory Research, Quarterly Progress Report, January 1-March 31, 1983; compiled by Allen J. Weiss, NUREG/CR-2331, BNL-NUREG-51454, Vol. 3, No. 1, 1983.

WULFF, W., (1983b),"LWR Plant Analyzer Development Program," Ch. 5 in Safety Research Programs Sponsored by the Office of Nuclear Regulatory Research, Quarterly Progress Report, July-September 30, 1983; compiled by Allen J. Weiss, NUREG/CR-2331, BNL-NUREG-51414, Vol. 3, No. 3, 1983.

WULFF, W. (1983c), "NRC Plant Analyzer Development," Proc. Eleventh Water Reactor Safety Research Information Meeting, held at National Bureau of Standards, Gaithersburg, MD, Oct. 24-28, 1983, U.S. Nuclear Regulatory Commission. To be published.

Wulff, W., (1983d), "LWR Plant Analyzer Development Program," Ch. 5 in Safety Research Programs Sponsored by the Office of Nuclear Regulatory Research, Quarterly Progress Report, October 1-December 31, 1983; compiled by Allen J. Weiss, NUREG/CR-2331, BNL-NUREG-51414, Vol. 3, No. 4, 1983.

Wulff, W., (1984), "LWR Plant Analyzer Development Program," Ch. 5 in Safety Research Programs Sponsored by the Office of Nuclear Regulatory Research, Quarterly Progress Report, January 1-March 31, 1983; compiled by Allen J. Weiss, NUREG/CR-2331, BNL-NUREG-51414, Vol. 4, No. 1, 1984.

6. Code Assessment and Application (Transient and LOCA Analyses)

(P. Saha, J. H. Jo, and H. R. Connell)

This project includes the independent assessment of the latest released versions of LWR safety codes such as TRAC, RELAP5, and RAMONA-3B, and the application of these codes to the simulation of plant accidents and/or transients. Two major code application tasks namely, the RESAR-3S large break LOCA study and the BWR/4 MSIV closure ATWS analysis, have been completed, and are being documented in two separate topical reports.

The TRAC-BD1/MOD1 (Version 22) code has been implemented on the BNL computer and significant progress has been made in developing a TRAC-BD1/MOD1 input deck for simulating the FIST facility. A part of the NUFREQ-NP code has also been implemented at BNL.

The major activities performed during the reporting period of April to June 1984 are described below.

6.1 Code Implementation

6.1.1 TRAC-BD1/MOD1 Implementation (H. R. Connell)

The work to make the TRAC-BD1/MOD1 code operational on the BNL CDC-7600 computer was completed. Version 21 was implemented first, but was replaced by Version 22 when this later version became available at BNL.

A considerable amount of programming to revise the INEL Cyber 176 coding to the BNL CDC-7600 was carried over from the previous TRAC-BD1 implementation work. However, the innovations in the MOD1 version of TRAC imposed new difficulties, namely the conversion to FORTRAN 5 and the use of CDC Common Memory Manager (CMM) feature.

The overlay structure of the code and the use of CMM require a computer with 300gk central memory; the BNL CDC-7600 has only 160gk. It was, therefore, necessary to implement the "fixed common lengths" version of the code and to develop a segmentation scheme for loading the code at the BNL computer. This was done and the two sample problems were successfully run. This BNL version of the code will also be provided to the General Electric Company at San Jose, California.

6.1.2 NUFREQ-NP Implementation (H. R. Connell)

The BWR stability analysis code, NUFREQ-NP, was received from Rensselaer Polytechnic Institute, and the work to make this code operational at BNL was begun.

The NUFREQ-NP code is composed of two separate codes, a Thermal Hydraulic Program System and a Nuclear Program System, both written for an IBM 370 computer.

Conversion from an IBM system to a CDC system involves extensive FORTRAN modifications as well as developing a segmentation scheme such that the code can execute in the fixed central memory length of 160g$_8$k of the BNL CDC-7600 computer.

The Thermal Hydraulic Program system has been made operational on the BNL CDC-7600, and the sample problem ran successfully. However, the central memory requirements for the Nuclear Program System are so great that implementation of this program on the CDC-7600 is perhaps impossible. The use of a BNL VAX computer is being investigated for this purpose.

6.2 Code Assessment

6.2.1 Simulation of FIST Facility with TRAC-BD1/MOD1 (J. H. Jo)

The FIST (Full Integral Simulation Test) facility (Stephens, 1982) is a BWR safety test facility which was built to investigate small break LOCA and operational transients in BWRs and to complement earlier large break LOCA test results from TLTA (Two-Loop Test Apparatus) (Letzring, 1977). The FIST program is sponsored jointly by NRC, Electric Power Research Institute (EPRI) and General Electric Company (GE).

The facility is a full BWR height, integral test facility with volume scaling of 1/624 to the BWR/6 vessel and contains a single full-size BWR fuel bundle (electrically heated). The flow areas and the fluid volumes in all regions are also closely scaled to 1/624. Figure 6.1 shows the comparison of the FIST and a BWR/6 vessel. Table 6.1 shows the list of experiments conducted in Phase 1 of the program.

The TRAC-BD1/MOD1 input deck which was used to simulate the FIST Test 6PMC2, was obtained from Idaho National Engineering Laboratory (INEL). However, the input deck was extensively modified to better represent the separator-dryer region of the test facility. The major modification was to increase the number of the radial rings from 1 to 2 (thereby increasing the number of cells per level from 2 to 4) of the VESSEL module. Figure 6.2 shows the BNL nodalization of the VESSEL. The steady state calculation is in progress with this BNL input deck. The BWR-4 MSIV closure test, i.e., Test 4PMC1, is planned to be the first experiment to be simulated.

REFERENCES

LETZRING, W. J., (1977), "BWR Blowdown/Emergency Core Cooling Program, Preliminary Facility Description Report for the BD/ECC-1A Test Phase," GEAP-23592, December 1977.

STEPHENS, A. G., (1982) "BWR Full Integral Simulation Test Program," Contract No. NRC-4-76-215, NUREG/CR-2576, December 1982.

Table 6.1 Phase 1 FIST Tests

DATE	TEST #	DESCRIPTION	INITIAL POWER (MW)	AVAIL. ECCS	COMMENTS
12/09/82	6DBA1	BWR/6 DBA	5.08	HPCS, LPCS, LPCI(1)	Reverse Flow Leak 87 sec. from LPCI.
1/19/83	6SB2	SB, w/o HPCS	5.08	LPCS, LPCI(3)	6 Deffective heater rods fail.
4/07/83 to 4/15/83	6PNC1	Nat. Circulation	Note 1	NA	Nat. Circulation characterization.
4/14/83	6SB2B	SB, w/o HPCS	5.09	LPCS, LPCI (3)	Trip at 362 sec W/ 10 TC's at 950°F.
5/10/83	6DBA1B	BWR-6 DBA	5.05	HPCS, LPCS, LPCI(1)	Peak clad temperature 703°F.
5/16/83	6PMC1	BWR-6 MSIV clos.	4.64	All	No heatup.
5/19/83	6PMC2	Sep. effects test	4.64	RC1C, LPCS, LPCI(3)	Special effects test.
5/26/83	4PMC1	BWR-4 MSIV clos.	4.35	All	No heatup.
6/01/83	6PMC2A	BWR-6 MSIV clos. w/o HPCS	4.63	RCIC, LPCS, LPCI(3)	No heatup
6/14/83	6MSB1	MS line break	4.62	HPCS, LPCS, LPCI(1)	No heatup
6/16/83	6SB1	SB, Stuck SRV	4.62	LPCS, LPCI (3)	Peak clad temp. 714°F
6/21/83	6SB2C	SB, w/o HPCS	5.05	LPCS, LPCI(3)	Peak clad temp. 925°F

Note 1: 6PNC1 was a "quasi" steady state test run at 6 different power levels, 0.5, 1.0, 1.5, 2.0, 2.5, 3.0 MW.

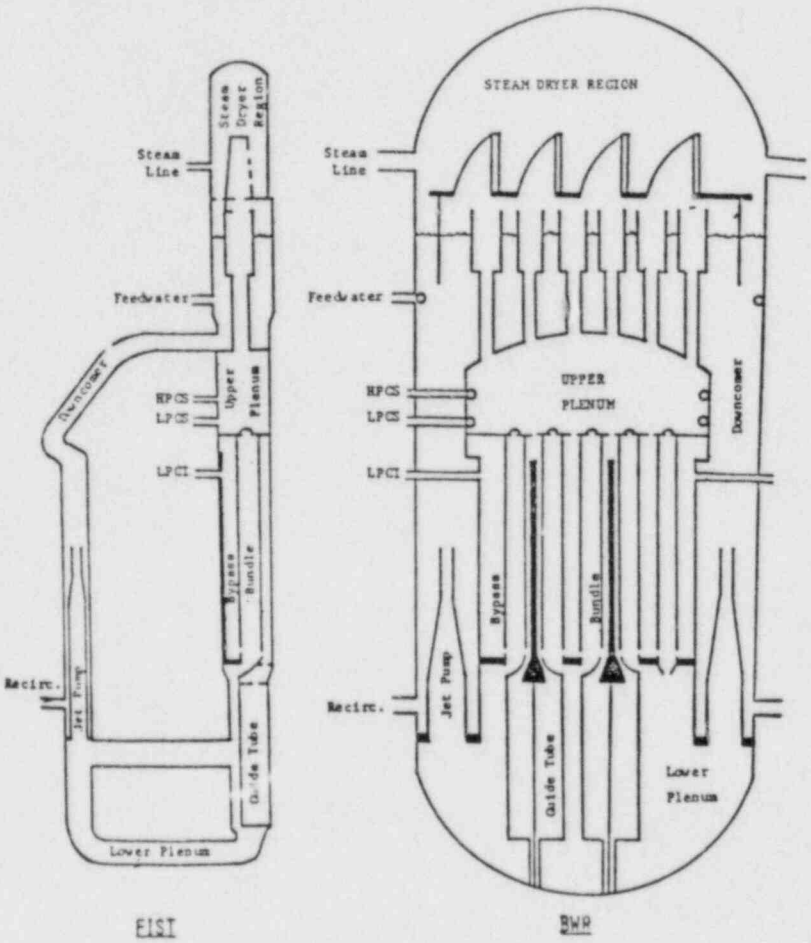

Figure 6.1 Comparison of FIST and BWR/6 Reactor Vessel.
(BNL Neg. No. 8-143-84)

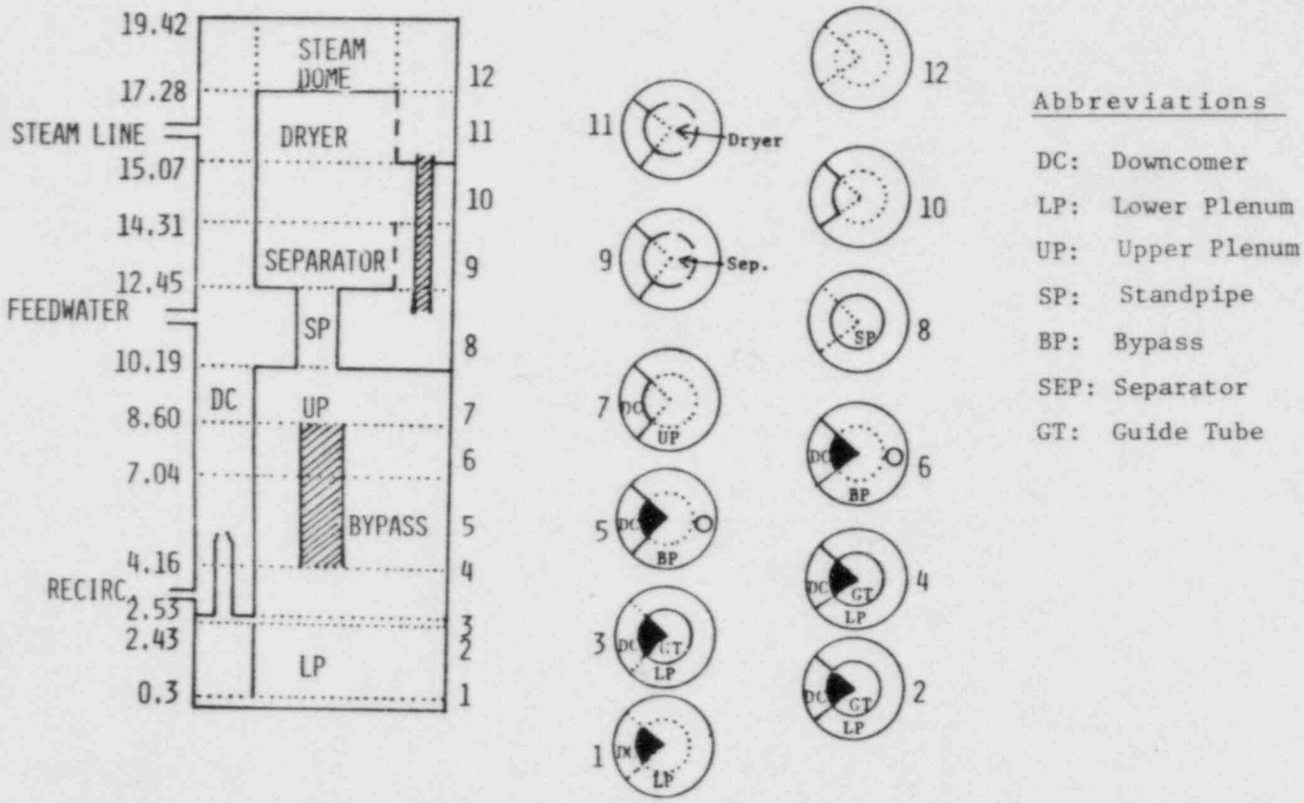

Figure 6.2 Vessel Nodalization for the FIST Facility.

7. Thermal Reactor Code Development (RAMONA-3B)

(P. Saha, L. Neymotin, G. C. Slovik, H. R. Connell, E. Cazzoli, P. Kohut and D. Cokinos)

This project includes the modifications, improvements and preliminary (or developmental) assessment of the BWR transient analysis code called RAMONA-3B. This is the only BWR systems transient code with three-dimensional neutron kinetics, and it is now available, at no cost, to U. S. organizations for the analysis of U. S. reactors.

During this reporting period of April to June 1984, several improvements and corrections have been made to the RAMONA-3B code. A two-day seminar on RAMONA-3B was also held at BNL for the benefit of the RAMONA users. Finally, significant progress has been made in the generation of 3-D neutronic cross sections for Browns Ferry Cycle 5. This last task is being jointly performed under this and another NRC program (FIN A-3273, Application of RAMONA to BWR ATWS).

The details of the progress achieved during the reporting quarter are described below:

7.1 Code Improvement/Correction

7.1.1 Recirculation Pump Model (L. Neymotin and E. Cazzoli)

During the Browns Ferry MSIV closure ATWS study under the NRC SASA program, it was discovered that the calculated recirculation pump speed did not reach near zero even after a long time after the pump trip. Comparison with Browns Ferry recirculation pump trip data also showed a deviation in the calculated pump speed at the later part (beyond 20 seconds) of the transient.

Further investigation revealed that the discrepancy was due to inadequate treatment of the pump friction torque in the present model (Wulff, 1984). A new recirculation pump model was, therefore, considered for RAMONA-3B.

The new model consists of the following non-dimensional form of the pump head and torque equations (or homologous curves) as developed earlier at BNL (Madni, 1978):

Pump Head

$$\frac{h}{\alpha^2} = C_0 + C_1 \left(\frac{\nu}{\alpha}\right) + C_2 \left(\frac{\nu}{\alpha}\right)^2 + \ldots + C_5 \left(\frac{\nu}{\alpha}\right)^5 \qquad (7.1)$$

$$\text{in the range of } 0 \leq \left|\frac{\nu}{\alpha}\right| \leq 1$$

$$\frac{h}{\nu^2} = C_o + C_1 \left(\frac{\alpha}{\nu}\right) + C_2 \left(\frac{\alpha}{\nu}\right)^2 + \ldots + C_5 \left(\frac{\alpha}{\nu}\right)^5 \qquad (7.2)$$

$$\text{in the range of } 0 \leq \left|\frac{\alpha}{\nu}\right| \leq 1$$

where

$h = H/H_R$ = Pump head/Pump rated head

$\alpha = \Omega/\Omega_R$ = Pump speed/Pump rated speed

$\nu = Q/Q_R$ = Pump flow rate/Pump rated flow rate

Pump Torque

$$\frac{\beta}{\alpha^2} = C_o + C_1 \left(\frac{\nu}{\alpha}\right) + C_2 \left(\frac{\nu}{\alpha}\right)^2 + \ldots + C_5 \left(\frac{\nu}{\alpha}\right)^5 \qquad (7.3)$$

$$\text{in the range of } 0 \leq \left|\frac{\nu}{\alpha}\right| \leq 1$$

$$\frac{\beta}{\nu^2} = C_o + C_1 \left(\frac{\alpha}{\nu}\right) + C_2 \left(\frac{\alpha}{\nu}\right)^2 + \ldots + C_5 \left(\frac{\alpha}{\nu}\right)^5 \qquad (7.4)$$

$$\text{in the range of } 0 \leq \left|\frac{\alpha}{\nu}\right| \leq 1$$

where

$\beta = \tau_{hyd}/\tau_R$ = Pump hydraulic torque/Pump rated hydraulic torque

The coefficients C_o through C_5 are the same as reported in (Madni, 1978). In addition, the following equation for pump speed is used:

$$I \frac{d\Omega}{dt} = \tau_{EL} - \tau_{hyd} - \tau_{fr} \qquad (7.5)$$

where,

I = Moment of inertia of the rotating element including shaft and impeller

τ_{EL} = Electric torque (zero after pump trip)

τ_{hyd} = Hydraulic torque

τ_{fr} = Friction torque

A polynomial equation of the form

$$\tau_{fr} = \tau_R \left(C_o + C_1\alpha + C_2\ \alpha|\alpha|\right) \qquad (7.6)$$

is used for the friction torque, and the values of the coefficients C_o through C_2 are taken from (Madni, 1978).

This new model requires the pump rated conditions (H_R, τ_R, Ω_R, Q_R) as inputs which are generally available from the pump manufacturer. In contrast to the current model, the new model does not require the recirculation loop loss coefficient which is difficult to determine.

The RAMONA-3B code has been updated and run for 150 sec. for a recirculation pump trip transient with the new model, and physically reasonable results for the recirculation pump speed and recirculation loop flow rate vs. time have been obtained. Specifically, the pump speed has reached almost zero (<0.5%) in 135 seconds and the recirculation loop flow rate has leveled at ~7% of the steady state value.

7.1.2 Void Fraction for Reactivity Calculations (L. Neymotin)

According to the RAMONA-3B nodalization schemes for hydraulics and neutronics calculations, each axial cell of a core neutronic channel coincides with a corresponding axial cell in a hydraulic channel, i.e., the number of axial neutronic and hydraulic cells is the same. The logic of the code, however, was such that an average value of void fractions over two adjacent hydraulic cells was supplied to the void reactivity calculation part of the code. Similar logic was also used in the moderator temperature evaluations for the moderator temperature reactivity feedback calculation.

The code has been run with the original and updated code versions after appropriate corrections were made, and the results for the steady state axial power profile are shown in Figure 7.1. A slight difference in the axial power distribution can be seen with the corrections; power decreased at the lower part and increased at the upper part of the core. This is physically reasonable considering positive reactivity insertion when underestimated void fraction is supplied to the neutronics for the core entrance region.

7.1.3 Static Driving Head Correction (L. Neymotin)

A correction to the static head calculation logic was made for the case when the water mixture level resides in the steam dome region. (In RAMONA-3B this region is defined as a steam filled volume just above the entrance to the Downcomer 1.) Previously, the driving head imposed by this water in the steam dome was not taken into consideration. The error would have been noticeable only in the natural circulation mode with the water level residing in the steam dome region.

7.2 RAMONA-3B Seminar (P. Saha, G. C. Slovik, L. Neymotin, H. R. Connell and D. Cokinos)

A two-day RAMONA-3B seminar was held at Brookhaven National Laboratory on May 30-31, 1984. Besides the BNL staff, eleven persons representing seven U. S. organizations attended the seminar. The BNL staff made detailed presentations on the RAMONA-3B capabilities and limitations, code models and numerics, card-by-card input description, code structure and implementation, RAMONA-3B assessment and application, and the BNL plan for future code improvements.

Responses from the seminar attendees were very positive. All agreed that RAMONA-3B with three-dimensional neutron kinetics and system simulation capability fulfills a major need in the BWR transient analysis area. An IBM-version of the code has been suggested by some of the attendees so that the code can be used by more organizations.

A copy of the hand-outs that were distributed during the seminar is available on request.

7.3 Generation of Browns Ferry Cycle 5 Nuclear Cross Sections (G. C. Slovik and P. Kohut)

The purpose of this task is to generate 3-D nuclear data or cross sections to be used in the RAMONA-3B calculations for the Browns Ferry ATWS study under the NRC SASA program. Since the fuel types in the current Browns Ferry type reactors are quite different from those in the Peach Bottom 2 reactor at the end-of-cycle 2 (for which 3-D cross sections were generated earlier at BNL), new cross sections for the Browns Ferry Cycle 5 have to be generated.

Five major fuel types were identified in Cycle 5 of the Browns Ferry nuclear reactor. Macroscopic cross sections for all of these fuel types have been calculated with the CASMO computer code which is a multi-group two-dimensional transport theory code for burn-up calculations on BWR (and PWR) assemblies. Approximately 200 CASMO calculations were required for each fuel type to generate the macroscopic cross sections over the typical range of exposures and void histories found in Cycle 5.

Work has begun in collapsing these macroscopic cross sections around specific exposure and void history combinations of Browns Ferry, Cycle 5, core using the BLEND code (Eisenhart, 1980) developed at BNL. Approximately twenty collapsed sets of cross sections will be generated and used in RAMONA-3B as the Browns Ferry Cycle 5 cross sections.

REFERENCES

EISENHART, L.D., and DIAMOND, D. J., (1980), "Automatic Generation of Cross Section Input for BWR Spatial Dynamics Calculations," BNL-NUREG-28796, November 1980.

MANDI, I.K. and CAZZOLI, E., (1978), "A Single-Phase Pump Model for Analysis of LMFBR Heat Transport Systems", NUREG/CR-0240, BNL-NUREG-50859, June 1978.

WULFF, W., et al., (1984) "A Description and Assessment of RAMONA-3B Mod. 0 Cycle 4: A Computer Code with Three-Dimensional Neutron Kinetics for BWR Transients," NUREG/CR-3664, BNL-NUREG-51746, January 1984, Section 4.4.4.4, pp. 146-149.

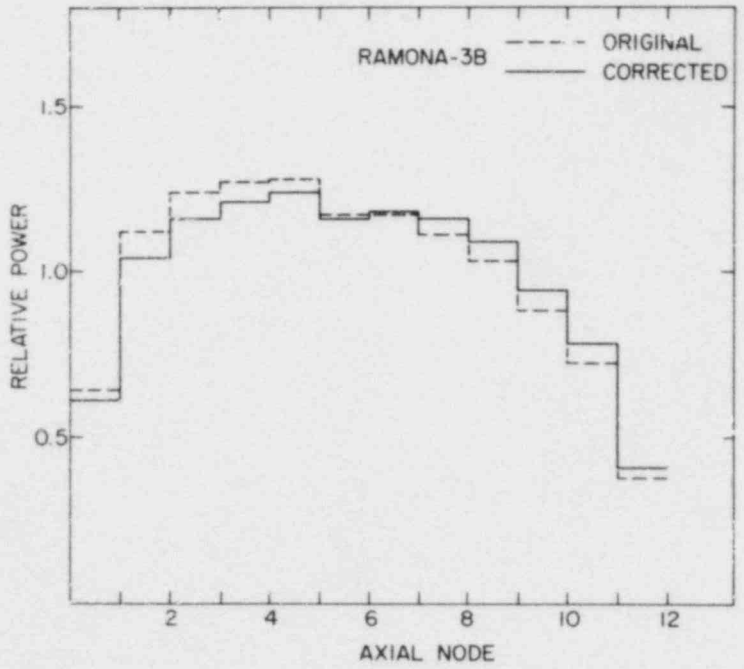

Figure 7.1 Comparison Between the Steady-State Axial Power Profiles Obtained Using the Corrected and Original Code (RAMONA-3B/MOD0/Cycle 7). (BNL Neg. No. 7-833-84)

8. Calculational Quality Assurance in Support of PTS

(P. Saha, U. S. Rohatgi and C. Yuelys-Miksis)

The objective of this project is to provide a peer review of the thermal-hydraulic calculations that have been performed at LANL (using the TRAC-PWR code) and INEL (using the RELAP5 code) for the NRC Pressurized Thermal Shock (PTS) study. Specifically, this includes a review of the plant decks and the calculations, and an assessment of the reasonableness of the results. The major activities performed during April to June 1984 are described below.

8.1 Preliminary Assessment of RELAP5 Thermal-Hydraulic Analysis of PTS Transients of H. B. Robinson Unit 2

(U. S. Rohatgi and C. Yuelys-Miksis)

Idaho National Engineering Laboratory has simulated eleven transients for the H. B. Robinson-2 PWR plant using RELAP5/MOD1.6. The scenarios for these transients were specified by Oak Ridge National Laboratory. Five of these transients are from the hot standby conditions and the remaining six are from the full power conditions. Except for Transients 9 and 11, RELAP5 calculations were made only for the early part (2000-4000 s); transient behaviors out to 7200 s were obtained by extrapolation.

In the remaining sections, the BNL comments based on the assessment of these eleven transients, as documented in the INEL informal report (Fletcher, 1983), have been summarized.

Transient 1: Main Steam Line Break from Hot Standby Conditions

The transient was initiated by a 0.093 m^2 break in the steam line of Steam Generator A. The code was successful in predicting the early sequence of events and the direction of heat transfer in the different steam generators. The calculation was terminated at 1800 seconds and the remaining part of the transient was estimated by extrapolation. The minimum downcomer fluid temperature of 386.2 K (235°F) occurred at 1026 seconds into the transient.

The uncertainties in the results are due to the condensation model, structure stored energy and multidimensional effects in the physical transient. Multidimensionality effects occur because each hot leg sees a slightly different fluid which may result in the hotter fluid going to the pressurizer, reducing the condensation there, and thereby slowing down the associated pressure drop. This higher system pressure will reduce the HPI and other safety injection flows which will result in a higher downcomer fluid temperature. This effect cannot be modeled by RELAP5. There are some other phenomena which were predicted, but not explained. These are: (1) the lag in pressure increase after the pressurizer level indicated a full pressurizer, (2) rapid drop in cold leg temperatures at 600 seconds, and (3) lack of oscillations in the cold leg fluid temperature in the presence of flow oscillations.

Transient 2: Double Ended Steam Line Break at Hot Standby

This transient was initiated by a 200% break in the steam line of Steam Generator A. The transient is quite similar to Transient 1 except for a faster pressure drop and cooling. The calculation was terminated at 1586 seconds and the rest of the transient up to 7200 seconds was predicted by extrapolation. The minimum downcomer fluid temperature of 369.8 K (206°F) occurred at 7200 seconds.

The uncertainty in the prediction is also due to the same phenomena as described in the previous transient. This calculation also showed sharp changes in cold leg temperatures and flow rates between 500-600 seconds which were not explained in the INEL report (Fletcher, 1983).

Transient 3: Stuck Open Steam Line PORV at Hot Standby

This transient is similar to the previous two steam line break transients except for a smaller size break and additional operator failure which allowed continuous injection of auxiliary feedwater throughout the transient. Most of the events were the same as in the previous two transients but occurred much later due to the smaller break. The code calculation was terminated at 3787 seconds and the remainder of the transient was predicted by extrapolation. The lowest downcomer fluid temperature of 397 K (256°F) occurred at the end of the transient at 7200 seconds.

This calculation is also subject to uncertainties due to inadequacies in describing the condensation phenomenon in the pressurizer during pressurizer fill up. Since the transient is slower and the code was run for a sufficiently long duration, the stored energy in the structure will be properly accounted for. The asymmetric behavior will still influence the transient in terms of less condensation in the pressurizer as explained in Transient 1. However, the calculation and extrapolation seem reasonable.

Transient 4: Three Steam Dump Valves Stuck Open at Full Power

This transient was also initiated by the secondary side blowdown as in the previous three transients, except that the plant was at full power conditions. The code calculation was terminated at 2500 seconds and the remainder of the transient was predicted by extrapolation. The lowest downcomer fluid temperature of 373 K (212°F) occurred at 4837 seconds.

This transient is suited to a one-dimensional analysis since the secondary side of all three steam generators secondary sides was blown down, resulting in good natural circulation in all three loops. The fluid conditions were also quite similar in all three loops. The primary side would eventually reach the saturation temperature corresponding to the ambient conditions. The code calculation and the subsequent extrapolation correctly predicted that behavior.

The calculation incurred the usual problems with condensation as the pressurizer was filling up, but the final results were not affected. Furthermore, it is not clear from the INEL report, why the nodalization was changed at 2157 seconds.

Transient 5: Overfeed with Auxiliary Feedwater at Full Power

This transient was initiated by the failure of the Auxiliary Feedwater (AFW) to come on when the Main Feedwater (MFW) was tripped. The operator manually started the auxiliary feedwater flow at 480 seconds. The code calculation was terminated at 3600 seconds and the remainder of the transient was extrapolated. The minimum downcomer temperature of 535 K (503°F) occurred at 3027 seconds.

All steam generators were available and auxiliary feedwater flowed to all of them. The transient was quite symmetric and amenable to the one-dimensional analysis of RELAP5. There was no stagnation as the Reactor Coolant Pump (RCP) stayed on and there were no large temperature variations in the primary side. There were a few minor uncertainties which were not explained in the INEL report. For example, why was there a variation in feedwater temperature for different steam generators? Why did the Steam Generator A receive the coldest feedwater? Why did the feedwater flow increase first in Steam Generator C? Despite these minor uncertainties, the results seem reasonable and the event sequence was as expected.

Transient 6: Small Hot Leg Break at Full Power

A small break (0.0635 m in diameter) at the bottom of the hot leg (Loop C with the pressurizer) initiated the transient. The code calculation was terminated at 2800 seconds and the remainder of the transient was predicted by extrapolation. The lowest downcomer fluid temperature of 310 K (100°F) occurred at 7200 seconds.

This transient exhibited strong multidimensional behavior in the beginning of the transient where a one-dimensional analysis would not be appropriate. However, since the minimum temperature occurred at the end of the transient when all the loops were stagnant, the RELAP5 formulation was adequate. The pressurizer remained empty, and so the system pressure was not affected by the condensation phenomenon in the pressurizer. The system did not repressurize and the primary side temperature reached the ECCS temperature as correctly predicted by the code calculation and extrapolation.

There are a few phenomena which need more clarification. Why is the Loop C steam generator secondary side pressure higher than the other two steam generators at the time of the initiation of motor driven auxiliary feedwater pump? Furthermore, why does this steam generator (SG-C) get most of the auxiliary feedwater and fill up earlier? Loop flows exhibit considerable oscillations before the loops are stagnant. What causes these oscillations? In addition, why is the downcomer fluid temperature so much higher than the cold leg temperatures between 1000 and 2000 seconds? The difference is on the order of 100 K.

Transient 7: Stuck Open PORV With Reactor at Full Power

This transient was initiated by a primary side upset when the PORV valve was stuck open and the primary side started to blow down. The operator action closed this valve at 600 seconds and ended the depressurization of the primary side. The remaining system worked as designed.

The calculation was terminated at 2200 seconds, when the primary side became liquid solid and there was no HPI or auxiliary feedwater flow into the system. Beyond this point, the primary side pressure would be maintained at 2535 psia (17.5 MPa) by the safety relief valve, and the primary side temperature would be controlled by the saturation temperature corresponding to the steam dump valve set pressure. The INEL report correctly showed this behavior for the extrapolations. However, there would be minor oscillations in all the fluid conditions which cannot be predicted by extrapolation. The minimum downcomer fluid temperature of 538 K (509°F) occurred at 947 seconds.

The calculation in the first 2200 seconds proceeded as expected. There were some differences in the flow behavior in three loops, which are not easily explainable. Loop C and Loop B were quite close in flow rates, temperatures and timings of events, while Loop A showed delay in initiation and termination of auxiliary feedwater (AFW). Furthermore, between 900 and 1400 seconds, Loop A experienced the coldest cold leg temperature, highest flow, and highest steam generator secondary side pressure. The natural circulation was maintained by the sinks which, in this case, were the steam generators. It is not clear how a larger flow rate was maintained in Loop A when the secondary side had probably the highest saturation temperature and the least capacity to absorb heat.

Transient 8: Small Hot Leg Break at Hot Standby

This transient is similar to Transient 6 discussed earlier. This was a primary side upset with a small hot-leg break in the pressurizer loop and system blowdown from hot standby conditions, unlike Transient 6, where the reactor was initially at full power. The remaining systems worked as designed and the operators followed the appropriate guidelines.

The calculation was terminated at 1740 s due to oscillations which would require smaller time steps and larger computer running time. The final temperature would be close to the LPI/HPI fluid temperature in the extrapolated part of the transient as cooling was due to these injections only. The minimum downcomer fluid temperature of 310 K (100°F) was estimated to occur at 7200 seconds (Fletcher, 1983).

There are a few questions about the extrapolating procedure. The sources of energy were the core power and heat transfer from the steam generator secondary side. The extrapolation predicted a constant primary side pressure and temperature up to 2700 seconds, at which time the secondary side was cooled to the saturation temperature (~464 K) and the primary side was cooled to ~375 K. Furthermore, the rate of heat transfer between the primary and secondary sides was assumed to be a constant, but in reality it

will decrease. Therefore, the primary side conditions will not remain constant until 2700 seconds but will vary. This will delay the initiation of LPI and subsequent cooling.

The calculation up to 1740 seconds seems reasonable. Although the code has the capability of modeling a break at different locations in the horizontal pipe, but to the best of our knowledge has not been assessed. The break may receive some voids even when it is not covered as some vapor may be entrained into the break flow. It is not clear if the code accounts for this entrained vapor. In addition, the code predicted oscillations at the end of the calculation, and it is not clear what caused it and if they were physical? It is important as these oscillations warmed up the downcomer fluid. However, it only affected the lowest downcomer fluid temperature reached during the code calculation which is higher than the downcomer fluid temperature at the end of the transient.

Transient 9: Steam Generator Tube Rupture at Hot Standby

In this transient, a single tube in Steam Generator A ruptured near the cold leg side creating two breaks from which the primary side fluid flowed into the secondary side. As the secondary side pressure was very close to the saturation pressure of the primary side, the flow was always single phase liquid and not choked. The calculation was run for 7200 seconds and there was no need for extrapolation. The minimum downcomer fluid temperature of 465 K (378°F) occurred at the end of the transient at 7200 seconds.

The calculation exhibited considerable oscillations in the mass flow rates and temperatures after 3000 seconds. These are not physical as stated in the INEL report and are due to code limitations. This problem was circumvented by injecting the HPI flow in the vessel downcomer and the results exhibited no oscillation. The new flow parameters agreed well with the corresponding values in the initial calculation. However, this adjustment in the model will preclude any warming up of the HPI fluid due to cold leg walls.

Loop A had the lowest flow rate, and it was mostly affected by the HPI flow. The modeling change of directly injecting HPI into the vessel also had the most influence on Loop A fluid conditions. In the real situation, however, there may be some delay due to the fluid transit time, and a finer nodalization between the HPI point and the vessel may account for it. The original calculation predicted a lower downcomer fluid temperature, and additional sensitivity studies, such as finer nodalization, should have been made before the injection point was shifted to the vessel.

Transient 10: Steam Generator Tube Rupture at Full Power

This transient is similar to the previous transient (Transient No. 9) except that the reactor was at full power. There was a single tube rupture near the cold leg side of the steam generator A. However, the course of this transient was quite different from the similar transient at hot standby.

This calculation was terminated at 2400 seconds and the remaining prediction of this transient until 7200 seconds was by extrapolation. The pumps were always running; so there was good mixing and less variation in the fluid conditions in different loops. Furthermore, the steam generators were not receiving any feedwater after 1200 seconds, and the secondary and primary side fluid conditions were governed by the steam generator dump valve setting (7 MPa). The secondary side temperature at this pressure is 559 K and the primary side temperature will remain close to it. The extrapolation seems reasonable.

This transient is quite mild as the temperature variations in different loops throughout the transient were less than 10K. The only uncertainty is the increased heat transfer in the steam generator which is explained as flow reversal due to condensation in the secondary side. However, it is not clear what caused it since there was no feedwater coming in. This event only caused a temperature variation of 3 K. The calculation, in general, looks reasonable.

Transient 11: Loss of Secondary Heat Sink with Primary System Feed and Bleed Recovery at Full Power

This transient was initiated by the failure of the secondary side feedwater system to deliver any feedwater; the situation was made worse by by the operator action of feed and bleed, thereby cooling the primary side. This calculation was terminated at 8100 seconds and further prediction of the transient until 11000 seconds was by extrapolation. The minimum downcomer fluid temperature occurred at the end of the transient at 11000 seconds and it was 422 K (300°F).

The extrapolation seems reasonable as pressure drop was due to contraction of liquid and loss of fluid at the PORV. The main energy loss was at the PORV and energy addition was due to core power and ECC injections. As the system pressure was decreasing, the flow at the PORV decreased while injection flow increased. At some pressure, there would be a balance between liquid contraction and the PORV flow against injection flow rate, which would determine the final pressure. However, the system temperature continued to decrease.

The first 8100 seconds of the transient was computed by the code. The sequence of events were as expected for this type of transient. There are, however, a few phenomena which have not been clearly explained in the INEL report. There are contradictory statements about the direction of heat transfer in the steam generator. If the steam generator secondary sides are also the heat source, what maintains the natural circulation in Loops A and B? Furthermore, if the heat transfer is negligible in the SG-A and SG-B, what is maintaining the natural circulation? The cold leg flow in Loop C cannot be stagnant as stated in the report, but it should be at least equal to the HPI flow. Furthermore, it is not clear why the normalized level of the SG-B and SG-C secondary side had very little effect of feedwater header blowdown while there was a large effect on the SG-A secondary side level? This transient will also have strong multidimensional effects due to PORV

flow affecting Loop C first. However, the calculation predicted flow reversal of almost the same magnitude for all three loops due to PORV opening. In reality, Loop C is expected to be affected the most.

Summary and Conclusion

RELAP5 is a one-dimensional code and it cannot model the asymmetric behavior of some of the transients. The code always predicts the same fluid conditions for all of the hot legs. In some of the transients the cold legs fluid conditions are quite different and the asymmetry may be carried through the core to the corresponding hot legs. This usually occurs in the transients which have flow stagnation in some of the loops. Most of the transients computed by INEL had asymmetric initiators but only the steam line break transients had flow stagnation and large differences in cold leg fluid conditions. These transients should be assessed either with a multidimensional code or a limiting one-dimensional analysis with no mixing in the vessel for estimating the uncertainty due to multidimensionality of the transients.

Two other major items which are common to all the transients are the condensation effect in the pressurizer and steam generator secondary side, and the effect of stored energy in the structure. INEL has made a reasonable compromise in modeling the pressurizer filling phenomenon. The code generally overpredicts the condensation, but in the case of pressurizer filling, the calculation maintained a good condensation rate for the first volume and the remaining filling is by adiabatic compression. There is a need to assess the code's ability to predict the pressurizer filling rate with separate effect tests. It was observed from the review of the Calvert Cliffs PTS transients (Jo, 1984) that the stored energy in the structures influenced the course of transients between 2000 s to 4000 s. This will be more significant for hot standby conditions where the core power is less and the structure stored energy is a much larger fraction of the total energy. The calculation should be continued at least up to 4000 s before the results are extrapolated. Note that the rate of heat transfer from the structure varies as the transient proceeds.

REFERENCES

FLETCHER, C.D., et al., (1983) "RELAP5 Thermal-Hydraulic Analysis of Pressurized Thermal Shock Sequences for the H. B. Robinson Unite 2 Pressurized Water Reactor," EGG-SAAM-6476, December 1983.

JO, J., et al., (1984) "Review of TRAC Calculations for Calvert Cliffs PTS Study," BNL-NUREG report to be published, 1984.

II. DIVISION OF ENGINEERING TECHNOLOGY

SUMMARY

Stress Corrosion Cracking of PWR Steam Generator Tubing

The experimental program on stress corrosion cracking (SCC) at Brookhaven National Laboratory (BNL) is aimed at the development of a quantitative model for predicting the behavior of Inconel 600 tubing in high temperature aqueous media. Much of this has been done in an ongoing experimental program in which empirical relationships are being established between SCC failure time or crack velocity and factors influencing cracking. These include stress, strain and environmental and metallurgical variables. Environments are related to the ingredients of primary or secondary water. Cold work of Alloy 600 is included, and activation energies are determined.

SSC was earlier found in four U-bends of production tubing exposed in deaerated, pure water at 315°C, and provided a continuous Arrhenius plot from 365°C to 315°C. One or two more cracks occurred during this quarter. CERT in secondary water ingredients and tests at constant load were not active during this period. Computer programs remain available for handling the proposed model used for predictive purposes for Inconel 600 steam generator tubing, but the CERT data have to be improved before this can become reliable. Simulated denting tests remain in progress. Model verification with tubing from the Surry steam generator at PNL is still strongly advocated.

In primary water, important observations of strain rate effects in CERT have been made.

Probability Based Load Combinations for Design of Category I Structures

The probability-based load combination criteria for design of concrete containment structures have been developed. The details of the proposed criteria are described in a draft report entitled, "Probability-Based Load Combination Criteria for Design of Concrete Containment Structures." This draft report is currently under review.

A comparison of the current ASME code and proposed criteria has been carried out. The reliability analysis results show that the overall limit state probabilities for the containments designed by the proposed criteria are much closer to each other. These results are expected because the load factors in the proposed criteria are obtained from the minimization.

Mechanical Piping Benchmarking Problems

A preliminary copy of the report entitled, "Alternate Procedures for the Seismic Analysis of Multiply Supported Piping Systems," was prepared and issued to select reviewers. The report describes the entire Multiple Supported Piping Study. The three additional tasks under this effort were completed. A summary of the key results from the Multiple Supported Piping Study, including the three additional tasks, was presented to the PVRC Committee for Piping at their New York meeting.

Identification of Age Related Failure Modes

The objective of this program is to determine what aging and service wear effects are likely to impair plant safety, and what methods of inspection and surveillance will be effective in detecting significant aging effects.

The first groups of components to be addressed are small motors in mild environments, battery chargers/inverters, and circuit breakers and relays.

The program for each component will proceed through three phases: a reseach phase, an experimental phase, and an evaluation and conclusion phase. At the end of this quarter, the motor research phase is 50% completed, and the experimental phase will be conducted in the next quarter.

9. Stress Corrosion Cracking of PWR Steam Generator Tubing

(D. van Rooyen)

The objective of this program is to develop quantitative data to serve as a predictive basis for determining the useful life of Alloy 600 tubing in service. For this purpose, tests are being run on production tubing of Inconel 600 at different carbon levels to examine the various factors that influence the cracking of tubing. Verification is planned with tubing to be obtained from a decommissioned steam generator.

The present experimental program addresses two specific conditions, i.e., 1) residual stress conditions where deformation occurs but is no longer active, such as when denting is stopped and 2) where plastic deformation of the metal continues, as would occur during active denting. Laboratory media consist of pure water as well as solutions to simulate environments that would apply in service; tubing from actual production is used in carrying out these tests.The environments include both normal and "off" chemistries for primary and secondary water. Material condition also includes various degrees of cold work.

9.1 Constant Load

No experimental work was done in this area during this quarter, but refinements in the calculations of the applied cross-sectional stress in earlier tests have been made. The existing curves have been re-plotted for inclusion in future reports. The corrections give a slight increase in stress for a given failure time.

9.2 CERT

CERT data on SCC require a better distinction between the initiation and propagation stages than can be achieved by our present extrapolation technique. Corrections are needed to improve the quantitative determination of SCC induction times. New data confirm an activation energy of 33 Kcal/mole for crack growth, pending the introduction of a better correction in the calculation.

Data for CERT in primary water are sufficiently complete to show trends for some of the ingredients, principally the effect of H_2, H_3BO_3 and pH. AVT data are less clear.

Several additional experiments have been run in primary water at different strain rates. These have shown that the percentage of the fracture surface that represents IGSCC increases inversely with strain rate. Certain rates, which depend on the condition of the material and the temperature, can be outside the region where susceptibility is found and can give wrong results.

9.3 Dents

We have discontinued plans for the new test that would permit simulation of an active dent. Static dents continue in test.

9.4 U-bends

Split tube type U-bends at lower temperatures continue to supplement the existing data in the range 325°C-365°C. The possibility remains that the carbon level of the Inconel influences the crack initiation/temperature relationship. The larger number of replicate samples that have been exposed in water at 315°C have now shown cracking for 0.01, 0.02, and 0.03% carbon, but not yet at 0.05% carbon. The 0.01% material is now almost completely cracked.

9.5 Future Work

Future work will be the continuation of long-term tests. However, it is strongly recommended that work on the model, especially in crack propagation rates, be re-started to complete the quantitative relationships. These may be simplified by limited further work, and without this additional effort the work to date may lose much of its potential application. Verification with tubes from service is still pending -- tubes should be provided from the Surry or other steam generators.

10. Probability Based Load Combinations for Design of Category I Structures

(H. Hwang, M. Reich, J. Pires, P. C. Wang,
M. Shinozuka, B. Ellingwood and S. Kao)

10.1 Load Combination Criteria for Design of Concrete Containments

The probability-based load combination criteria for design of concrete containment structures have been developed. The proposed criteria are in a load and resistance factor design (LRFD) format. In order to test the performance objectives of the proposed criteria, four representative structures are selected using a Latin hypercube sampling technique. Next, the reliability analysis method developed by Brookhaven National Laboratory is employed to assess the reliability of these representative containments. Furthermore, an objective function is defined and a minimization technique is developed in order to find the optimum load factors. The load factors for accident pressure due to LOCA and safe shutdown earthquake are derived for three target limit state probabilities. Other load factors are also discussed on the basis of prior experience with probability-based design criteria for ordinary building construction. Finally, tentative load combinaton design criteria are recommended. The details of the proposed criteria are described in a draft report entitled "Probability-based Load Combination Criteria for Design of Concrete Containment Structures". This draft report is currently under review by the review panels listed in Section 10.3.

Tentative design load combinations corresponding to a target limit state probability of 1.0×10^{-6}, mean values of material strengths, and $a_{max} = 2a_{SSE}$ for PWR containments are:

$$\left.\begin{aligned} &1.2\ D + 1.6\ L + T_o + R_o \\ &0.9\ D + 1.1\ P_a + T_a + R_a \\ &1.2\ D + L + 1.6\ E_{ss} + T_o + R_o \\ &0.9\ D - 1.6\ E_{ss} \end{aligned}\right\} \leq \phi_i\ R_i \qquad (10.1)$$

It is clear that the use of such criteria would entail no major change in the way that routine structural design calculations are performed. However, in contrast to existing design procedures, the proposed criteria are risk-consistent and have a well-established rationale.

The major features of the proposed load combination design criteria are summarized as follows:

1. The load combinations are in a Load and Resistance Factor Design (LRFD) format together with the principal load-companion loads concept.

2. Load factors and resistance factors are, in general, selected on the basis of limit states and a target limit state probability. In this study, the resistance factors and some load factors are preassigned to simplify the optimization of the design criteria.

3. The load factor for accidental pressure, γ_p, is equal to 1.1 for $P_{f,T} = 1.0 \times 10^{-6}$ and mean values of the material strengths. This new γ_p is smaller than 1.5 used in current design criteria. However, if the variation of the material strength are included, the load factor for accidental pressure will be 1.2.

4. One design earthquake, i.e., SSE, is selected to represent seismic hazards. In current practice, however, two kinds of design earthquake, i.e., SSE and OBE are employed. Furthermore, the annual probability of exceeding the SSE is assumed to be 4×10^{-4} per year. For $P_{f,T} = 1.0 \times 10^{-6}$, the load factor for SSE is equal to 1.6, if $a_{max} = 2a_{SSE}$; it will be equal to 2.4, if $a_{max} = 3a_{SSE}$.

5. The load combination involving both accidental pressure and SSE, i.e., abnormal/extreme environmental conditions in the current ASME code, is not recommended for inclusions in the proposed design criteria.

6. The dead load factor, is set to be 1.2 or 0.9 depending on whether or not dead load has a stabilizing effect. Furthermore, for permanent equipment loads, which currently are considered as dead loads, the load factor is set to be 1.0.

7. The live load factor is set to be 1.6 or 1.0 depending on if it is a principal load or a companion load.

8. The load factor γ_{ps} on the prestress effect is set equal to 1.0 if the limit state is ductile. However, if the prestress stabilizes the structure or has a beneficial effect (e.g., shear), γ_{ps} is set to be 0.9.

9. The load factors for temperature loads either due to operating or accidental conditions are set equal to 1.0.

10. The load factors for those loads which produce only local effects on structures, are tentatively set equal to 1.0.

11. The nontornadic wind load is not recommended for inclusion in the load combinations. The load factor for tornado loads is set equal to 1.0.

10.2 A Comparison of ASME Code and Proposed Criteria

ASME Code

For design of a reinforced concrete containment subjected to dead load, accidental pressure due to LOCA and earthquake ground acceleration, the current ASME code requires that a designer should provide structural resistance against the following load combinations:

A. Service Load Category

1. Severe environmental

$1.0\ D + 1.0\ E_o$

B. Factored Load Category

2. Extreme environmental

$1.0\ D + 1.0\ E_{ss}$

3. Abnormal

$1.0\ D + 1.5\ P_a$

4. Abnormal/severe environmental

$1.0\ D + 1.25\ P_a + 1.25\ E_o$

5. Abnormal/extreme environmental

$1.0 + 1.0\ P_a + 1.0\ E_{ss}$

in which E_o is the load effect due to operating basis earthquake (OBE). It is assumed that $E_o = 1/2\ E_{ss}$. For this comparison, samples 1 and 3 as indicated in the previous quarter report are used.

The design of containments is carried out as below. The element stress resultants for dead load and accidental pressure are obtained from static finite element analysis. For seismic analysis, the response spectrum analysis method is employed. The horizontal and vertical response spectra used in this study are those specified in the Regulatory Guide 1.60. The damping ratio is taken to be 7 percent of critical for SSE and 4 percent of critical for OBE as specified in the Regulatory Guide 1.61. The square root of the sum of squares (SRSS) is used to combine the responses in three directions.

For this comparison only the design with respect to membrane force and/or bending moment is considered. From the analysis it is concluded that the most critical elements, which requires the largest amount of rebars, are element 102 in the hoop direction and element 6 in the meridional direction.

The stresses under various load combinations are shown in Table 10.1. The stress distribution across the section is assumed to be linear.

The allowable stresses for rebars and concrete under service and factored load categories specified in the ASME codes are as follows:

service load category:

$$f_s \leqslant 0.5\ f_y$$

$$f_c \leqslant 0.40\ f'_c \text{ (membrane)} \qquad (10.2)$$

$$f_c \leqslant 0.45\ f'_c \text{ (membrane plus bending)}$$

factored loading category:

$$f_s \leqslant 0.9\ f_y$$

$$f_c \leqslant 0.60\ f'_c \text{ (membrane)} \qquad (10.3)$$

$$f_c \leqslant 0.75\ f'_c \text{ (membrane plus bending)}$$

where

f_s: stress in reinforcing steel
f_c: concrete compressive stress at the extreme fiber of the cross section.

Based on the element stresses in Table 10.1 and the allowable stresses described above, the amount of the minimum required rebar area are shown in Table 10.2, where the governing load combination is also indicated.

Proposed Criteria

For $P_{f,T} = 1.0 \times 10^{-6}$, and mean values of the material strengths, and $a_{max} = 2a_{SSE}$, the proposed load combination for design of the concrete containments are as follows:

$$\begin{aligned} &0.9\ D + 1.1\ P_a \\ &1.2\ D + 1.6\ E_{SS} \\ &0.9\ D - 1.6\ E_{SS} \end{aligned} \qquad (10.4)$$

Using this recommended load combination and the proposed design procedure, the minimum required rebar area in the most critical elements and the governing load combinations are also shown in Table 10.2. It can be seen from this table, the proposed code results in less amount of reinforcing bars except one case.

Reliability assessments of containments designed by the ASME code and the proposed criteria are carried out by the method developed by BNL. The de-

tails of these assessments are described in the report. The results of the reliability assessments of the containment structures are shown in Table 10.3 and Table 10.4, respectively. It can be seen from these tables, the overall limit state probabilities for the two containments designed by ASME code are quite different, 2.15×10^{-6} vs. 6.89×10^{-18} (Table 10.3) while the overall limit state probabilities for the containments designed by the proposed code are much closer to each other, 7.26×10^{-7} vs. 2.22×10^{-7} (Table 10.4). The results are expected because the load factors in the proposed load combination criteria are obtained from the minimization.

10.3 Peer Review Panel

A peer review panel for the load combination program has been formed. This review panel consists of nine members as follows:

1. J. P. Allen
   Stone & Webster Engineering Corp.
2. Gerhard Haaijer
   American Institute of Steel Construction, Inc.
3. Kenneth Y. Lee
   Bechtel Power Co.
4. Clarence A. Moorre
   EG&G Idaho, Inc.
5. Frederick L. Moreadith
   EG&G Idaho, Inc.
6. John Stevenson
   Stevenson & Associates
7. John C. Tsai
   Offshore Power Systems
8. Joseph J. Ucciferro
   United Engineers & Constructors, Inc.
9. Adolf Walser
   Sargent & Lundy

The first peer review panel meeting was held on June 29, 1984 at United Engineering Center, New York City. In the meeting the progress to date was presented to and discussed with the review panel.

Table 10.1 Element Stresses Under ASME Load Combinations.

Load Combination	Element Stresses	Sample 1 X (Element) 102	Sample 1 Y (Element) 6	Sample 3 X (Element) 102	Sample 3 Y (Element) 6
1.0 D+ 1.0 E_o	σ(psi)	10.1	134.6	25.2	458.1
	m(lb-in/in)	8.96 3	6.945 4	2.83 3	1.929 5
1.0 D + 1.0 E_{SS}	σ	15.5	232.0	39.6	825.5
	m	1.79 3	9.576 4	4.26 3	2.886 5
1.0 D + 1.5 P_a	σ	1152.1	520.8	1106.8	331.4
	m	1.24 3	5.481 5	8.19 3	5.478 5
1.0 D + 1.25 P_a + 1.25 E_{SS}	σ	971.5	646.0	952.4	1069.3
	m	2.102 4	5.121 5	1.003 4	6.752 5
1.0 D + 1.0 P_a + 1.0 E_{SS}	σ	782.8	606.1	776.6	1182.1
	m	9.74 3	4.316 5	9.16 3	6.400 5

NOTE: 8.96 3 = 8.96×10^3.

Table 10.2 Comparison of Required Rebar Area.

Sample	Direction	A_s (in^2/in)	
		ASME Code	Proposed Code
1	X	0.577 (1.0 D + 1.5 P_a)	0.452 (0.9 D + 1.1 P_a)
	Y	0.566 (1.0 D + 1.25 P_a + 1.25 E_o)	0.303 (0.9 D + 1.1 P_a)
3	X	0.557 (1.0 D + 1.5 P_a)	0.433 (0.9 D + 1.1 P_a)
	Y	0.895 (1.0 D + 1.0 P_a + 1.0 E_{SS})	1.00 (0.9 D - 1.6 E_{SS})

Table 10.3 Reliability Assessments of Containments Designed by ASME Code.

	Load Combination	Expected Number of Occurrences	Conditional Limit State Probability	Unconditional Limit State Probability	Critical Elements
Sample 1	$D + P_a$	6.72 -2	6.71 -23	4.51 -24	97,...120
	D + E	4.36 -1	1.58 -17	6.89 -18	6,7,18,19
	$D + P_a + E$	2.81 -8	3.22 -13	9.04 -21	6,7,18,19
	Overall			6.89 -18	
Sample 3	$D + P_a$	6.72 -2	2.68 -20	1.80 -21	97,...120
	D + E	8.00 0	2.69 -7	2.15 -6	6,7,18,19
	$D + P_a + E$	5.22 -7	3.32 -7	1.73 -13	6,7,18,19
	Overall			2.15 -6	

NOTE: $a_{max} = 2a_{SSE}$.

Table 10.4 Reliability Assessments of Containments Designed by Proposed Criteria.

	Load Combination	Expected Number of Occurrences	Conditional Limit State Probability	Unconditional Limit State Probability	Critical Elements
Sample 1	$D + P_a$	6.72 -2	2.52 -6	1.69 -7	97,...120
	$D + E$	4.36 -1	1.21 -7	5.27 -8	6,7,18,19
	$D + P_a + E$	2.81 -8	5.41 -3	1.52 -10	6,7,18,19
	Overall			2.22 -7	
Sample 3	$D + P_a$	6.72 -2	2.35 -9	1.58 -10	97,...120
	$D + E$	8.00 0	9.07 -8	7.26 -7	6,7,18,19
	$D + P_a + E$	5.22 -7	1.17 -7	6.11 -14	6,7,18,19
	Overall			7.26 -7	

NOTE: $a_{max} = 2a_{SSE}$.

11. Mechanical Piping Benchmark Problems

(P. Bezler, M. Subudhi, Y.K. Wang and S. Shteyngart)

11.1 Physical Benchmark Development

The physical benchmark development effort continued to receive only cursory attention during this period owing to the need to expedite completion of the Multiple Supported Piping Study. For the most part, efforts were made to assure that all the information necessary to perform an evaluation of the NRC/EPRI Main Pipe Line 1 were available at BNL. Towards this end, ANCO was requested to provide a comprehensive list of all instrumentation with as-built locations. This information was received at the end of the period and will be used to revise the analytical model of the system. The input forcing function data, previously transmitted by ANCO, was reviewed. This data includes time history records of the acceleration of each sled in the forcing direction and displacement records of the two end point sleds (S1 & S4). It will be necessary to develop the displacement records for the two inboard sleds (S2 & S3) from the acceleration records, using the Trifunac Methods, prior to the benchmark evaluation. This effort was initiated at the end of this period.

11.2 Multiple Supported Piping System

The total project resources were devoted to the Multiple Supported Piping Study. All the data was processed and a report describing the entire study was prepared. A draft of this report was transmitted to and reviewed by the NRC Technical Monitor. Following the review, the corrected draft was submitted for preparation of preliminary copies and transmitted to PVRC committee members and others designated by the NRC Technical Monitor. The report is entitled, "Alternate Procedures For the Seismic Analysis of Multiply Supported Piping Systems", dated May 1984.

The report provides a complete description of the entire study and tabulations of all the results. The following recommendations concerning the use of the Independent Supported Motion method of analysis were advanced. These recommendations are based on the BNL evaluation of all the piping system results including those developed for the BNL models. It is felt that adoption of these recommendations would provide estimates for the total response which are reduced by a factor of two or more as compared to those developed using the current SRP methodology.

(i) Dynamic Component of Response

(a) The independent support motion response spectrum method should be certified as acceptable for the evaluation of the dynamic component of response.

(b) SRSS combination between support group contributions should be adopted in the independent support motion response spectrum analysis.

(ii) Pseudo-Static Component of Response

For displacements, pipe moments and support forces

(a) Method 5 (grouping by elevations) with absolute combination between groups should be used for preliminary design.

(b) Method 4 (grouping by attachment points) with absolute combination between groups should be used for final design.

For accelerations

(a) Absolute combination between support groups should be adopted.

(iii) Combined Response

(a) SRSS combination between the dynamic and static components of the response should be adopted.

As mentioned in the last quarterly, three additional tasks were undertaken in this study. These involved an evaluation of the "Center of Mass Approach", an assessment of the study results for critical locations and a application of the independent support motion methodology to a modified form of the AFW model. All calculations for these tasks were completed during the period. A letter report detailing these results is in preparation.

The preliminary copy of the study report was completed and issued in time for the PVRC Committee for Piping meeting in New York in May. A description of the study results as well as a description of the key results for the additional tasks were presented to the committee at that meeting.

At the request of the NRC Technical Monitor a paper entitled, "Standard Problems to Evaluate Piping Response Computer Codes", was prepared and submitted for inclusion at the MITI-USNRC Seismic Information Exchange Meeting to be held in Palo Alto, CA., in July 1984. It is anticipated that the paper will be accepted and presented at that meeting.

12. Identification of Age Related Failure Modes
(J.H. Taylor)

The objectives of this program are twofold: 1) to determine what aging and service wear effects are likely to impair plant safety, and 2) to determine what methods of inspection and surveillance will be effective in detecting significant aging effects prior to the loss of safety function so that proper maintenance and timely repair or replacement can be implemented.

The objectives mentioned above will be obtained by addressing components used in nuclear power plants on an individual basis. The selection of components to be studied will be made by using risk analysis, failure histories, special NRC interests, and expert judgement. The components to be addressed are small motors in mild environments, battery chargers/inverters, circuit breakers and relays.

The program will proceed through three phases for each component: review of operating data, aging assessment, and recommendation for surveillance and monitoring. As of the end of the third quarter of FY 1984, significant progress has been made on the motors, which is detailed below. Work on the other components is scheduled for the next quarter.

12.1 Review of Operating Data - Motors (M. Subudhi, L. Burns)

The acquisition of motors (and other components for future use) is being pursued at operating and decommissioned reactors. Some motors have been identified at a decommissioned plant. They are of an older design and their relevancy to contemporary equipment is under evaluation.

Available sources of information are being researched to provide input to the scope and type of examinations to be conducted and towards defining the functional parameters important for defect characterization, and determination of the aging and service wear effects that are likely to impair plant safety. Typical examples of the sources of information are failure analyses and reports by other national laboratories, licensees, architect engineers, and equipment manufacturers. Preliminary results indicate that aging is not a problem that affects the performance of motors. That is, motor failures are caused not by aging but by improper maintenance or by external stresses, such as failures of the driven equipment. A NUREG report will be issued in the first quarter of FY 1985.

12.2 Aging Assessment - Motors (F. Cifuentes and J. Curreri)

A test plan has been prepared, which includes visual examinations, operational tests, and seismic testing according to a generic floor response spectra. This testing will be conducted at BNL. The test apparatus has been assembled and the testing will be conducted in the fourth quarter of FY 1984.

III. DIVISION OF RISK ANALYSIS AND OPERATIONS

SUMMARY

Analysis of Human Error Data for Nuclear Power Plant Safety Related Events

Brookhaven National Laboratory has been tasked in this program to develop and apply realistic human performance data and models to help evaluate the human's role in nuclear power plant (NPP) safety. To meet this objective, the major current efforts are being placed in the following areas of investigation, namely:

- The use of Performance Shaping Factors (PSFs) and quantified expert judgment in the evaluation of human reliability - the Success Likelihood Index Method (SLIM).

- The development and testing of the Multiple Sequential Failure (MSF) Model.

- The usefulness of Probabilistic Risk Assessment (PRA) related human reliability data in resolving human factors regulatory issues.

As a result of these efforts, BNL has developed several documents which report on the findings in the above areas, namely:

- Human Error Probability Estimation Using Licensee Event Reports (NUREG/CR-3519).

- SLIM-MAUD: An Approach to Assessing Human Error Probabilities Using Structured Expert Judgment (NUREG/CR-3518).

Human Factors Aspects of Safety/Safeguards Interactions

Brookhaven National Laboratory has been tasked in this program to describe potential staff interaction problems during safety-related events to prevent or mitigate those problems. In addition, the nature of these interactions is to be examined to identify any performance deficiencies or conflicts.

Emergency Action Levels

Brookhaven National Laboratory has been tasked in this program to develop guidance for Emergency Action Levels (EALs) that can be integrated into Emer-

gency Operating Procedure (EOP) guidelines. From this guidance, a method will be developed that can be applied by licensees to verify that the EALs incorporated into their EOPs are usable in the control room under accident conditions. This should result in a reliable and timely basis for declaring emergencies without being too complex or burdensome to those who are trying to safely mitigate an accident. Thus far, a preliminary assessment has been made to integrate EALs and EOPs based on the degradation of the fission product barrier criteria.

Protective Action Decisionmaking

In this program, BNL staff are developing a technical basis for NRC guidance on protective action decisionmaking based on an evaluation of the consequences of nuclear power plant accidents. Potential actions under consideration include sheltering, evacuation, and relocation. In the past, specific recommendations have proven to be difficult to justify because of uncertainties in potential accident sequences. Consequently, BNL will establish strategies appropriate to those sequences for which emergency planning is necessary, emphasizing credible failure modes, links to emergency action levels based on in-plant observables and containment status, and other factors such as weather. A final NUREG report will be written in a manner understandable to laypeople.

13. Analysis of Human Error Data for Nuclear Power Plant Safety Related Events

(W. J. Luckas, Jr.)

Brookhaven National Laboratory (BNL) has been tasked in this program to develop and apply realistic human performance data and models to help quantify and qualify the human's role in nuclear power plant (NPP) safety. To meet this objective, the major current efforts are being placed in the following areas of investigation, namely:

- The use of Performance Shaping Factors (PSFs) and quantified expert judgement in the evaluation of human reliability - the Success Likelihood Index Method (SLIM).
- The development of the Multiple Sequential Failure (MSF) Model.
- The usefulness of Probabilistic Risk Assessment (PRA) related human reliability data in resolving human factors regulatory issues.

13.1 Success Likelihood Index Method (SLIM) Development

(E. A. Rosa)

The use of Performance Shaping Factors (PSFs) and quantified expert judgment using SLIM is important in the evaluation of human reliability. It should be noted that the amount of authentic quantitative human reliability data that exists is small (and is likely to remain small for the foreseeable future). It is therefore likely that subjective judgment and extrapolation will continue to play an important part. Nevertheless, present extrapolation techniques are covert, unsystematic, and rely on the knowledge of a limited number of judges. They do not systematically take into account the ways in which PSFs combine together to affect the probability of success in particular situations. Moreover, certain tasks cannot effectively be quantified using reductionist approaches. For these tasks, involving diagnosis, decision making and other cognitive activities, a holistic technique will probably be necessary.

Quantified subjective judgment has emerged from the previous analysis as being of critical importance for human reliability evaluation. SLIM is a quantified subjective judgment approach which uses PSFs as comprising any or all of the factors which combine to produce the observed likelihood of success. The basic premise of the approach is that when an expert judge (or judges) evaluate(s) the likelihood that a particular task will succeed, he or she is essentially considering the utility of the combination of PSFs in the situation of interest in either enhancing or degrading reliability. SLIM has the means of positioning a task on a subjective scale of likelihood of success, which is subsequently transformed to a probability scale. This positioning is derived by considering the judges' perceptions of the effects of the PSF in determining task reliability. NUREG/CR-2986 documents the initial appraisal of SLIM.

During the third quarter of FY 1984, the draft of NUREG/CR-3518 entitled "SLIM-MAUD: An Approach to Assessing Human Error Probabilities Using Structured Judgment," was finalized. The addition of Multi- Attribute Utility Decomposition (MAUD) to the basic SLIM procedure represents the incorporation of an interactive microcomputer based program into the elicitation procedures so that assessors may generate their own PSFs. The assessor generated PSFs are evaluated for theoretical consistency by the program and then converted to failure probabilities. An assessment of progress on the development of the MAUD addition to SLIM is an essential precursor to the actual field testing of the technique.

The principal objective of current work devoted to SLIM development is a comprehensive test of the MAUD-based implementation of SLIM. The first task to be accomplished in the test was a classification session whose purpose was the grouping of human actions on the basis of the PSFs influencing the actions. This task was completed during the third quarter of FY 1984. In addition, the remaining tasks of the test plan were operationalized and are now undergoing a final scheduling.

13.2 Multiple Sequential Failure Model Development and Testing

(P. K. Samanta, J. N. O'Brien)

The dependence of human failure on multiple sequential action is important in the evaluation of human reliability. NUREG/CR-2211 has analyzed the nature of this dependence and has distinguished it from other types of multiple failures. Human error causes selective failure of components depending on when the failure started. Two models have been initially developed for quantifying the failure probability in a multiple sequential action. The first is very general in nature and does not require any dependent failure data. The failure probability obtained from this model is a conservative one with associated uncertainty. The uncertainty is calculated considering many possible sources such as data, coupling, and modeling. In the second model, details of the process in multiple sequential failures (MSF) are taken into account. The model increments the conditional failure probabilities by a certain amount from their lower bounds (independent failure probability). This approach provides important insights into the influence of dependence of failures on system reliability. The model can be used effectively to choose an optimum system considering the individual failure probability, dependence factor, and the amount of redundancy in a system.

During the third quarter of FY 1984, the small-scale psychological experiment being used to test the model was further developed. Programming of test sequences was initiated and experimental tasks were further refined. Subject training approaches were further developed along with other experimental design considerations. Subjects were being selected and expected to be performing in the experiment during the next quarter.

13.3 PRA Human Reliability Data
(J. N. O'Brien)

An assessment of the usefulness of PRA human reliability data in resolving human factors regulatory issues facing NRC has been undertaken. In order to accomplish this, two efforts are being undertaken. First, a list of all human factors issues is being assembled and the technical research questions which must be addressed to resolve them developed. Second, all PRAs are being reviewed to illicit exactly what type of data is presented. After both of these efforts are completed, PRA data will be compared to the human factors technical questions to determine their usefulness.

During the third quarter of FY 1984, a taxonomy for classifying human reliability data and a method for locating these data were developed. Also, technical readers have been analyzing PRA documents for key words relating to human reliability data while a coding scheme is being developed for expert reader classification of identified human reliability data. In addition, a discussion paper on human factors regulatory issues has been completed. This paper is being used to formalize a comprehensive set of technical research questions relevant to regulation of human factors in nuclear power plants.

REFERENCES

COMER, M. K., KOZINSKY, E. J., SECKEL, J. S., AND MILLER, D. P. (1983). "Human Reliability Data Bank for Nuclear Power Plant Operations," NUREG/CR-2744.

EMBREY, D. E. (1983). "The Use of Performance Shaping Factors and Quantified Expert Judgement in the Evaluation of Human Reliability: An Initial Appraisal," NUREG/CR-2986.

EMBREY, D. E., HUMPHREYS, P., AND ROSA, E. A. (1984). "SLIM-MAUD: An Approach to Assessing Human Error Probabilities Using Structured Judgment," NUREG/CR-3518.

HALL, R. E., FRAGOLA, J., AND LUCKAS, W. J., JR., Tech. Eds. (1981). Conference Record for NRC/BNL/IEEE Standards Workshop on Human Factors and Nuclear Safety, NUREG/CP-0035.

HALL, R. E., FRAGOLA, J., AND WREATHALL, J. (1982). "Post Event Human Decision Errors; Operator Action Tree/Time Reliability Correlation," NUREG/CR-3010.

LUCKAS, W. J., JR. AND HALL, R. E. (1981). "Initial Quantification of Human Errors Associated with Reactor Safety System Components in Licensed Nuclear Power Plants," NUREG/CR-1880.

LUCKAS, W. J., JR., LETTIERI, V., AND HALL, R. E. (1982). "Initial Quantification of Human Error Associated with Specific Instrumentation and Control system Components in Licensed Nuclear Power Plants," NUREG/CR-2416.

SAMANTA, P. K. AND MITRA, S. P. (1981). "Modeling of Multiple Sequential Failures During Testing, Maintenance, and Calibration," NUREG/CR-2211.

SAMANTA, P. K., HALL, R. E., AND SWOBODA, A. L. (1981). "Sensitivity of Risk Parameters to Human Errors in Reactor Safety Study for a PWR," NUREG/CR-1879.

SCHMALL, T. M., Ed. (1979). Conference Record for NRC/BNL/IEEE Standards Sponsored December 1979 Workshop on Human Factors and Nuclear Safety.

SPEAKER, D. M., THOMPSON, S. R., AND LUCKAS, W. J., JR. (1982). "Identification and Analysis of Human Errors Underlying Pump and Valve Related Events Reported by Nuclear Power Plant Licensees," NUREG/CR-2417.

SPEAKER, D. M., VOSKA, K. J., AND LUCKAS, W. J., JR. (1983). "Identification and Analysis of Human Error Underlying Electrical/Electronic Component Related Events Reported by Nuclear Power Plant Licensees," NUREG/CR-2987.

VOSKA, K. J. AND O'BRIEN, J. N. (1984). "Human Error Probability Estimation Using Licensing Event Reports," NUREG/CR-3519.

14. Human Factors Aspects of Safety/Safeguards Interactions

(J. N. O'Brien)

Brookhaven National Laboratory has been tasked in this program to describe potential safety/safeguards interaction problems during safety-related events and recommended actions to prevent or mitigate those problems. In addition, the nature of these interactions is to be examined to identify any performance deficiencies or conflicts.

The first step of this effort is to examine and address human factors issues which arise from consideration of impacts on the ability of personnel at nuclear power plants to effectively perform their duties as documented in NUREG-0992. Of particular interest are situations at plants which may involve conflicts in roles and missions between security measures and the other organizational units which operate the plant. This program sets out to examine the human factors aspects of these potential problems and, further, to recommend measures to prevent or mitigate any potential adverse impacts on safety.

In order to effectively address potential problems involving conflicts between security requirements and operational practices, potentially troublesome situations and human factors issues relevant to them must be identified. This involves the consideration of a wide range of situations and human factors issues. Once situations have been identified and relevant human factors issues defined, a systematic examination will reveal how potential conflicts can be prevented or mitigated.

After potentially troublesome situations and relevant human factors issues are identified, a matrix will be constructed with situations on one axis and human factors on the other. The cells in the matrix represent the basis of the analysis from which proposals will be developed to prevent or mitigate adverse effects.

The scope of the resultant report will include input from a number of individuals in the fields of operational safety, security, and human factors. However, no site visits will be conducted. Instead, the data contained in the NUREG-0992 is considered to be representative of that which would come from site visits since that is how the committee's data were generated. NUREG-0992 has been extensively analyzed and conclusions are drawn on the basis of that information and subject to review by a panel of experts in the relevant fields. No formal attempt has been made to corroborate or verify the data presented in NUREG-0992.

During the third quarter of FY 1984, an expert panel was convened to finalize the matrix of potentially troublesome situations and revelant human factors issues. Also, a detailed survey form and structured interview guide has been developed to help to elicit expert opinion on the nature of the safety/safeguards interactions to identify problem areas.

15. Emergency Action Levels

(W. J. Luckas, Jr.)

Brookhaven National Laboratory (BNL) has been tasked in this program to develop guidance for Emergency Action Levels (EALs) that can be integrated into Emergency Operating Procedure (EOP) guidelines. From this guidance, a method will be developed that can be applied by licensees to verify that the EALs incorporated into their EOPs are usable in the control room under accident conditions. This should result in a reliable and timely basis for declaring emergencies without being too complex or burdensome to those who are trying to safely mitigate the accident.

EALs are a plant specific, predetermined observable and/or measurable set of indications (such as a particular set of control room instrument readings having reached specific off-normal values) which are used to declare one of the Emergency Classes (Alert, Site Area Emergency, or General Emergency). A more descriptive term for EALs would be emergency declaration indicators.

After appropriate examination, an attempt is being made to utilize currently available EALs developed by utilities, such as Kansas Gas and Electric Company on their Wolf Creek Generating Station, that use the degradation of fission-product barrier approach as a starting point. The EAL guidance will be verified by testing it against the example initiating conditions listed in Appendix 1 of NUREG-0654.

During the third quarter of FY 1984, a demonstration of the incorporation of EALs into three specific sample sequences along with their accompanying writeups describing the operator's preceptions and actions during the sequences were developed to show how the fission product barrier criteria is used in predicting the declaration of the appropriate emergency classes. The accident sequences used were an Anticipated Transient Without Scram in a BWR, a Small Break LOCA with no Recirculation of Emergency Core Cooling in a PWR, and Complete Station Blackout in a BWR. In addition, a preliminary assessment of the adaptability of the BWR Owners' Group Emergency Procedure Guidelines to integrate EALs and EOPs based on the degradation of the fission product barrier criteria.

16. Protective Action Decisionmaking

(W. T. Pratt, A. G. Tingle, H. Ludewig,
W. R. Casey*, and A. P. Hull*)

16.1 Background

NRC regulations require that, in the case of a major nuclear power plant accident, licensees recommend protective actions to reduce radiation dose to the public. When certain emergency action levels are exceeded, the licensee recommends protective actions to State and local officials. The nature of the protective actions recommended is determined by which emergency action levels are exceeded.

In practice drills, decisions on protective action recommendations have proven to be difficult. NUREG-0654 states that if containment failure is imminent, sheltering is recommended for areas that cannot be evacuated before the plume arrives, but evacuation is recommended for other areas. The assumption in NUREG-0654 is that there would be a greater dose savings if the population were sheltered during plume passage rather than evacuated, but this assumption has not been proven. Furthermore, the recommended protective actions must be based on estimated containment failure times, which are difficult to determine.

Alternatively, other NRC publications suggest that the appropriate response would be early evacuation of everyone within a distance of about 2 or 3 miles for all events that could lead to a major release even if containment failure is imminent or a release is underway. Those at greater distances should take shelter. Further, if a release occurs, the appropriate action would be for monitoring teams to find "hot spots" (radiation dose rate exceeding about 1 R/hr) and for people to evacuate these "hot spots."

16.2 Project Objectives

The objectives of the activities to be performed in this project are to:

(1) characterize the family of potential accident sequence for which emergency planning is necessary,

(2) establish strategies appropriate to these sequences, emphasizing credible failure modes,

(3) identify those factors which would influence the implementation of these strategies,

(4) determine how these factors should be incorporated into the decisionmaking process, and

---

*BNL Safety and Environmental Protection Division

(5) develop a guidance report on the protective actions to be recommended for combinations of these factors.

The final NUREG report for the project will be written in a simplified manner that can be readily grasped by people not intimately familiar with accident consequence modeling. In addition, the report will also have a clear and concise summary understandable to laypeople.

16.3 Technical Approach

The technical approach is based on an evaluation of the consequences of nuclear power plant accidents as they relate to protective action decision-making. The evaluation includes a careful review of previous work (e.g. NUREG/CR-2339, NUREG-0654, NUREG/CR-2025, NUREG-0396, and reports and memoranda by the NRC staff) and its applicability to protective action decision-making. The approach is also based on a consideration of a wide range of potential accident sequences and on up-to-date assessments of containment performance. Thus the technical basis will reflect the new fission product source term information under development by the NRC/RES Accident Source Term Program Office (ASTPO). BNL staff are closely following the activities of ASTPO and, in addition, are participating in the SARP Containment Loads Working Group and in the Containment Performance Group. The work of these groups will be integrated into our development of protective action strategies.

The evaluation will be based in large part on results obtained from the CRAC2 computer code (Consequence of Reactor Accident Code, version 2). The output is being analyzed in terms of dose vs. distance for a variety of release characterizations, weather sequences, and protective action strategies.

In accordance with the above, we have selected the following six facilities to represent the range of potential reactor and containment designs:

Zion: PWR with a large dry containment
Surry: PWR with a subatmospheric containment
Sequoyah: PWR with an ice condenser containment
Brown's Ferry: BWR with a Mark I containment
Limerick: BWR with a Mark II containment
Grand Gulf: BWR with a Mark III containment

16.4 Project Status

16.4.1 Summary of Activities

In April BNL staff made a presentation on the project status to the NRC staff at a meeting in Washington, D.C. The presentation focused on three principal subjects:

- The role of containment performance in reducing potential source terms during severe accident sequences was discussed. In particular, the ability of the plant operator to assess certain critical plant conditions which indicate the direction of an accident was stressed.

- Using the SST1 source terms, calculations were presented comparing dose to individuals as a function of distance from the reactor, weather conditions, and protective action strategies. These calculations were presented in the format to be used in our draft report.

- Several protective action strategies were considered using guidelines based upon preventing loss of life and minimizing radiation exposure during severe accident sequences.

The NRC Project Manager visited BNL in May to present current NRC views on Protective Action Decisionmaking and to present feedback on the presentation given by BNL to the NRC. The NRC feels that all PAD work should be based on new source terms and consider the role of containment performance. This is consistent with our general approach to this project and was reflected in our presentation to NRC staff. During the visit, BNL demonstrated that the results from the Emergency Action Levels Project (FIN A-3271) are vital to rational protective decisions and showed examples of strategies linked to EAL's. The coordination of the two projects was the basis for much of the work this quarter.

Several CRAC 2 calculations were performed based upon the new source term data and a consideration of the role of containment performance. Coordination with the Emergency Action Levels Project has led us to consider sequences initiated by an ATWS, complete station blackout, and small break LOCA. This coordination assures that recommended protective actions will be linked to key in-plant observables.

16.4.2 Preliminary Conclusions

The results of these analyses to date have permitted certain preliminary conclusions to be developed.

(1) In-plant conditions: BNL staff have been evaluating specific accident sequences to determine if readily identifiable plant conditions exist which permit selection of appropriate protection action strategies. Preliminary results indicate that such links do exist and that protective action strategies can be based on in-plant observables for those accident sequences examined to this point.

(2) Warning time: BNL staff analysis of severe accidents indicates that warning times of several hours or more can be expected for the more probable accident sequences, e.g. small break LOCA or transients. Short warning times of 1 hour or less are associated only with less probable accident sequences such as ATWS, which should be readily identified.

(3) Weather: The importance of weather in defining the consequences of a radioactive release has been convincingly reconfirmed in our analyses of different accident scenarios. The type of weather occurring at the time of a release can dramatically affect the type of protective action recommended and the size of the area for which protective action is warranted. Since weather is an observable condition,

it is apparent that the recommended protective action strategies should be highly weather dependent.

(4) Plume rise: In the accident scenarios that BNL staff have evaluated, the energy of release is an important parameter affecting downwind doses. It appears that this information will also be important in selecting the appropriate strategy.

NRC FORM 335 (11-81)

U.S. NUCLEAR REGULATORY COMMISSION

BIBLIOGRAPHIC DATA SHEET

1. REPORT NUMBER (Assigned by DDC)
NUREG/CR-2331
BNL-NUREG-51454, Vol. 4, No. 2

4. TITLE AND SUBTITLE (Add Volume No., if appropriate)
Safety Research Programs Sponsored by Office of Nuclear Regulatory Research, Quarterly Progress Report April 1 - June 30, 1984

2. (Leave blank)

3. RECIPIENT'S ACCESSION NO.

7. AUTHOR(S)
Compiled by Allen J. Weiss

5. DATE REPORT COMPLETED
MONTH: September YEAR: 1984

9. PERFORMING ORGANIZATION NAME AND MAILING ADDRESS (Include Zip Code)
Brookhaven National Laboratory
Department of Nuclear Energy
Upton, New York 11973

DATE REPORT ISSUED
MONTH: November YEAR: 1984

6. (Leave blank)

8. (Leave blank)

12. SPONSORING ORGANIZATION NAME AND MAILING ADDRESS (Include Zip Code)
U. S. Nuclear Regulatory Commission
Office of Nuclear Regulatory Research
Washington, D. C. 20555

10. PROJECT/TASK/WORK UNIT NO.

11. FIN NO.
A-3014,15,16,24,41, A-3208,15, 19,25,26,27,57,61,66,68,70,71,75

13. TYPE OF REPORT
Quarterly

PERIOD COVERED (Inclusive dates)
April 1 - June 30

15. SUPPLEMENTARY NOTES

14. (Leave blank)

16. ABSTRACT (200 words or less)

This progress report will describe current activities and technical progress in the programs at Brookhaven National Laboratory sponsored by the Division of Accident Evaluation, Division of Engineering Technology, and Division of Risk Analysis & Operations of the U.S. Nuclear Regulatory Commission, Office of Nuclear Regulatory Research.

The projects reported are the following: High Temperature Reactor Research, SSC Development, Validation and Application, CRBR Balance of Plant Modeling, Thermal-Hydraulic Reactor Safety Experiments, Development of Plant Analyzer, Code Assessment and Application (Transient and LOCA Analyses), Thermal Reactor Code Development (RAMONA-3B), Calculational Quality Assurance in Support of PTS; Stress Corrosion Cracking of PWR Steam Generator Tubing, Probability Based Load Combinations for Design of Category I Structures, Mechanical Piping Benchmark Problems, Identification of Age-Related Failure Modes; Analysis of Human Error Data for Nuclear Power Plant Safety Related Events, Human Factors Aspects of Safety/Safeguards Interactions, Emergency Action Levels, and Protective Action Decision Making.

17. KEY WORDS AND DOCUMENT ANALYSIS

17a. DESCRIPTORS

High Temperature Graphite Reactor
Super System Code
MINET Code
Thermal-Hydraulic Reactor Safety
Emergency Action
Plant Analyzer
RAMONA-3B
Pressurized Thermal Shock
Stress Corrosion Cracking
Protective Action
Load Combinations
Nuclear Plant Aging
Human Error
Human Factors

17b. IDENTIFIERS/OPEN ENDED TERMS

18. AVAILABILITY STATEMENT

19. SECURITY CLASS (This report)

21. NO OF PAGES

20. SECURITY CLASS (This page)

22. PRICE
S